OULU 2015
C 523

ACTA UNIVERSITATIS OULUENSIS

Hirley Alves

ON THE PERFORMANCE ANALYSIS OF FULL-DUPLEX NETWORKS

UNIVERSITY OF OULU GRADUATE SCHOOL;
UNIVERSITY OF OULU,
FACULTY OF INFORMATION TECHNOLOGY AND ELECTRICAL ENGINEERING,
DEPARTMENT OF COMMUNICATIONS ENGINEERING;
FEDERAL UNIVERSITY OF TECHNOLOGY - PARANÁ

ACTA UNIVERSITATIS OULUENSIS
C Technica 523

HIRLEY ALVES

ON THE PERFORMANCE ANALYSIS OF FULL-DUPLEX NETWORKS

Academic dissertation to be presented with the assent of the Doctoral Training Committee of Technology and Natural Sciences of the University of Oulu for public defence in Kainuunsali (L2), Linnanmaa, on 27 March 2015, at 14 p.m.

UNIVERSITY OF OULU, OULU 2015

Acta Univ. Oul. C 523, 2015

Supervised by
Professor Matti Latva-aho

Reviewed by
Professor George K. Karagiannidis
Doctor Himal A. Suraweera

ISBN 978-952-62-0765-0 (Paperback)
ISBN 978-952-62-0766-7 (PDF)

ISSN 0355-3213 (Printed)
ISSN 1796-2226 (Online)

Cover Design
Raimo Ahonen

JUVENES PRINT
TAMPERE 2015

Alves, Hirley, On the performance analysis of full-duplex networks.
University of Oulu Graduate School; University of Oulu, Faculty of Information Technology and Electrical Engineering, Department of Communications Engineering; Federal University of Technology - Paraná
Acta Univ. Oul. C 523, 2015
University of Oulu, P.O. Box 8000, FI-90014 University of Oulu, Finland

Abstract

In this thesis we study Full-Duplex (FD) cooperative networks from different perspectives, using concepts of information theory, communication theory and applied statistics. We provide a comprehensive performance analysis of cooperative communications systems operating with FD relays. We demonstrate that FD relaying is feasible even when experiencing strong self-interference, and we show its application under different scenarios. More importantly, the results attained through this work serve as a benchmark for design as well as deployment of current and future wireless communications technologies.

Our first contribution is a comprehensive overview of the state-of-the-art on FD communications, more specifically on FD relaying, and we revisit some of the main properties of cooperative schemes. Another contribution comes from an extensive analysis of outage probability, throughput and energy efficiency of FD relaying over Rayleigh fading channels. Besides the mathematical framework introduced herein, we also show that in some cases cooperative Half-Duplex (HD) schemes achieve better performance than FD relaying with self-interference. Therefore, we draw a discussion on the trade-offs between HD and FD schemes as well as between throughput and energy efficiency. Then, we investigate the performance of FD relaying protocols under general fading settings, namely Nakagami-m fading. Our findings allow a better understanding of effects of the residual self-interference and line-of-sight on a FD relaying setup. Our final contribution lies on the performance analysis of secure cooperative networks relying on information theoretical metrics to provide enhanced privacy and confidentiality to wireless networks. Thus, we provide a comprehensive mathematical framework for composite fading channels. Even though experiencing strong self-interference, we demonstrate that FD relaying is feasible also under secrecy constraints, thus perfect secrecy can be achieved.

Keywords: cooperative relaying, full duplex relaying, performance analysis, physical layer security

Alves, Hirley, Suorituskykyanalyysi kaksisuuntaisissa verkoissa.
Oulun yliopiston tutkijakoulu; Oulun yliopisto, Tieto- ja sähkötekniikan tiedekunta, Tietoliikennetekniikan osasto; Federal University of Technology - Paraná
Acta Univ. Oul. C 523, 2015
Oulun yliopisto, PL 8000, 90014 Oulun yliopisto

Tiivistelmä

Tässä työssä tutkitaan kaksisuuntaisia (Full-Duplex, FD) yhteistoiminnallisia verkkoja informaatioteorian, tietoliikenneteorian ja sovelletun tilastotieteen näkökulmista. Työssä suoritetaan kattava suorityskykyarviointi yhteistoiminnallisten FD-välittimien muodostamassa tietoliikenneverkossa. FD-releointi osoitetaan toimintakelpoiseksi useissa toimintaympäristöissä ja sovelluksissa jopa voimakkaan omahäiriön vallitessa. Mikä tärkeintä, työssä saavutetut tulokset muodostavat vertailukohdan sekä nykyisten että tulevien langattomien verkkoteknologioiden suunnitteluun ja toteutukseen.

Aluksi esitetään perusteellinen katsaus uusimpiin FD-tiedonsiirtomenetelmiin, etenkin FD-välitykseen, sekä kerrataan yhteistoiminnallisten tekniikoiden pääpiirteet. Seuraavaksi analysoidaan laajasti FD-välitinyhteyden luotettavuutta sekä spektrinkäyttö- ja energiatehokkuutta Rayleigh-häipyvissä radiokanavissa. Matemaattisen viitekehyksen lisäksi osoitetaan myös, että joissain tapauksissa yhteistoiminnalliset vuorosuuntaiset (Half-Duplex, HD) menetelmät ovat parempia kuin FD-releointi omahäiriön vallitessa. Niinpä työssä käydään keskustelua kaupankäynnistä HD- ja FD -menetelmien kesken kuten myös spektrinkäyttö- ja energiatehokkuuden kesken. Seuraavaksi tutkitaan FD-releoinnin suorityskykyä yleistetymmässä häipymäympäristössä eli Nakagami-m -kanavassa. Saavutetut tulokset auttavat ymmärtämään paremmin jäljelle jäävän omahäiriön ja näköyhteyslinkkien vuorovaikutussuhteet FD-välitinjärjestelmän suunnittelussa. Lopuksi käsitellään tietoturvattuja yhteistoiminnallisia verkkoja informaatioteoreettisin mittarein, joilla pyritään tarjoamaan langattomien verkkojen käyttäjille parempaa yksityisyyden suojaa ja luottamuksellisuutta. Tätä varten työssä esitetään perusteelliset matemaattiset puitteet yhdistettyjen häipyvien kanavien tutkimiseen. Tuloksena osoitetaan, että myös salassapitokriteerien kannalta on mahdollista käyttää voimakkaan omahäiriön kokemaa FD-releointia vahvan salauksen saavuttamiseen.

Asiasanat: fyysisen kerroksen turvallisuus, kaksisuuntainen yhteistoiminnallinen releointi, suorituskykyarviointi, yhteistoiminnallinen releointi

To Antonio, Sirley and Phâmela.

Acknowledgements

I would like to express my sincere gratitude to my Professors Matti Latva-aho and Richard Demo Souza for their guidance, friendship and flexible supervision, providing me fully support whenever needed. In addition, my thanks extends to Mehdi Bennis, who invited me to come to Oulu and join CWC back in 2011, and with whom I have worked closely and befriend.

I also would like to thank Prof. Marcelo Pellenz, Prof. Gustavo Fraidenraich, Prof. Evelio Fernández, Prof. Mérouane Debbah, Prof. Daniel Benevides da Costa, Prof. José Cândido for their friendship as well as our work collaboration. I also extend my gratitude to my follow up group, Antti Tölli, Nandana Rajatheva and Mehdi Bennis, for their valuable inputs and friendly discussions. Additionally, I would like to thank the pre-examiners for their valuable comments and suggestions, which definitely enhanced the content of this thesis.

I would like to thank all friends I have made in my years at LabSC and CWC, especially Amin, Animesh, Ari, Behnaam, Davide, Diana, Edgar, Fatih, Fernando, Francesco, Glauber, Hamid, Harri, Hossein, Jani, Jarkko, João Rebelatto, Joukko, Kakitani, Kalle, Keeth, Madhu, Manosha, Marian, Markku, Markus, Matti, Mohammed, Namal, Nuwan, Pekka, Petri, Qiang Xue, Samuel, Satya, Simon, Sumudu, Uditha, Ulrico, Visa amongst others. Moreover, I would like to thank Brett & Laura, Carlos & family, Destino & family and Pedro & Carol whose friendship excel our work environment and with whom I share great memories. A very special thanks goes to my long time friends Jonne & Caro (and their families), for receiving me with open arms, and as well for their support and company. Yet, I am grateful that Jonne & Caro invited me to join the band, and consequently for all the extra fun we have playing, composing, recording... Another special thanks goes to my girlfriend Priscila for her support and joyfulness of my success.

I also would like to thank the whole administrative staff from CWC, specially Anu, Elina, Hanna, Jari, Juha-Pekka, Kirsi, Mari, Timo and Varpu. I want to express my gratitude to Infotech Graduate School, Tekniikan Edistämissäätiö, Elisa Oy. Foundation, Riita and Jorma J. Takanen Foundation, Tauno Toning Foundation and Nokia Foundation for the financial support of this work.

Em conclusão, agradeço minha querida família – meu pai Antonio, minha mãe Sirley and minha irmã Phâmela – pelo amor incondicional, fé nas minhas aspirações, e sábios conselhos além do apoio irrestrito. A eles dedico esta tese.

Hirley Alves
Oulu, March 2, 2015

List of abbreviations

3GPP 3rd Generation Partnership Project

AF Amplify-and-Forward

ADC Analog-to-Digital Converter

ARQ Automatic Repeat reQuest

AWGN Additive White Gaussian Noise

BC Broadcast Channel

CDF Cumulative Distribution Function

CSI Channel State Information

DAC Digital-to-Analog Converter

DF Decode-and-Forward

FDF Fixed-Decode-and-Forward

SDF Selective-Decode-and-Forward

DL Downlink

FD Full-Duplex

FDBM Full-Duplex Block Markov

FDMH Full-Duplex Multi-Hop

HARQ Hybrid Automatic Repeat reQuest

HD Half-Duplex

IDF Incremental-Decode-and-Forward

IRST Incremental Redundancy Space-Time

i.i.d. independent and identically distributed

IFA Intermediate Frequency Amplifier

LNA Low-Noise Amplifier

LTE Long Term Evolution

LoS Line-of-Sight

MAC Multiple-Access Channel

MIMO Multiple-Input Multiple-Output

mmWave Millimeter Wave

MRC Maximum Ratio Combining

PA Power Allocation

PDF Probability Distribution Function

PHY Physical Layer

QoS Quality of Service

R Relay

RA Rate Allocation

RV Random Variable

SC Selection Combining

SDF Selective Decode-and-Forward

SINR Signal-to-Interference plus Noise Ratio

SNR Signal-to-Noise-Ratio

SQP Sequential Quadratic Programming

UL Uplink

List of symbols

δ	Self-interference mitigation coefficient
$\mathrm{erfc}\,(\cdot)$	Complementary error function
Γ	Random Variable representing SNR
$\Gamma(\cdot)$	Gamma function
$\Gamma(\cdot,\cdot)$	Incomplete gamma function
γ_{ij}	Signal-to-noise-ratio of the link between nodes i and j
$\mathrm{K}_{\nu}(\cdot)$	Modified Bessel function of the second kind
$\mathsf{Gamma}(\alpha,\beta)$	Gamma distribution with shape α and rate β
$\mathsf{GGamma}(\alpha,\beta,1,1)$	Generalized gamma distribution with shape α and rate β
$\mathsf{U}(\cdot,\cdot,\cdot)$	Confluent hypergeometric function of the second kind
$\min\{\cdot\,,\,\cdot\}$	Minimum function
ν	Path loss exponent
Ω_{ij}	Average fading power of the Nakagami-m distribution
$\mathrm{E}\,[\cdot]$	Mathematical expectation
$\mathrm{Re}(\cdot)$	Real part of complex number
$\overline{\gamma}$	Average SNR
$\Pr[\theta]$	Probability of and given event θ
ρ	Correlation coefficient
σ_w	Noise' standard deviation
τ	Processing delay
$\sim$	Distributed according to
$\tilde{x}$	Relay's unity energy transmitted symbol
d_{ij}	Distance between nodes i and j
$F_W(\cdot)$	Cumulative distribution function of a random variable W

$f_W(\cdot)$	Probability distribution function of a random variable W
h_{ij}	Fading channel coefficient between nodes i and j
L	Number of blocks
m_{ij}	Shape parameter of Nakagami-m distribution
N_0	Noise power spectral density
p_X	Probability distribution function of random variable X
P_i	Transmit power of node i
q_X	Approximated probability distribution function of random variable X
w_i	Zero-mean complex Gaussian noise at node i
x	Source's unity energy transmitted symbol
y_i	Received signal at node i
$\mathcal{I}_{ij}$	Mutual information between nodes i and j
$\mathcal{R}$	Achievable rate
*	Complex conjugate

Contents

1 Introduction

In the last few years wireless networks have become ubiquitous and an indispensable part of our daily life due to a broad range of applications. In the next years, a myriad of connected devices will change the way we live, make business, gather into social groups and interact. As a result, the next generation of mobile access networks will experience a thousand-fold increase in traffic volume compared to today's standards, which will require new technologies and practices as well as a rearrangement of the spectrum [1–3].

In order to meet these demands with high quality of service, not only high bit rates are required but also low error performance. Therefore, we first need to circumvent the disruptive characteristics of the wireless medium, mainly multipath and fading effects. Many techniques have been proposed over the years [4, 5], for instance channel coding is often employed as a way to overcome the effects of multipath. When the spatial domain of the channel is exploited, both multipath and fading can be tackled by the use of multiple antennas, commonly known as Multiple-Input Multiple-Output (MIMO) techniques [4].

Amongst the MIMO techniques are diversity schemes [4], whose main goal is to provide the receiver with several realizations of the signal and therefore effectively circumvent the effects of fading in wireless communications, which consequently enhances reliability through the use of multiple transmit and/or receive antennas [4–6]. However, as pointed out in [4] MIMO techniques offer various benefits, which do not come for free. For instance, wireless devices are constrained in size, complexity and power, which, by its turn, renders current diversity methods harder to implement in practical applications.

In order to overcome such constraint, cooperative diversity emerged as a promising technique for future wireless communication systems. Cooperation among nodes offers enhanced spatial diversity and network connectivity, improved power and spectrum efficiency as well as increased communication reliability [4–14]. Therefore, cooperative networks have been the focus not only of academia [4–14] but also of the industry [10–12]. For instance, earlier releases of 3rd Generation Partnership Project (3GPP) [10] already included relaying as a viable technique to boost performance, remaining in the scope of current systems

such as Long Term Evolution (LTE) and LTE-advanced [11]. In addition, cooperative systems are foreseen as a key technology also in the upcoming wireless systems [12–14].

The relay channel was introduced by Van der Meulen [15] and is composed of three nodes, namely source (S) and destination (D), while the third node acts as a helper and it is known as relay (R). The basic idea behind the relay channel is that the source broadcasts its information to both relay and destination. Then, the relay forwards the source's signal to the destination, which properly combines the signals received through the two independent paths (source-destination and R-D links). Thus, the destination perceives a virtual MIMO channel which allows a single antenna device to achieve spatial diversity as if it were a multiple antenna one [5–9].

Throughout these last decade, a variety of cooperative schemes have been proposed and applied to different network configurations. For instance, in [16] the authors claim that through cooperation transmission power is reduced, since the distance among nodes is smaller, consequently the interference within the network will be also smaller. Based on that cooperation is an important part of energy-efficient networks, given that a node can save energy through cooperation.

Cooperative schemes are also associated with multiple antenna (MIMO) technologies as discussed in [17]. As observed in [17], cooperative MIMO, known as virtual or distributed MIMO, utilizes distributed antennas on multiple radio devices to achieve some benefits similar to those provided by point-to-point MIMO systems. In this context, the wireless network is able to coordinate among distributed antennas and achieve considerable performance gains such as improvements in spectral efficiency and network coverage. More specifically, in [11] the authors explore the application of such cooperative schemes in LTE-advanced systems, showing that great system spectrum efficiency and performance improvements can be achieved. Another application of cooperative schemes is into the scope of machine-to-machine communications as pointed out in [14, 18]. Additionally, cognitive radio is also a propitious way to improve spectrum efficiency of wireless communications [19, 20]. Such schemes become an even more powerful tool when associated with cooperative schemes. In that case, significant gains can be achieved in spectrum sensing and sharing, interference constraint adaptive cooperative feedback, rateless network coding, and interference coordination [19, 20]. All in all, we observe that cooperative schemes are exploited in

a wide range of applications [11, 14, 16–21], and are also a promising technology for future wireless communications networks [11–14].

1.1 Multiplexing loss in cooperative schemes

In spite of all the progress achieved so far [4–14], there are still several open issues in cooperative schemes. Amongst these, may be even one of the greatest, challenges resides the multiplexing loss, which is inherent of cooperative schemes that operate with Half-Duplex (HD) radios [5, 6, 22]. The multiplexing loss appears because the relay, in a first slot, hears the broadcast from the source, and then on a second instant conveys the received message to the destination. In this sense, multiplexing loss presents itself as the on of the major drawbacks of cooperative schemes. Several schemes have been proposed on an attempt to overcome such issue; however, those solutions are in general quite intricate, see, for instance, [22–24]. For instance, [23] requires the use of one more relay in order to overcome the multiplexing loss, while in [22] a spectrally efficient relay selection scheme is proposed, which by its turn assumes the existence of several relays. In this sense, both works have an stringent requirement for more nodes, which may not be always available or it may be out of the interest of the nodes to cooperate, for instance due to a lack of proper incentives. In [24], the authors assume three node setup, in which the relay is able to accumulate messages. Then, exploiting its infra-structured deployment the relay can transmit the accumulated messages in a single frame with high data rate.

Until recently, communication standards rely heavily on HD radios, therefore transmission and reception occur in different instants. Nevertheless, this paradigm has changed and nowadays Full-Duplex (FD) radios are becoming a reality, such radios are able to simultaneously transmit and receive [25–47].

1.1.1 Full-duplex communications

Full-Duplex (FD) communications are becoming a reality and have gained considerable attention from academia and industry [25–47]. However, current FD systems suffer from a power leakage between the transmit and receive antennas, which is known as self-interference [26, 29, 30]. Therefore, there are still several unanswered questions such as: how to overcome self-interference? Which can-

cellation technique gives better performance? Could self-interference be brought down to noise level ? How to model and cope with residual self-interference? Currently, some of these questions are partially answered, since many of those questions are under scrutiny but there is yet plenty of work ahead. In the context of cooperative schemes, FD relaying deals not only with multiplexing loss, but at the same time promotes increased link capacity and opens new ways to reuse the spectrum [30].

Several works have dealt with the self-interference cancellation problem [25–42]. Analytical and empirical results show that self-interference can be mitigated, but so far cannot be brought down to noise floor [26–38]. Thus, the FD transceiver experiences the reminder of the self-interference, namely residual self-interference, which by its turn can be modeled as a fading channel [40–48].

All in all, the main conclusion amongst all those works [25–47] is that FD communication is feasible, even though suffering strong self-interference and, consequently, residual self-interference.

It is in this context that lies the work presented throughout this thesis. We explore and analyze several FD cooperative schemes as well as their applications in current and future wireless communications systems. For instance, we assess the performance of HD and FD cooperative schemes in terms of outage probability, throughput and energy efficiency over Rayleigh fading channels, and discuss the trade-offs between them. Later, we evaluate FD relaying under general fading settings, in order to better understand effects of distinct (non-) Line-of-Sight (LoS) configurations on the residual self-interference. Then, another important aspect of current and upcoming wireless communication networks is security, which we also grasp by means of information-theoretical tools, namely Physical Layer (PHY) security [49–51]. PHY-security appears as an alternative to complement cryptographic-based security systems, which are often implemented at the higher layer of communication protocols [49–51]. Furthermore, PHY-security opens a new way to enhance the robustness and reduce the complexity of conventional cryptography systems since it is unbreakable and quantifiable (in confidential bps/Hz) regardless of the eavesdropper's computational power [49]. Therefore, herein we assess the performance PHY-secured cooperative systems in terms of secrecy capacity and outage probability[1].

[1]Owing to readability, we opt to leave a more detailed discussion on PHY security enclosed to Chapter 5.

Bearing all this in mind, herein we provide a comprehensive performance analysis, by means of analytical and numerical results, which serves as a benchmark for design and deployment of cooperative networks.

1.2 Contributions and outline of the thesis

The work presented in this thesis focuses on the performance of cooperative FD networks which has been done analytically and corroborated by Monte Carlo simulations. In what follows, we outline this thesis and provide the main contributions of each chapter. Thus,

- **Chapter 2:** We present a comprehensive overview of the current state-of-the-art on FD communications, more specifically FD relaying. Additionally, we revisit some of the main properties of cooperative schemes and introduce the FD relaying model as well as the main performance metric used throughout this thesis.
- **Chapter 3:** We analytically evaluate outage probability, throughput and energy efficiency of cooperative FD relaying over Rayleigh fading channels. Additionally, we compare the performance of cooperative FD relaying, as well as a multi-hop FD scheme, to two incremental cooperative HD relaying methods: Incremental Redundancy Space-Time (IRST), which is one that achieve the best performance among HD schemes, and Selection Combining (SC), which is the simplest retransmission scheme. Besides the mathematical framework provided, we also show that cooperative HD schemes can achieve a smaller outage probability and a higher throughput than cooperative FD relaying with self-interference. Our main contribution lies on the discussion of such trade-offs between HD and FD schemes, as well as throughput and energy efficiency.
- **Chapter 4:** We investigate the performance of some FD relaying protocols under general fading settings, more specifically under Nakagami-m fading. For that purpose, we introduce a new accurate approximation for the product of two Nakagami-m Random Variables (RVs) as well as for the sum of Gamma RVs. With these results we are able to characterize the outage probability of the proposed FD relaying protocol in a easy to compute closed-form expression. Our findings allow us to better understand effects of the residual self-interference on a FD relaying setup, since distinct (non-) LoS configura-

tions can be emulated, which can be directly related to the quality of the antenna isolation and self-interference cancellation employed at the FD relay.

- **Chapter 5:** We consider the concept of PHY security, which is a information theoretic tool which comes as a way to complement cryptographic-based security systems. We discuss the main advances in cooperative PHY security associated with FD relaying schemes and composite fading channels. To do so, we introduce a comprehensive performance analysis on three major scenarios. For each scenario we evaluate the appropriate metric, providing easy-to-compute closed-form expressions. Moreover, we demonstrate that even though experiencing strong self-interference, FD relaying is feasible under secrecy constraints.
- **Chapter 6:** We conclude the thesis and discuss some directions for future work.

It is noteworthy that in this thesis we increment complexity of the system model chapter by chapter. Therefore, the fundamentals of FD relaying are introduced in Chapter 2. Then, Chapter 3 focuses on the performance analysis of FD relaying schemes under Rayleigh fading channel. Chapter 4 extends this initial assessment and provides an analysis of Nakagami-m fading, which allows the emulation of different conditions of the network, such as fading severity and LoS. Last, Chapter 5 adds an analysis on composite fading channels, under a PHY security constrains and FD relaying.

In each chapter, we employ a model that captures the main mechanisms of the network. Hence, even though the similarities in the network modeling, each chapter is based on different assumptions and provide new insights, which are justified and discussed therein.

1.3 Author's publications related to the thesis

This thesis is based on five published international journal papers [45, 46, 52–54], and four related conference papers [43, 55–57]. In [43, 55] an initial assessment on the performance of FD relaying schemes is provided, later these works are extended in order to encompass a deeper analysis and further comparisons with the state-of-the-art on HD relaying, yielding [45, 46]. The aspect of secrecy and confidentiality on FD cooperative networks is drawn in [52, 53, 56, 57].

In a initial work [52, 56] the author proposed a scheme that exploits spatial diversity as a way to enhance security. Then, motivated by the outcomes of FD relaying and information-theoretic security the author performs an investigation on secure FD cooperative schemes, whose results are presented in [53, 57]. In [54] network level analysis is performed, and we show how secrecy metrics are affected by the disposition of the desired receiver, the eavesdropper and the legitimate transmitter.

Besides [43, 45, 46, 52, 53, 55–57], the author published other journals [24, 44, 58–60] and conference papers [61–70]. Additionally, by the time this thesis was finished, the author had submitted [53, 54, 71–76]. Amongst these publications are the ones closely related to this thesis [58–60, 65, 76]. For instance, an initial assessment on HD cooperative networks is presented in [58, 59]. These works inspired the author the pursuit of new methods to increase performance of HD cooperative systems, which ultimately lead to FD relaying. Later, [44] introduces a performance assessment of heterogeneous networks, where the legacy network is underlaid by FD femtocells. Additionally, [65] investigates the use of FD nodes in two-way relaying networks. Notice that those results are not embodied herein, those works have distinct system models and setups which would be a cumbersome task to harmonize to the reminder of the thesis. Therefore, this thesis focus on general framework whose main insights can be applied to distinct applications as we have done in [44] and [65].

Furthermore, under the scope of cognitive networks, we focused on underlay relaying networks and an extensive analysis of both HD and FD schemes is provided in [60, 66, 71, 75]. Additionally, [74] renders a performance analysis of Amplify-and-Forward (AF) FD relaying schemes, while in [68, 69] a more general framework is investigated and we investigate how highly dense deployments of small cells perform when FD nodes communicate under composite fading channels. The impact due to extra interference from co-channel users and how that compares to the intrinsic residual self-interference is identified, and performance is compared to benchmark HD scenarios.

During his thesis work the author has established a vast collaboration network with professors and researchers from various distinguished universities such as Supelec (France), State University of Campinas, Unicamp, Federal University of Ceará, UFC, São Paulo State University, Unesp-SJBV, and especially with the Federal University of Technology - Paraná – UTFPR (where the author

completed his under graduation studies). Furthermore, the author is part of a double degree program between University of Oulu and UTFPR and all results have been obtained under the co-supervision of Prof. Richard Demo Souza and Prof. Matti Latva-aho. This extensive collaboration led to several publications [43, 45, 46, 53–56, 61–76].

2 Cooperative communications: a general overview

In this chapter, we outline the most relevant aspects of cooperative communications: from the relay channel classification up to FD relaying protocols. This overview will serve as a guideline for the developments introduced in the next chapters.

2.1 Relay channel

The relay channel is depicted in Fig. 1. Notice that h_{ij} represents the channel coefficients between the nodes $i \in \{\mathrm{S}, \mathrm{R}\}$ and $j \in \{\mathrm{R}, \mathrm{D}\}$ with $i \neq j$. After the broadcast from the source, the relay helps the communication by forwarding source's message to the destination [15, 77], represented by the dotted line in Fig. 1.

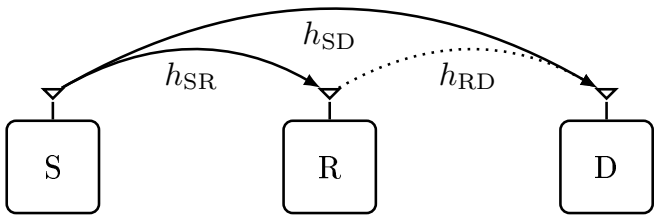

Fig 1. The relay channel is composed of: source (S), relay (R) and destination (D). Notice that the relay helps the source to convey its message to destination. The solid lines are used to denote the channels during the first phase of the cooperative protocol, while the dotted line used to denote the channel during the second phase of the protocol, when the relay forwards source's message. Channel coefficients are denoted by h_{ij}, where $i \in \{\mathrm{S}, \mathrm{R}\}$ and $j \in \{\mathrm{R}, \mathrm{D}\}$ with $i \neq j$.

There are several ways to classify the relay channel:

- **Superposition:** in [78, 79] the authors investigate superposition schemes, where diversity comes, for example, from superposition modulation.
- **Orthogonal transmission:** are the focus on [4–9], and [24, 58, 59, 61] such strategies exploit different repetition protocols in order to enhance the perfor-

mance of such cooperative schemes.

- **Ad-hoc/infra-structured relaying:** infra-structured relays are deployed by the service provider [24, 58, 61, 80, 81], while ad-hoc relays generally are other users of the network. The advantage of infra-structured over ad-hoc relaying lies on a better positioning and channel fading conditions as pointed out in [80, 81].
- **Return channel:** in [58, 82, 83] the authors exploit the presence of a return channel, which allows the destination to exchange information with source and/or relay, and therefore allows the use of Automatic Repeat reQuest (ARQ) strategies as investigated in [82, 83]. For instance, [24] exploits accumulation of retransmitted messages, in order to achieve higher throughput and increased reliability, while [58] evaluates the performance and energy efficiency of incremental relaying protocols. Further, in [59, 61] the authors investigate different cooperative Hybrid Automatic Repeat reQuest (HARQ) schemes and discuss the trade-offs of each scheme in terms of outage probability and throughput.
- **Operation mode:** the relay can operate either in HD or FD fashion [4–9]. For instance, in HD mode, the relay transmits and receives in orthogonal slots either in time or frequency [7, 58, 59]. Such HD schemes have been widely investigated in the literature, although they are inherently spectrally inefficient [22, 24], cooperative HD schemes suffer from multiplexing loss, since Relay (R) first listens and then forwards the message which requires at least two slots for cooperation [22, 24]. On the other hand, in FD mode transmission and reception occur simultaneously [26, 40–47, 84, 85].

Moreover, FD relaying has received more attention of the academy and industry in the recent years [25–28, 30–48]. The main reason behind this growing interest is that FD schemes outperform HD schemes [7, 40–48], ideally doubling the spectral efficiency. In FD mode, cooperative protocols do not suffer from multiplexing loss inherent of HD schemes [22, 24], and therefore FD protocols achieve much higher rates. Thus, in recent years due to such high potential, FD communication has become a promising technology to increase performance of cooperative as well as point-to-point networks, this added to the fact that it has been shown that practical FD communication is feasible [25–28, 30–48, 68, 69, 86–90], further discussion will be presented next.

2.1.1 Cooperative protocols

The behavior of the relay is dictated by the cooperative protocols whose general picture is given in Fig. 2. Notice that Fig. 2 depicts HD protocols, which demand at least two slots, either in time or frequency, to operate. In general, cooperative protocols can be divided into two major phases: broadcast from the source, as shown in Fig. 2a; and cooperative phase[2], as shown in Fig. 2b.

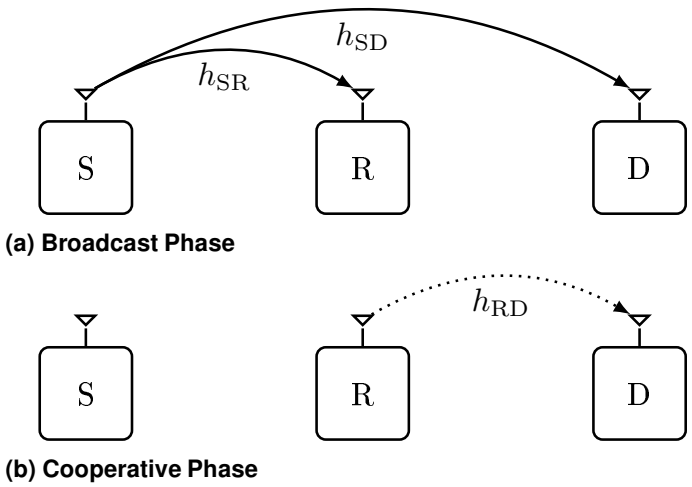

Fig 2. HD cooperative protocols operate in two distinct phases: (*a*) Broadcast Phase: first the source broadcasts its message to relay and destination (solid lines). Then, (*b*) Cooperative phase: the relay acts by forwarding source's message to the destination in a second slot (dotted line).

The two most known cooperative protocols are: AF and Decode-and-Forward (DF) [6–8, 91]. In the AF protocol the relay amplifies source' signal and then forwards it to the destination [6, 7]. On the other hand, in the DF protocol the relay decodes the source's message and then forward it to the destination [6, 7]. The DF protocol has three main variants commonly known as fixed, selective and incremental. In Fixed-Decode-and-Forward (FDF) the relay always forwards the message even if it was incorrectly decoded [6]. On the other hand, in Selective Decode-and-Forward (SDF) the relay only forwards the message if it was decoded

[2]We distinguish here HD and FD protocols. While cooperative phase refers to HD protocols, we termed as multiple access phase the second half of the FD protocols.

free of errors [6]. The Incremental-Decode-and-Forward (IDF) protocol accounts for the presence of a return channel, and therefore the relay only forwards the message if it is error free and if requested by the destination [6, 7, 58, 59].

Cooperative HD protocols suffer from multiplexing loss, since the communication happens in two distinct instants [22, 24]. Due to the great potential of cooperative schemes several solutions have been proposed trying to overcome such issue [22–24]. For instance, in [24] the authors propose a HD cooperative protocol that allows the relay to accumulate a given number of messages, and then forward a single frame carrying a concatenation of all decoded messages. This new frame is transmitted with a rate proportional to the number of accumulated messages, exploiting the deployment of infra-structured relays. In general such relays are strategic deployed and its positioning yields some LoS towards the destination. Alternatively, in [23] successive relaying is introduced, thus at least two relays are needed and while one listens to the source broadcast the other forwards the message to destination. This technique does not suffer from multiplexing loss, however imposes the use of two or more relays besides the coordination among the cooperative parties. Therefore, it becomes disadvantageous in scenarios where there is a scarcity of resources or even in heavily loaded networks, where nodes are often busy such that cooperation may be not possible.

Another alternative to overcome the spectral inefficiency of HD cooperative protocols is at a cost of a return channel between nodes [6, 7, 58, 59], again such protocols are known as incremental. For instance, in our earlier works [58, 59] we investigate the combination of rate and power allocation techniques and the use of repetition and parallel coding with IDF protocol. The results show that there is trade-off between the resource allocation schemes and the Signal-to-Noise-Ratio (SNR), which means that one technique is favored over the other depending on SNR constraints. It is also shown that a simple repetition scheme becomes more suitable for practical purposes since it requires a simpler receiver than parallel coding methods with similar performance.

In this context, FD relaying appear as an interesting alternative once FD cooperative protocols do not suffer from multiplexing loss and achieve higher capacity than HD cooperative protocols [7, 8]. Hereafter, we focus on the FD relaying protocols and practical aspects of their implementations. The discussion drawn next serves as ground to the subsequent chapters, where a detailed

performance analysis is presented.

2.2 Full-duplex relaying

An ideal FD relay transmits and receives simultaneously, which considerably enhances performance of the relay channel [7, 8], such scenario is depicted in Fig. 3a. Throughout this thesis we assume that the relay is equipped with two distinct radio interfaces, such that transmission and reception are isolated from each other, and each has its own dedicated antenna, as illustrated in Fig. 3a. Notice that, in this case perfect isolation is assumed between transmit and receive antennas. Nevertheless, perfect isolation (ideal) between transmitted and received signals is not yet possible, and in fact it is a cumbersome task [25–28, 30–39]. Notice that in Fig. 3b the self-interference is represented by the dotted line in between the relay's antennas.

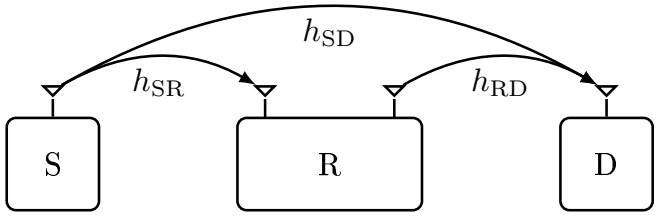

(a) Ideal FD Relay

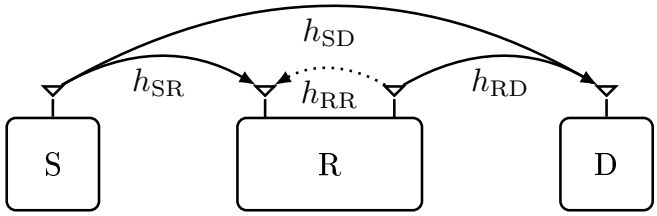

(b) FD Relay with Self Interference

Fig 3. In FD relaying transmission and reception occur simultaneously, therefore broadcast and cooperative (multiple access) phases are concurrent. Ideal relaying is not yet possible, therefore the FD relay experiences self-interference, which is denoted by the channel coefficient h_{RR} (dotted line).

2.2.1 Self-interference cancellation

Intuitively FD communication should be easily attainable given that the signals are known and all needed is extra circuitry to subtract it from the receiving end. However, in practice this assumption does not hold since the radios considerably distort the transmitted signal which appear due to the (non-)linearities of the radio circuitry and noise [25–28, 30–39].

Then, in order to tackle such strenuous task, practical FD schemes have been proposed such that the power leakage between transmitted and received signals, known as self-interference, is taken into account and several mitigation techniques have been proposed [25–28, 30–39]. Self-interference cancellation is the key enabler of FD communications, which allows to exploit the full potential of FD communications [30, 34].

We can classify the self-interference cancellation schemes in two large groups, as follows:

- **Passive techniques:** consists of antenna separation and also shielding the reception form the transmission at the FD radio. The main goal is to isolate and shield the reception from transmission.

- **Active techniques:** operate on analog and/or digital domain. The main objective in the analog domain is to suppress the self-interference in the analog receiver circuitry-chain before the Analog-to-Digital Converter (ADC). While in the digital domain, the goal is to cancel the self-interference after the ADC by resorting to sophisticated signal processing schemes.

Notice that there are many option and tradoffs involved in the design of the receiver chain in order to cope with the self-interference cancellation. To each solution there are advantages and downsides as well. For instance, in order to cope with non-idealities of the receiver-chain (such as distortions and phase-noise) an analog-domain signal processing circuit would be necessary, which becomes costly and cumbersome to implement. On the other hand, canceling the interfering transmit signal in the digital domain is facilitated by the use of sophisticated adaptive digital signal processing techniques. However, such techniques suffer from cancellation precision non-idealities in the analog domain (for instance, power amplifier distortions, phase-noise, quantization noise). Bering this in mind, we can classify the self-interference cancellation schemes is by defin-

ing two large groups with respect to the domain, thus

- **Analog Cancellation:** analog cancellation circuitry and/or analog signal processing.

- **Digital Cancellation:** sophisticated signal processing schemes.

In what follows we discuss some of the recent advances on active and passive. For instance, the issue of self-interference cancellation on FD radios is investigated through experimental results in [25, 26]. In [25] a practical FD system is proposed and it is shown that the self-interference can be attenuated by more than 39 dB through transmit and receive antenna separation. Later, in [26] the authors extend their initial results and show that attenuation levels up to 75 dB can be achieved.

Later, [33] presents a measurement-based study of the capabilities and limitations of key mechanisms for passive self-interference mitigation, showing that more than 70 dB of passive suppression can be achieved in certain environments. The authors also relate the antenna suppression with frequency selectivity of the residual self-interference signal which, by its turn, implicates in higher-order filters or per-subcarrier cancellation. In addition, [36] evaluates the impact of amplitude and phase errors on the estimation of self-interference. Thus, based on the Rician model introduced by [26], the authors analytically investigate the impact of LoS and non-LoS on the self-interference, showing that poor antenna isolation (*e.g.* larger LoS factor) is the bottleneck of self-interference cancellation.

The nonlinearities aspects of the transmitter and receiver chains are exploited in [37]. The authors focus on the nonlinear distortions occurring in the transmitter power amplifier and receiver chain, focusing as well on the dynamic range requirements of ADCs. Their results point out that the nonlinear distortion produced by the transmitter power amplifier and the quantization noise at ADCs become a great issue on a FD transceiver. Further, in [38] the authors focus on active self-interference cancellation. A detailed self-interference model is introduced, such model includes power amplifier nonlinear distortion as well as transmitter and receiver mixer amplitude and phase imbalances. In order to tackle the self-interference issue the authors propose a widely-linear digital self-interference cancellation process which outperforms current linear solutions and enables low-cost FD transceivers.

A summary of the recent advances on active and passive self-interference cancellation as well as a discussion of the role of FD radios in the upcoming generation of wireless technologies is provided in [30]. Similar investigations on hardware design and implementation are carried out also in [27, 28, 30–39] and similar conclusions are drawn. Further more, Table 1 summaries the recent advances on self-interference cancellation, and indicates the overall cancellation achieved and which technique is employed: analog (A), digital (D) or hybrid (H). Notice that hybrid cancellation employs both analog and digital cancellation.

Table 1. Summary of the recent advances on Self-Interference Cancellation for FD radios

	Self-Interference Cancellation		
Reference	**Solutions**	**Domain**	**Cancellation**
[34]	Characterization of analog interference mitigation schemes for compact FD radios, resorting to polarized antenna and self-tunable cancellation circuits.	A	75 dB
[31]	Experimental characterization of passive and active cancellation: antenna separation and digital cancellation.	D	60 dB
[35]	Characterization of digital interference cancellation accounting for non-linearities of power amplifier as well as I/Q imbalances. The desired signal is iteratively removed from the received one for more accurate channel estimation and cancellation.	D	75 dB

Continued on next page

Table 1, continued from previous page

	Self-Interference Cancellation		
References	**Solutions**	**Domain**	**Cancellation**
[25]	Measurement based characterization of passive and active cancellation schemes: antenna separation (20 and 40 cm), analog and digital cancellation.	H	80 dB
[26]	Measurement based characterization of the distribution of the self-interference. Self-interference is modeled as a Rician fading channel.	H	74 dB
[27, 28]	Characterization of passive and active cancellation schemes: analog and digital cancellation. Discussion on the use of FD radios on real-time feedback channels.	H	80 dB
[33]	Characterization of passive cancellation schemes through distinct antenna separation techniques, which are able to achieve 70 dB attenuation. Associated with digital cancellation the total average attenuation arrives to 95 dB.	H	95 dB
[92–96]	Precoding strategies for self-interference mitigation in single and multi-user scenarios.	D	

Continued on next page

Table 1, continued from previous page

References	Self-Interference Cancellation		
	Solutions	**Domain**	**Cancellation**
[38]	Introduces a detailed self-interference model, accounting for power amplifier nonlinear distortion as well as transmitter and receiver mixer amplitude and phase imbalances. Resorts to widely-linear digital self-interference cancellation process which enables low-cost FD transceivers.	D	–
[37]	Discuss the impact on FD transceiver performance due to nonlinear distortion at the transmitter power amplifier and receiver chain and on the dynamic range requirements of ADCs.	A	–

2.2.2 Performance analysis of FD schemes

Despite all the advances in interference attenuation and cancellation attained in the last few years, with current technology it is not possible to fully mitigate and reduce the self-interference to the noise floor level [26, 28, 30]. Nevertheless, whenever self-interference is attenuated, at levels around 70 dB, FD communication becomes feasible. The receiver is able to cope with the remaining of the self-interference, which is known as residual self-interference. Thus, even though experiencing residual self-interference, FD communication is achieved and its performance is evaluated for several scenarios depending on the residual self-interference levels, as we shall see in what follows.

Earlier works conjectured that the residual self-interference could be modeled as a RV [48, 97, 98], and later experimental results confirmed such assumption, as

pointed out in [26]. This model is quite intuitive and allows the analysis of many scenarios which can include the emulation of various (non-)LoS configurations [26, 46, 97]. Bearing this in mind, many works have carried out this assumption, of residual self-interference as a fading channel, and many techniques that deal with residual interference have been proposed [26, 40–42, 48, 99, 100]. Fig. 4 summarizes the current self-interference cancellation techniques. We divided the methods into two major categories: digital and analog cancellation. The intersection gives us the joint strategies, which present the best performance by suppressing self-interference up to 95 dB. Fig.4 also includes a third category which accounts for the residual self-interference, which appears as a result of analog and digital cancellation techniques. For instance, therein are the general fading models for residual self-interference.

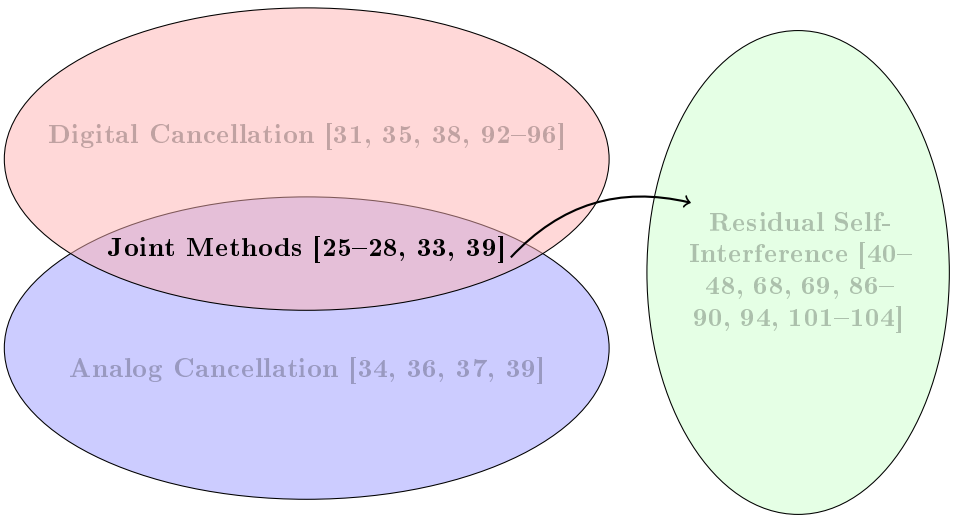

Fig 4. Overview of self-interference cancellation techniques for FD communications

Performance analysis of distinct FD protocols are also investigated in [32, 40, 42, 47, 97, 99, 100] as well as in [43–46, 68, 69, 74]. For instance, [99, 100] discuss the feasibility of full-duplex relaying as well as compare the performance of AF HD to its FD counterpart. Additionally, [43, 45] provide an extensive comparison between HD and FD schemes. The authors compare FD DF scheme to the state-of-the-art on HD DF relaying, which are the methods that associate

repetition coding with HARQ strategies [59]. Still, [32, 40, 74] deal with FD AF relaying, from performance analysis to power allocation and self-interference mitigation. For instance, [40] provides a performance analysis of a gain control scheme, which maximizes the Signal-to-Interference plus Noise Ratio (SINR) with reduced the transmit power. Then [74] shows that, when the direct link is accounted as a useful source of information rather than interference, performance enhances and that such scheme achieves diversity order of one. We recall that due to self-interference FD relaying suffers from zero diversity order. In order to tackle such issue the authors in [42] propose an hybrid relaying scheme, where the FD relay is able to switch modes from FD to HD given the network constraints. Extending this idea the authors in [102] consider also multiple FD relays under AF protocol, such that the best relay is opportunistically chosen to cooperate in either FD or HD fashion depending on some network constraints. In [101] the authors propose a self-interference cancellation scheme that allows FD relays to achieve diversity order greater than zero due to a block based relaying strategy, which brings time diversity enhancement over independent fading realizations.

Furthermore, in [97] all channels coefficients follow Rician distribution, while [46] models the residual self-interference, as well as all other channel coefficients, as Nakagami-m fading. Both works assess the impact of distinct channel parameters on the performance of a FD cooperative protocol.

Moreover, multiple antenna relaying settings are evaluated in [32, 41, 92, 94–96, 103–107]. Another application of FD relaying is in a multi-user MIMO setting, which is investigated in [92, 93], where Uplink (UL) and Downlink (DL) transmissions occur simultaneously and the authors rely on precoding schemes to enhance spectral efficiency and deal with the self-interference.

Furthermore, a network level analysis of FD communicating devices is performed in [68, 69] and it is shown that the self-interference dominates the aggregate interference component. Moreover, FD networks outperform HD networks in terms of both spectral efficiency and outage probability when self-interference is attenuated by more than 70 dB.

Next, Table 2 outlines on the performance analysis of FD schemes and also indicates fading models for the residual self-interference, as well as applications of FD communication to different scenarios.

Table 2. Performance analysis of FD schemes

Reference	Self-Interference Cancellation
[36]	Evaluates the impact of amplitude and phase errors on the estimation of self-interference. Based on the Rician model introduced by [26] the impact of LoS and non-LoS on the self-interference
[40, 42]	Performance analysis and power allocation strategies for FD relaying schemes. Introduces the idea of hybrid relays, which operate under FD or HD depending on system constraints.
[40, 42–45, 101]	Performance analysis, outage probability, as well as power allocation strategies for FD relaying schemes: AF, DF, hybrid relays and relay selection. Residual self-interference modeled as Rayleigh fading.
[43–45]	Outage probability and throughput analysis of FD relaying schemes. Residual self-interference modeled as Rayleigh fading. Energy efficiency assessment is provided in [45], while [44] investigates the use of FD femtocells as relays.
[46, 76, 97]	Modeling residual self-interference though general fading distributions, Rice and Nakagami-m.
[74, 86, 89, 102]	Performance analysis of FD AF relaying schemes. For instance, the issue of FD relay selection under AF protocol is investigated in [102].
[43, 45–47]	Performance analysis of FD DF relaying schemes. A selective DF scheme is introduced in [47], which is a sub-case of [43, 45].
[71, 75]	Assess outage probability and power allocation policies for underlay cognitive radio networks with FD relays.
[68, 69]	Assess spectral efficiency and outage probability in the network level of highly dense deployment of FD nodes.

Continued on next page

Table 2, continued from previous page

References	Self-Interference Cancellation
[30]	Comprehensive discussion on the applicability of self-interference cancellation schemes to future wireless networks.

All in all, one common conclusion amongst those works is that it is possible to achieve high performance even in the presence of strong self-interference [25–28, 30–39], which means that FD communication is feasible. All in all, given that the FD node is able to considerably attenuate the self-interference, so that FD communication becomes feasible. Therefore, the performance of different FD protocols can be evaluated.

In the following, we introduce the two FD protocols that will be evaluated under different scenarios in the next chapters.

2.3 Full-duplex relaying protocols

Here we introduce two FD relaying protocols namely Full-Duplex Multi-Hop (FDMH) and Full-Duplex Block Markov (FDBM) [7, 8, 77, 108]. These protocols were initially proposed for the relay channel with ideal FD relay [7, 8, 108]. We compare the FDMH scheme, which is the simplest relaying technique since it relies on the idea of multi-hopping, to FDBM, which is the best known performance achieving FD relaying method [7, 77, Ch. 15.7].

Both FDMH and FDBM operate under DF protocol [7, 77, 108]. The FD DF protocol can be decomposed into two channels: Broadcast Channel (BC) and Multiple-Access Channel (MAC), similarly to the HD case as discussed above. However, here the whole process occurs within one single time slot. In the first phase, namely broadcast phase, the source broadcasts its message to relay and destination. Differently from HD cooperative schemes, the multiple access phase starts simultaneously with the broadcast phase under the FD mode, in which the relay forwards the received message to the destination. Thus, we can write

the received signal at the relay as

$$y_{\mathrm{R}} = \sqrt{P_{\mathrm{S}}\, d_{\mathrm{SR}}^{-\nu}}\, h_{\mathrm{SR}}\, x + \sqrt{P_{\mathrm{R}}\, \delta}\, h_{\mathrm{RR}}\, \tilde{x} + w_{\mathrm{R}}, \tag{1}$$

while the received signal at the destination is

$$y_{\mathrm{D}} = \sqrt{P_{\mathrm{S}}\, d_{\mathrm{SR}}^{-\nu}}\, h_{\mathrm{SR}}\, x + \sqrt{P_{\mathrm{R}}\, d_{\mathrm{RD}}^{-\nu}}\, h_{\mathrm{RD}}\, \tilde{x} + w_{\mathrm{D}}, \tag{2}$$

where h_{ij}, $i \in \{\mathrm{S}, \mathrm{R}\}$ and $j \in \{\mathrm{R}, \mathrm{D}\}$, denotes fading channel coefficients, P_i is the transmit power, d_{ij} represents the distance between the nodes i and j, and $\nu \geq 2$ denotes the path loss exponent. Additionally, w_j is zero-mean complex Gaussian noise with unity variance ($\sigma_w^2 = 1$). In addition, x represents the unity energy transmitted symbol, while $\tilde{x}$ is the unity energy transmitted symbol re-encoded by the relay. It is noteworthy that x and $\tilde{x}$ are not necessarily identical once the relay may use a different codeword from the source.

2.3.1 The encoding/decoding process

The decoding and encoding schemes used in both protocols, FDMH and FDBM, were initially proposed in [108], and are extended to fading scenarios in [7, 45].

Both protocols rely on a combination of block Markov encoding at source and relay, associated with coding for cooperative multiple access channel and superposition coding [7, 108], which is also named as irregular encoding/successive decoding [7]. As pointed out in [7] the same achievable rates can be achieved through different strategies such as: regular encoding/sliding-window decoding [109]; and regular encoding/backward decoding [110].

Furthermore, those two strategies are more suitable for quasi-static fading channels, once they are less likely to fail in the intermediate decoding steps [7] when compared to irregular encoding/successive decoding proposed by [108]. Bearing this in mind, we adopt throughout this thesis regular encoding and backward decoding [7, 110, 111].

Thus, as proposed in [7, 110, 111], the message is divided into L blocks , as shown in Fig. 5. Moreover, $\tilde{x}$ is delayed compared to x [42, 108] such that $\tilde{x}[l] = x[l - \tau]$, where $1 \leq l \leq L$ and $\tau \geq 1$ represents the processing and delay. In order to facilitate to the reader and for easy comparison, we assume hereafter

that $\tau = 1$, which means that the message from the relay is only delayed by one block. Moreover, as pointed out in [42] this delay is large enough to guarantee that the simultaneously received signals are uncorrelated, and therefore can be jointly decoded.

In order to illustrate this processes Fig. 5 depicts the block transmission scheme with backward decoding where the message is divided into L blocks, notice that even though the relay is delayed by one block with respect to the source, performance is not affected for large L [47, 108].

A first analysis on such decoding schemes for practical FD relaying, accounting for the effects of residual self-interference, is done in [45]. Later, it is extended in [47], where the authors generalize the backward decoding scheme for any delay and number of blocks. Also it is shown that the performance is not affected for large L or as far the ratio between delay and the number of blocks is small.

2.3.2 Achievable rates of FD cooperative protocols

The overall achievable rate of the both protocols (FDMH and FDBM) is given as [7, 110, Sect. IV-B], [45, 47]

$$\mathcal{R}_{\mathrm{FD}} = \min\left\{\mathcal{R}_{\mathrm{BC}}\,,\,\mathcal{R}_{\mathrm{MAC}}\right\}, \tag{3}$$

where we assume regular encoding and backward decoding, and express (3) as a function of the achievable rates in each phase of the FD protocol: $\mathcal{R}_{\mathrm{BC}}$ for the BC; and $\mathcal{R}_{\mathrm{MAC}}$ for MAC.

First, the achievable rate of the BC phase is [7, 45, 47]

$$\mathcal{R}_{\mathrm{BC}} = \log_2\left(1 + (1-\rho^2)\,\frac{\gamma_{\mathrm{SR}}}{\gamma_{\mathrm{RR}}+1}\right) \tag{4}$$

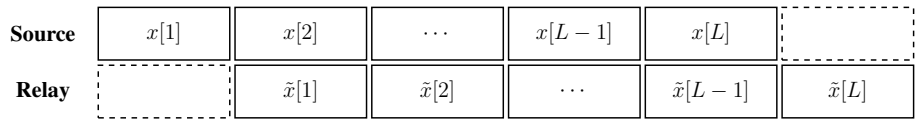

Fig 5. Source and relay block transmission. Notice that the frame is divided into L blocks and the relay's transmission is delayed by only one block ($\tau = 1$).

where $\gamma_{ij} \triangleq P_{\mathrm{i}} \, |h_{ij}|^2$ represents the SNR of the link between nodes i and j, and notice that γ_{RR} represents the SNR of the residual self-interference at the relay. Additionally, ρ represents the correlation coefficient between source and relay messages [108]. Notice that for the FDMH we assume independent codewords, therefore $\rho = 0$ and (4) reduces to $\mathcal{R}_{\mathrm{BC}} = \log_2 \left(1 + \frac{\gamma_{\mathrm{SR}}}{\gamma_{\mathrm{RR}}+1}\right)$.

The FDMH protocol is in essence a multi-hop protocol, and therefore, it is reasonable to assume that the direct link between source and destination (S-D) cannot be decoded, and instead such link is seen as additional interference at the destination. Then, the achievable rate of the MAC phase ($\mathcal{R}_{\mathrm{MAC}}$) is written as [43, 45]

$$\mathcal{R}_{\mathrm{MAC}}^{\mathrm{FDMH}} = \log_2 \left(1 + \frac{\gamma_{\mathrm{RD}}}{\gamma_{\mathrm{SD}} + 1}\right), \tag{5}$$

Differently from the FDMH protocol, in the FDBM case the S-D link is seen as useful information rather than interference, and therefore based on [7] the achievable rate is then given as

$$\mathcal{R}_{\mathrm{MAC}}^{\mathrm{FDBM}} = \log_2 \left(1 + P_{\mathrm{S}} \, |h_{\mathrm{SD}}|^2 + P_{\mathrm{R}} \, |h_{\mathrm{RD}}|^2 + 2\sqrt{P_{\mathrm{S}} \, P_{\mathrm{R}}} \, \mathrm{Re}(\rho \, h_{\mathrm{SD}} \, h_{\mathrm{RD}}^*)\right), \tag{6}$$

where $\mathrm{Re}(\cdot)$ denotes the real part of complex number and * represents the complex conjugate of x.

Herein, we introduced FD relaying protocols and we provide a general idea of their operation. Then, we will employ the concepts introduced above into different settings and scenarios in the following chapters.

2.4 Summary

In this chapter we briefly summarized some concepts of cooperative communications. As discussed above, through cooperation even single antenna devices can achieve spatial diversity by sharing resources. Therefore, cooperation comes as a promising alternative to boost performance of current and upcoming wireless networks. Cooperation becomes even more attractive in applications that are constrained, for instance, due to size and cost.

Moreover, herein we also discussed the advantages of FD relaying. We presented the key idea behind practical FD communication and challenges to

cope with self-interference. As discussed above, complete mitigation of self-interference is not possible, which results in residual self-interference. The residual self-interference can be modeled as a RV, which facilitates the performance evaluation of different FD networks. Finally, we outline the FD protocols that are evaluated throughout this thesis.

All in all, these concepts are relevant to understand our assumptions and developments in the next chapters, where we analyze in details the FD relaying schemes. It is important to note that our main results are enclosed from Chapter 3 to Chapter 5. In each of them, the network is modeled in order to capture the main mechanisms of the network. Hence, even though the similarities in the network modeling, each chapter is based on different assumptions that provide new insights, which are discussed therein.

3 Outage, throughput and energy efficiency analysis of some half and full duplex cooperative relaying schemes

3.1 Motivation and related work

Through cooperation among nodes even single antenna devices can achieve spatial diversity [6, 112, 113]. Moreover, cooperative protocols can operate either in a HD or FD fashion. As mentioned in Chapter 2 and investigated in [22, 24], HD cooperative protocols are spectrally inefficient, in the sense that two time slots are used to transmit a message from source to destination, whereas in the FD mode the relay simultaneously transmits and receives in the same frequency. However, "ideal FD operation", in which transmitted and received signals are perfectly isolated, is not possible. In practice, transmitted power is normally much larger than received power [7], which turns the isolation a difficult task. Non-cooperative and cooperative FD schemes where residual self-interference is assumed between the transmitted and received signals were investigated in [25, 26, 40, 48, 99, 100, 114]. For instance, in [99] it is shown that FD relaying with self-interference is feasible even if there is a strong power leakage between the transmitted and the received signals, and that FD relaying enhances capacity when compared to multi-hop HD relaying. Similar conclusions are obtained in [40, 48]. Additionally, such relaying schemes are of great interest of the industry [10, 34], for instance, in band FD operation is being investigated, for instance, since Release 10 of 3GPP [10] and [44] introduces a performance assessment of heterogeneous networks, where the legacy network is underlaid by FD femtocells.

Besides the boost in performance achieved through cooperation, cooperative diversity is seen as an energy efficient strategy since, for instance, a target Quality of Service (QoS) can be achieved with lower power consumption [6, 115]. Furthermore, in the recent years energy efficient wireless protocols have been focus of both academia and industry [10, 116–119]. The objective of power consumption analysis is to propose alternatives to extend the battery lifetime of mobile devices as well as to reduce carbon emissions, and reduce energy consump-

tion of the network as a whole [10, 116–119]. In [120–122] power consumption was analyzed for non-cooperative and cooperative networks. Moreover, the authors have accounted for different node densities and the circuitry consumption for transmitting and receiving data. In [120], the transmit power of the non-cooperative and the cooperative systems are considered to be fixed. Thus, the energy efficiency is maximized by the optimization of the packet length and the modulation order of each scheme. The performance analysis showed that the cooperative transmission outperforms the non-cooperative in terms of energy consumption when there is a great distance between the source and the destination. In [121], by establishing an acceptable limit for the packet loss, the transmit power is minimized based on the outage probability of each transmission scheme. The results show that the cooperative network can be more energy efficient than the non-cooperative network when source and destination are far apart. In [122], by defining an end-to-end throughput requirement, it is shown that incremental cooperation is more energy efficient than direct transmission and than multi-hop transmission, even at small transmission ranges. Moreover, in [123] energy efficiency analysis is carried out considering HD and FD multi-hop schemes in the Additive White Gaussian Noise (AWGN) relay channel. The results show that the HD multi-hop relay may require at least 50% more bandwidth than FD multi-hop relay with the same rate and power constraints.

In this chapter we analytically evaluate the outage, throughput and energy efficiency of cooperative FD relaying with interference under Rayleigh fading channel. Moreover, as previously discussed in Chapter 2, we adopt the Block Markov encoding at source and relay [7, 108]. We recall that, as seen in Chapter 2, the Block Markov encoding has the same achievable rates as regular encoding and backward decoding, which is also pointed out in [7]. While in [40, 48, 99] the authors consider multi-hop HD relaying, here we compare the performance of cooperative FD relaying to that of two incremental cooperative HD relaying methods: IRST transmission and SC [59]. In IRST the relay only cooperates if requested by the destination. Once requested, the relay sends additional parity bits, together with the source, by means of a space-time codeword, which is then appropriately combined by the destination with the first source transmission [59, 124–129]. By its turn, in SC, which is the simplest IDF scheme, the relay also cooperates only if requested. In such case the relay retransmits the source message (while the source is silent), and the destination applies SC

between the original source transmission and the relay retransmissions.

Other operation modes for HD relaying could be considered, but our choice for IRST and SC is justified by the fact that IRST is a very high performance due to accumulation of the achievable rate at a cost of strict synchronization. While SC is very simple and the worst performing HD scheme based on the DF protocol [59]. Therefore, we are able to compare FD relaying to a sample of the most complex and high performance HD schemes and to a sample of the most simple and less performing HD methods.

3.2 System model

Consider a system with three cooperating terminals as discussed in Chapter 2. Fig. 6 depicts the network under consideration, where we assume that all channels coefficients are subject to quasi-static Rayleigh fading. Moreover, we account for the self-interference (dotted line in Fig. 6). We model the self-interference channel also as Rayleigh fading, because we assume that this link is dominated by the scattering component of the channel. This is a reasonable assumption since the LoS component is considerably reduced by antenna isolation or represents a residual interference after the usage of an interference cancellation scheme [25, 26, 48]. In [25, 26] an experiment-driven analysis of FD wireless was carried out. The authors evaluate passive and active cancellation techniques and showed that self-interference can be attenuated up to 74 dB. However, such attenuation is not enough to bring the self-interference to the noise floor [26]. Additionally, we assume perfect Channel State Information (CSI) at the receivers. The chan-

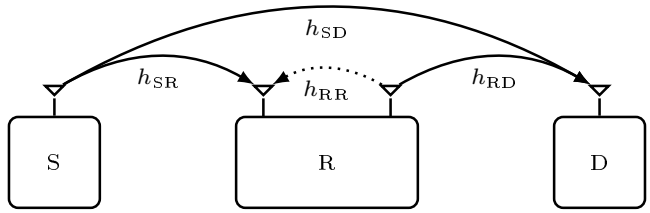

Fig 6. Three-node cooperative network: source (S), relay (R) and destination (D). Residual self-interference is present at the relay and represented by the dotted line. Notice that the direct link is also perceived at the destination.

nel noise is considered to be a complex AWGN with variance $N_0/2$ per dimension. Without loss of generality, we assume that the noise power is $N_0 = 1$. Moreover, we consider that the relay can operate either in FD or HD mode.

3.2.1 Full-duplex relaying

In the FD mode, the source broadcasts the message x, which is heard by both relay and destination (when the direct link exists). At the same time the relay sends a message $\tilde{x}$ to destination. Moreover, the transmission from the relay to destination interferes in its own reception of the message sent by the source. Following the above and as pointed out in Chapter 2, the received signals at the relay and at the destination can be written as:

$$y_{\mathrm{R}} = \sqrt{P_{\mathrm{S}}}\, h_{\mathrm{SR}}\, x + \sqrt{P_{\mathrm{R}}\delta} h_{\mathrm{RR}}\, \tilde{x} + w_{\mathrm{R}}, \tag{7}$$

$$y_{\mathrm{D}} = \sqrt{P_{\mathrm{R}}} h_{\mathrm{RD}}\, \tilde{x} + \sqrt{P_{\mathrm{S}}}\, h_{\mathrm{SD}}\, x + w_{\mathrm{D}}, \tag{8}$$

where h_{ij} are the complex fading channel coefficients with $i \in \{\mathrm{S}, \mathrm{R}\}$ and $j \in \{\mathrm{R}, \mathrm{D}\}$, where h_{RR} is the complex fading coefficient of the self-interference link [48]. The average transmit power at source and relay are P_{S} and P_{R} while w_{R} and w_{D} are the noise at relay and destination, $d_{ij}^{-\nu}$ is the path loss distance between nodes i and j with ν begin the path loss exponent. Notice that all channels are Rayleigh distributed where $\Omega \triangleq \Omega_{ij} \triangleq \mathrm{E}\left[|h_{ij}|^2\right] \triangleq d_{ij}^{-\nu}$ represents the corresponding average fading power. Again, notice that $\Omega_{\mathrm{RR}} \triangleq \mathrm{E}\left[|h_{\mathrm{RR}}|^2\right] \triangleq \delta$, where δ coefficient represents average strength of the residual self-interference cancellation, which encompass active and passive cancellation techniques [26, 30].

3.3 Half-duplex relaying

In the HD mode, the transmissions are orthogonal in time, and we assume the presence of a feedback channel, so that nodes use the incremental DF protocol. In the first time slot, the source broadcasts a message to relay and destination,

so that:

$$y_{\mathrm{R}} = \sqrt{P_{\mathrm{S}}}\, h_{\mathrm{SR}}\, x_{\mathrm{S}} + w_{\mathrm{R}}, \tag{9}$$

$$y_{\mathrm{D}} = \sqrt{P_{\mathrm{S}}}\, h_{\mathrm{SD}}\, x_{\mathrm{S}} + w_{\mathrm{D}}. \tag{10}$$

If an error is detected, destination requires a retransmission. Then, two cases are considered, depending if source and relay transmit concurrently in the second time slot or not. In case they do (the IRST method), then the relay cooperates with the source, and the received signal at destination given as:

$$y'_{\mathrm{D}} = \sqrt{P_{\mathrm{S}}}\, h_{\mathrm{SD}}\, x' + \sqrt{P_{\mathrm{R}}}\, h_{\mathrm{RD}}\, \tilde{x}' + w_{\mathrm{D}}, \tag{11}$$

where x' and $\tilde{x}'$ are symbols from a space-time codeword. The signals y'_{D} and y_{D} are combined at destination and a new decoding attempt is carried out. Then, in case the relay retransmits in the second slot while the source is silent (the SC method). Hence, $x' = 0$ and $\tilde{x}' = \tilde{x}$, the receiver applies SC between y'_{D} and y_{D}. For instance, an application of the SC in cooperative network under AF protocol is performed in [91].

3.4 Cooperative FD and HD schemes

In this section we introduce two FD relaying schemes: FDMH and FDBM. The latter is the best performance achieving FD relaying protocol [7] while the former is the simplest FD relaying protocol. Likewise, we also introduce two HD protocols: SC and IRST. The SC protocol is the simplest HD relaying protocol, only the transmission with the highest SNR is decoded at destination. On the other hand, the IRST protocol combines different (re-)transmissions which increases the overall mutual information.

3.4.1 Full-duplex multi hop (FDMH) relaying

The FDMH scheme is a simple multi-hop relaying protocol. We assume that destination sees the direct link as interference rather than useful information, which may represent a scenario where the destination is not as sophisticated as in the FDBM case. Bearing this in mind, we can white the SNR at the relay

and destination, respectively, as

$$\gamma_{\mathrm{R}} = \frac{|h_{\mathrm{SR}}|^2 \ P_{\mathrm{S}}}{|h_{\mathrm{RR}}|^2 \ P_{\mathrm{R}} + 1}, \tag{12}$$

$$\gamma_{\mathrm{D}} = \frac{|h_{\mathrm{RD}}|^2 \ P_{\mathrm{R}}}{|h_{\mathrm{SD}}|^2 P_{\mathrm{S}} \ + 1}, \tag{13}$$

where P_{S} and P_{R} represent the source and relay transmit power, respectively. Then, the mutual information of the source-relay and relay-destination links, respectively, are

$$\mathcal{I}_{\mathrm{SR}} = \log_2 (1 + \gamma_{\mathrm{R}}), \tag{14}$$

$$\mathcal{I}_{\mathrm{RD}} = \log_2 (1 + \gamma_{\mathrm{D}}), \tag{15}$$

Theorem 3.1. *Assuming that all RVs are independent, the overall outage probability of FDMH scheme is*

$$\mathcal{P}_{\mathrm{FDMH}} = 1 - \frac{\exp\left(-\dfrac{P_{\mathrm{R}}\,\Omega_{\mathrm{RD}}\left(2^{\mathcal{R}}-1\right) + P_{\mathrm{S}}\Omega_{\mathrm{SR}}\left(2^{\mathcal{R}}-1\right)}{P_{\mathrm{S}}\,\Omega_{\mathrm{SR}}\,P_{\mathrm{R}}\,\Omega_{\mathrm{RD}}}\right) P_{\mathrm{S}}\,\Omega_{\mathrm{SR}}\,P_{\mathrm{R}}\,\Omega_{\mathrm{RD}}}{\left(P_{\mathrm{R}}\,\Omega_{\mathrm{RD}} + (2^{\mathcal{R}}-1)P_{\mathrm{S}}\,\Omega_{\mathrm{SD}}\right)\left(P_{\mathrm{S}}\,\Omega_{\mathrm{SR}} + (2^{\mathcal{R}}-1)P_{\mathrm{R}}\ \Omega_{\mathrm{RR}}\right)}. \tag{16}$$

Proof. As in the HD multi-hop case [6] and assuming that all RVs are independent, an outage event occurs whenever the source-relay link is in outage or when the relay fails to transmit. Mathematically the outage is given as

$$\mathcal{P}_{\mathrm{FDMH}} = \mathcal{P}_{\mathrm{SR}} + (1 - \mathcal{P}_{\mathrm{SR}})\,\mathcal{P}_{\mathrm{RD}}, \tag{17}$$

$$= \Pr\left[\mathcal{I}_{\mathrm{SR}} < \mathcal{R}\right\} + \Pr\left[\mathcal{I}_{\mathrm{SR}} > \mathcal{R}\right] \Pr\left[\mathcal{I}_{\mathrm{RD}} < \mathcal{R}\right], \tag{18}$$

which allows us to write the overall outage probability as a function of the outage probabilities of the individual links, namely source-relay and relay-destination. □

Next, we assess the outage probability of the source-relay and relay-destination link through the next theorem.

Theorem 3.2. *Assuming independent and exponentially distributed RVs, the outage probability is*

$$\mathcal{P}_{\mathrm{ij}} = 1 - \frac{\exp\left(-\dfrac{2^{\mathcal{R}}-1}{P_i\,\Omega_{ij}\,\kappa}\right) P_i\,\Omega_{ij}}{P_i\,\Omega_{ij} + \dfrac{2^{\mathcal{R}}-1}{\kappa} P_k \Omega_{kj}}, \tag{19}$$

where $i \in \{\mathrm{S}\}$, $j \in \{\mathrm{R}\}$ *and* $k \in \{\mathrm{R}\}$ *for the source-relay link, while for the relay-destination link the indexes are* $i \in \{\mathrm{R}\}$, $j \in \{\mathrm{D}\}$ *and* $k \in \{\mathrm{S}\}$.

Proof. The proof follows as

$$\begin{aligned}
\mathcal{P}_{ij} &= \Pr\left[\mathcal{I}_{ij} < \mathcal{R}\right] \\
&= \Pr\left[\log_2\left(1 + \kappa\,\gamma_j\right) < \mathcal{R}\right], \qquad (20) \\
&= \Pr\left[\frac{\left|h_{ij}\right|^2\ P_i}{\left|h_{kj}\right|^2\ P_k + 1} < \frac{2^{\mathcal{R}}-1}{\kappa}\right]. \qquad (21)
\end{aligned}$$

Let us define define $X = \left|h_{ij}\right|^2\ P_i$ which is exponentially distributed and $Y = \left|h_{kj}\right|^2\ P_j + 1$ is mean shifted exponentially distributed. Then, we compute the distribution of $Z = \kappa\,X/Y$ [130, pg. 186] given by $f_Z(z) = \int_0^\infty y f_{X,Y}(yz, y)dy$, where $\kappa \neq 0$ is a scaling factor used to generalize the result. Once that this distribution is calculated, it is possible to compute the Cumulative Distribution Function (CDF), which fortunately has closed-form solution and is given as in (19). □

Then, from Theorem 3.2 and setting $\kappa = 1$ we obtain the outage probability of the source-relay link as

$$\mathcal{P}_{\mathrm{SR}} = 1 - \frac{\exp\left(-\frac{2^{\mathcal{R}}-1}{P_{\mathrm{S}}\,\Omega_{\mathrm{SR}}}\right) P_{\mathrm{S}}\,\Omega_{\mathrm{SR}}}{P_{\mathrm{S}}\,\Omega_{\mathrm{SR}} + (2^{\mathcal{R}}-1)\ P_{\mathrm{R}}\,\Omega_{\mathrm{RR}}}. \tag{22}$$

Likewise, the outage probability of the relay-destination link is given by:

$$\mathcal{P}_{\mathrm{RD}} = 1 - \frac{\exp\left(-\frac{2^{\mathcal{R}}-1}{\Omega_{\mathrm{RD}}\,P_{\mathrm{R}}}\right) P_{\mathrm{R}}\,\Omega_{\mathrm{RD}}}{P_{\mathrm{R}}\,\Omega_{\mathrm{RD}} + (2^{\mathcal{R}}-1)\ P_{\mathrm{S}}\,\Omega_{\mathrm{SD}}}. \tag{23}$$

Once the FDMH scheme suffers interference from the direct link as well as

self-interference, the outage probability is limited by a performance floor as the as the transmit power increases. Such performance floor is characterized in the following theorem.

Theorem 3.3. *Assuming $P_{\mathrm{S}} = P_{\mathrm{R}} = P$ and that $P \to \infty$, the performance floor of the FDMH protocol is*

$$\lim_{P\to\infty} \mathcal{P}_{\mathrm{FDMH}} = 1 - \frac{\Omega_{\mathrm{SR}}}{(\,\Omega_{\mathrm{SR}} + (2^{\mathcal{R}} - 1)\Omega_{\mathrm{RR}})} \frac{\Omega_{\mathrm{RD}}}{(\,\Omega_{\mathrm{RD}} + (2^{\mathcal{R}} - 1)\,\Omega_{\mathrm{SD}})} \tag{24}$$

Proof. The proof is straightforward from the properties of the limits and given that $\lim_{x\to\infty} \exp(-1/x) = 1$. □

Remark 3.1. *Note that even without self-interference, $\delta = 0$. Hence, $\Omega_{\mathrm{RR}} = 0$ and the performance floor does not tend to zero due to the interference from the direct link.*

Assuming a transmission rate of $\mathcal{R}$, the average spectral efficiency (information rate) seen at destination of the FDMH scheme is

$$\mathcal{T}_{\mathrm{FDMH}} = \mathcal{R}\,(1 - \mathcal{P}_{\mathrm{FDMH}})\,. \tag{25}$$

3.4.2 Full-duplex block Markov (FDBM) relaying

The capacity for the relay channel is still an open problem. In view of this unanswered issue, the best achievable rate known in the literature is attained when the Block Markov encoding technique is employed [8, 77, 97, 98, 108]. The Block Markov DF relaying scheme is based on the Block Markov encoding at source and relay, combined with superposition coding and coding for cooperative multiple access channel and random coding [77, Chap. 15] and also [7, 108]. Notice that a more detailed analysis on the decoding method and achievability can be found in [7, 8, 77, 108]. Additionally, for further analysis on ideal FDBM on Rayleigh fading channels, please refer to [7, 98].

As aforementioned, the achievable rate of FDBM is given by the minimum of the achievable rates of the source-relay link (BC) and of a MAC, which is composed of the concurrent transmissions from source and relay to destination

[7]. Thus,

$$\mathcal{I}_{\mathrm{FDBM}} = \min\left\{\mathcal{I}_{\mathrm{SR}}, \mathcal{I}_{\mathrm{MAC}}\right\}, \tag{26}$$

where the achievable rate $\mathcal{I}_{\mathrm{SR}}$ is given by [98]:

$$\mathcal{I}_{\mathrm{SR}} = \log_2\left(1 + \left(1-\rho^2\right)\gamma_{\mathrm{R}}\right), \tag{27}$$

while the variable ρ is the correlation coefficient between source and relay messages [7] and γ_{R} is the SINR given by

$$\gamma_{\mathrm{R}} = \frac{\left|h_{\mathrm{SR}}\right|^2 \ P_{\mathrm{S}}}{\left|h_{\mathrm{RR}}\right|^2 \ P_{\mathrm{R}} + 1} \tag{28}$$

Remark 3.2. *It is noteworthy that ρ can maximize the mutual information of the FDBM scheme [5]. Once we assume CSI only at the receivers, we consider that ρ is fixed for all fading states. Thus, under this simplifying assumption, ρ is designed to minimize the outage probability which leads to $\rho = 0$ as we discuss later in Section 3.7.*

We assume in γ_{R} that the residual self-interference is accounted for as an additional uncorrelated interference at the relay.

Remark 3.3. *As pointed out in [42] the delay between source and relay messages is large enough to guarantee that the simultaneously received signals at relay are uncorrelated, and therefore the residual self-interference is seen as interference (cf. Chapter 2). Moreover, the residual self-interference is the remaining interference after applying analog and digital cancellation. Thus, as experimental results indicate the residual self-interference can be modeled as an independent RV [26].*

The achievable rate in the MAC formed by relay-destination and source-destination links is [7, 97, 98]:

$$\mathcal{I}_{\mathrm{MAC}} = \log_2\left(1 + P_{\mathrm{S}}\ \left|h_{\mathrm{SD}}\right|^2 + P_{\mathrm{R}}\ \left|h_{\mathrm{RD}}\right|^2 + 2\sqrt{P_{\mathrm{S}}\ P_{\mathrm{R}}}\,\mathrm{Re}\left(\rho\, h_{\mathrm{SD}}\, h_{\mathrm{RD}}^*\right)\right). \tag{29}$$

Then, we know from Theorem 4.1 that the overall outage probability of FDBM

is given as

$$\mathcal{P}_{\mathrm{FDBM}} = \Pr\left[\min\left(\mathcal{I}_{\mathrm{SR}}\,,\,\mathcal{I}_{\mathrm{MAC}}\right) < \mathcal{R}\right], \tag{30}$$

$$= \mathcal{P}_{\mathrm{SR}} + \mathcal{P}_{\mathrm{MAC}} - \mathcal{P}_{\mathrm{SR}}\,\mathcal{P}_{\mathrm{MAC}}. \tag{31}$$

In order to find $\mathcal{P}_{\mathrm{FDBM}}$ we first develop the outage probability of the source-relay link, taking into account the effect of the self-interference. Then, by means of Theorem 3.2 and with $\kappa = 1-\rho^2$ the outage probability of the source-relay of the FDBM scheme is

$$\mathcal{P}_{\mathrm{SR}} = 1 - \frac{\exp\left(-\dfrac{2^{\mathcal{R}}-1}{P_{\mathrm{S}}\,\Omega_{\mathrm{SR}}\,(1-\rho^2)}\right) P_{\mathrm{S}}\,\Omega_{\mathrm{SR}}}{P_{\mathrm{S}}\,\Omega_{\mathrm{SR}} + \dfrac{2^{\mathcal{R}}-1}{1-\rho^2}\,P_{\mathrm{R}}\,\Omega_{\mathrm{RR}}}. \tag{32}$$

Theorem 3.4. *Assuming independent RVs and transmission rate $\mathcal{R}$, the outage probability of the MAC phase of FDBM protocol is*

$$\mathcal{P}_{\mathrm{MAC}} = 1 - \frac{\alpha\,\exp\left(-\dfrac{2^{\mathcal{R}}-1}{\alpha}\right) - \beta\,\exp\left(-\dfrac{2^{\mathcal{R}}-1}{\beta}\right)}{\alpha-\beta}, \tag{33}$$

where α and β are

$$\alpha = \frac{a}{2} + \sqrt{b}, \tag{34}$$

$$\beta = \frac{a}{2} - \sqrt{b}, \tag{35}$$

with

$$a = (P_{\mathrm{R}}\,\Omega_{\mathrm{RD}} + P_{\mathrm{S}}\,\Omega_{\mathrm{SD}}), \tag{36}$$

$$b = \frac{a^2}{4} - P_{\mathrm{S}}\,\Omega_{\mathrm{SD}}\,P_{\mathrm{R}}\,\Omega_{\mathrm{RD}}\,\left(1-\rho^2\right). \tag{37}$$

Proof. Please refer to [43, 45, 98]. Notice that the outage probability of the MAC phase of ideal FDBM was introduced in [98], in [43, 45] the authors extended this result to account for the effects of residual self-interference. □

Due to the presence of residual self-interference at the relay the FDBM pro-

tocol also presents a performance floor, which is given by the next theorem.

Theorem 3.5. *Assuming $P_{\mathrm{S}} = P_{\mathrm{R}} = P$ and that $P \to \infty$, the performance floor of the FDBM protocol is*

$$\lim_{P\to\infty} \mathcal{P}_{\mathrm{FDBM}} = \frac{\left(2^{\mathcal{R}} - 1\right) \Omega_{\mathrm{RR}}}{\left(2^{\mathcal{R}} - 1\right) \Omega_{\mathrm{RR}} + \Omega_{\mathrm{SR}} \left(1 - \rho^2\right)}. \tag{38}$$

Proof. Proof follows the rationale of Theorem 3.3. □

Remark 3.4. *Note that the performance floor increases with Ω_{RR} and $\mathcal{R}$. The existence of this floor limits the performance of FD relaying, making it possible for incremental HD relaying to outperform FDBM as we show and discuss in Section 3.7.*

Differently from the FDMH protocol, at high SNR regime, namely $P \to \infty$, the FDBM protocol does not present a performance floor as $\delta \to 0$, in other works, the better the isolation and interference cancellation at the FD node, the better the cooperative network performs. Assuming a transmission rate of $\mathcal{R}$, the average spectral efficiency (information rate) seen at destination of the FDBM scheme is

$$\mathcal{T}_{\mathrm{FDBM}} = \mathcal{R} \left(1 - \mathcal{P}_{\mathrm{FDBM}}\right). \tag{39}$$

Remark 3.5. *Differently from [98], here we investigate the effects of the residual self-interference on the FDBM protocol in terms of outage probability as well as throughput.*

3.4.3 Half-duplex relaying with selection combining

In the HD mode, the source broadcasts a message to relay and destination, then the relay forwards it to the destination. Recall that there is no self-interference in the HD mode, which can be also observed in (9) and (10).

The achievable rate of the source-destination link is $\mathcal{I}_{\mathrm{SD}} = \log_2(1 + \gamma_{\mathrm{SD}})$,

therefore the outage probability of the source-destination link can be written as

$$\mathcal{P}_{\mathrm{SD}} = \Pr\left[\mathcal{I}_{\mathrm{SD}} < \mathcal{R}\right] \tag{40}$$

$$= \Pr\left[\gamma_{\mathrm{SD}} < 2^{\mathcal{R}} - 1\right] \tag{41}$$

$$= 1 - \exp\left(\frac{1 - 2^{\mathcal{R}}}{P_{\mathrm{S}}\ \Omega_{\mathrm{SD}}}\right), \tag{42}$$

where the instantaneous SNR at the source-destination link is $\gamma_{\mathrm{SD}} = |h_{\mathrm{SD}}|^2\ P_{\mathrm{S}}$. Recall that γ_{SD} is exponentially distributed, then the outage probability of the source-destination link (assuming am attempted transmission rate $\mathcal{R}$) is attained from its CDF, which can be expressed as in (42).

Following the same rationale, we readily determine the outage probability of the source-relay and relay-destination links. Since the instantaneous SNR of both links also are exponentially distributed. Then, recall that the instantaneous SNR at the relay is $\gamma_{\mathrm{SR}} = |h_{\mathrm{SR}}|^2\ P_{\mathrm{S}}$ while at the destination is $\gamma_{\mathrm{RD}} = |h_{\mathrm{RD}}|^2\ P_{\mathrm{R}}$.

Next, we write the achievable rates of the source-relay and relay-destination links as $\mathcal{I}_{\mathrm{SR}} = \log_2(1 + \gamma_{\mathrm{SR}})$ and $\mathcal{I}_{\mathrm{RD}} = \log_2(1 + \gamma_{\mathrm{RD}})$, the outage probabilities in such links, $\mathcal{P}_{\mathrm{SR}}$ and $\mathcal{P}_{\mathrm{RD}}$, can be written just as above, but replacing Ω_{SD} by Ω_{SR} and Ω_{RD}, respectively, and P_{S} by P_{R} when appropriate.

In the case of SC, after the transmission from the source, the destination verifies if the message was correctly received or not. Suppose an error occurred, but the relay was able to decode the message. Then, the destination requests for a retransmission from the relay. Destination verifies the retransmitted frame received and if it is also in error a failure is declared. In other words, there was an outage and then the source proceeds with the next data frame.

Theorem 3.6. *The overall outage probability of the SC scheme is given by*

$$\mathcal{P}_{out}^{\mathrm{SC}} = \mathcal{P}_{\mathrm{SD}}\left(\mathcal{P}_{\mathrm{SR}} + (1 - \mathcal{P}_{\mathrm{SR}})\mathcal{P}_{\mathrm{RD}}\right). \tag{43}$$

Proof. Let us first define the outage probability of the SC after cooperation as

$$\mathcal{P}_{\mathrm{SC}} = \Pr\left\{\mathcal{I}_{\mathrm{SD}} < \mathcal{R},\ \mathcal{I}_{\mathrm{RD}} < \mathcal{R}\right\}, \tag{44}$$

$$= \mathcal{P}_{\mathrm{SD}} \cdot \mathcal{P}_{\mathrm{RD}}\,. \tag{45}$$

Since all RVs are independent and exponentially distributed (44) is expressed as

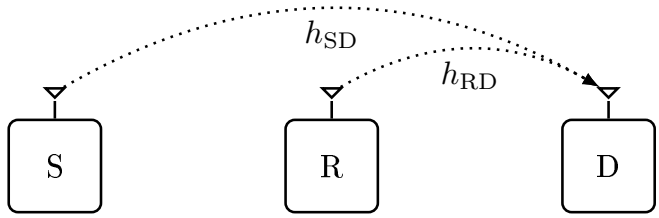

Fig 7. During the cooperative phase of the IRST protocol both source and relay synchronously retransmit. Thus, if a retransmission is requested by the destination, both source and relay send additional parity bits.

(45) [130]. Thus, an outage occurs if the source-destination link fails as shown in the first term or if the retransmission fails. Note that $\Pr\{\mathcal{I}_{\mathrm{SC}} < \mathcal{R} | \mathcal{I}_{\mathrm{SD}} < \mathcal{R}\} = \frac{\Pr\{\mathcal{I}_{\mathrm{SC}} < \mathcal{R}, \mathcal{I}_{\mathrm{SD}} < \mathcal{R}\}}{\Pr\{\mathcal{I}_{\mathrm{SD}} < \mathcal{R}\}} = \mathcal{P}_{\mathrm{RD}}$ is the probability that an error occurs after a retransmission from the relay, given that an error occurred after the transmission from the source. Bearing this in mind, we finally obtain (43). □

Given the outage probability of the SC scheme, the throughput is given as follows. The throughput of the SC method can be expressed as

$$\mathcal{T}_{\mathrm{SC}} = \mathcal{R}\,(1 - \mathcal{P}_{\mathrm{SD}}) + \frac{\mathcal{R}}{2} \cdot \mathcal{P}_{\mathrm{SD}} \cdot (1 - \mathcal{P}_{\mathrm{SR}}) \cdot (1 - \Pr\{\mathcal{I}_{\mathrm{SC}} < \mathcal{R} | \mathcal{I}_{\mathrm{SD}} < \mathcal{R}\}) \quad (46)$$

$$= \mathcal{R}\,(1 - \mathcal{P}_{\mathrm{SD}}) + \frac{\mathcal{R}}{2} \cdot \mathcal{P}_{\mathrm{SD}} \cdot (1 - \mathcal{P}_{\mathrm{SR}}) \cdot (1 - \mathcal{P}_{\mathrm{RD}})\,. \quad (47)$$

For the SC method the throughput notice that the first term in (47) comes from the direct transmission and destination can attempt to decode at rate $\mathcal{R}$. The second term comes from the cooperation from the relay. We recall that the factor $1/2$ appears due to the HD constraint since cooperation occurs in two time slots.

3.4.4 Incremental-redundancy space time (IRST) half-duplex relaying

In case of a requested retransmission, source and relay send additional parity bits (by means of a space-time codeword) which are then appropriately combined by the destination with the source's first transmission [59, 124–129]. Thus, different from the cooperative phase represented in Fig. 2b, in the IRST protocol both relay and source synchronously retransmit as depicted in Fig. 7. Thus, in case

of a retransmission the overall achievable rate seen at destination is [128]:

$$\mathcal{I}_{\mathrm{IRST}} = \log_2\left(1+\gamma_{\mathrm{SD}}\right) + \log_2\left(1+\gamma_{\mathrm{SD}}+\gamma_{\mathrm{RD}}\right). \tag{48}$$

Notice that the first term in (48) comes from first transmission, while the second term represents the synchronized transmission from source and relay.

It is noteworthy that if a retransmission is not required then $\mathcal{I}_{\mathrm{IRST}} = \log_2\left(1+\gamma_{\mathrm{SD}}\right)$ [126, 128]. Such case is also represented on the first term of the throughput in (57), as we shall discuss later herein.

Theorem 3.7. *Assuming exponentially distributed RVs and attempted transmission rate $\mathcal{R}$, the overall outage probability of the IRST schemes is*

$$\mathcal{P}_{out}^{\mathrm{IRST}} = \mathcal{P}_{\mathrm{SD}}\left(\mathcal{P}_{\mathrm{SR}} + \left(1-\mathcal{P}_{\mathrm{SR}}\right)\frac{\mathcal{P}_{\mathrm{IRST}}}{\mathcal{P}_{\mathrm{SD}}}\right), \tag{49}$$

where $\frac{\mathcal{P}_{\mathrm{IRST}}}{\mathcal{P}_{\mathrm{SD}}} = \mathcal{P}\left\{\mathcal{I}_{\mathrm{IRST}} < \mathcal{R} | \mathcal{I}_{\mathrm{SD}} < \mathcal{R}\right\}$ is the probability that an error occurs at destination after the IRST transmission from source and relay, given that an error occurred after the original source's transmission.

Proof. Let us first derive the outage probability of IRST, $\mathcal{P}_{\mathrm{IRST}} = \Pr[\mathcal{I}_{\mathrm{IRST}} < \mathcal{R}]$, given that the relay was able to decode the message from the source in the first transmission. Since γ_{SD} and γ_{RD} are independent and exponentially distributed, we can write

$$f_{\Gamma_{\mathrm{SD}},\Gamma_{\mathrm{RD}}}(\gamma_{\mathrm{SD}},\gamma_{\mathrm{RD}}) = \frac{1}{\bar{\gamma_{\mathrm{SD}}}\bar{\gamma_{\mathrm{RD}}}}\exp\left(-\left(\frac{\gamma_{\mathrm{SD}}}{\bar{\gamma_{\mathrm{SD}}}}+\frac{\gamma_{\mathrm{RD}}}{\bar{\gamma_{\mathrm{RD}}}}\right)\right) \tag{50}$$

where $\bar{\gamma_{\mathrm{SD}}} = P_{\mathrm{S}}\kappa_{\mathrm{SD}}\Omega_{\mathrm{SD}}$ and $\bar{\gamma_{\mathrm{RD}}} = P_{\mathrm{R}}\kappa_{\mathrm{RD}}\Omega_{\mathrm{RD}}$ are the mean values for the variables γ_{SD} and γ_{RD}, respectively. Now defining two new variables

$$Z_1 = \Gamma_{\mathrm{SD}} \tag{51}$$

$$Z_2 = (1+\Gamma_{\mathrm{SD}})(1+\Gamma_{\mathrm{SD}}+\Gamma_{\mathrm{RD}}) \tag{52}$$

Then applying the traditional methodology of changing of variables [130], it is possible to compute the Jacobian of this transformation as $J = 1+z_1$. With

this transformation, we can write

$$f_{Z_1,Z_2}(z_1,z_2)=\frac{1}{1+z_1}f_{\Gamma_{\rm SD},\Gamma_{\rm RD}}\left(z_1,\frac{z_2}{1+z_1}-1-z_1\right) \tag{53}$$

Note that the support now has changed from $(0\leq\Gamma_{\rm SD}<\infty,\,0\leq\Gamma_{\rm RD}<\infty\,)$ to $(0\leq Z_1<\infty)$, $((1+Z_1)^2\leq Z_2\leq\infty\,)$. With this in mind, it is possible to write the Probability Distribution Function (PDF) of the target variable, Z_2, as

$$f_{Z_2}(z_2)=\int_0^{\sqrt{z_2}-1}f_{Z_1,Z_2}(z_1,z_2)dz_1 \tag{54}$$

and finally

$$\mathcal{P}_{\rm IRST}=\int_1^{2^{\mathcal{R}}}f_{Z_2}(z_2)dz_2 \tag{55}$$

resulting in the final expression as

$$\mathcal{P}_{\rm IRST}=\frac{1}{\bar{\gamma_{\rm RD}}\bar{\gamma_{\rm SD}}}\int_1^{2^{\mathcal{R}}}\int_0^{\sqrt{z_2}-1}\frac{e^{-\frac{z_2}{\bar{\gamma_{\rm RD}}(z_1+1)}+\frac{z_1+1}{\bar{\gamma_{\rm RD}}}-\frac{z_1}{\bar{\gamma_{\rm SD}}}}}{z_1+1}dz_1dz_2. \tag{56}$$

It is important to note that $\Pr\left[\mathcal{I}_{\rm SD}<\mathcal{R},\mathcal{I}_{\rm IRST}<\mathcal{R}\right]=\Pr\left[\mathcal{I}_{\rm IRST}<\mathcal{R}\right]$, since if $\mathcal{I}_{\rm IRST}<\mathcal{R}$ then $\mathcal{I}_{\rm SD}<\mathcal{R}$ as $\mathcal{I}_{\rm IRST}\geq\mathcal{I}_{\rm SD}$. Therefore, $\Pr\left[\mathcal{I}_{\rm IRST}<\mathcal{R}|\mathcal{I}_{\rm SD}<\mathcal{R}\right]=\frac{\Pr[\mathcal{I}_{\rm IRST}<\mathcal{R}]}{\Pr[\mathcal{I}_{\rm SD}<\mathcal{R}]}$. Finally, once (56) is attained, the overall outage probability of IRST scheme is attained as in (49). □

Given a attempt transmit rate $\mathcal{R}$, the throughput of the IRST scheme is

$$\mathcal{T}_{\rm IRST}=\mathcal{R}\left(1-\mathcal{P}_{\rm SD}\right)+\frac{\mathcal{R}}{2}\mathcal{P}_{\rm SD}\,\left(1-\mathcal{P}_{\rm SR}\right)\left(1-\frac{\mathcal{P}_{\rm IRST}}{\mathcal{P}_{\rm SD}}\right). \tag{57}$$

3.5 Energy efficiency analysis

Energy efficiency has been one of the major concerns in the recent years in both academia and industry, since wireless communication networks have been growing rapidly and requiring large number base stations and small cells in order to attend the ever-increasing data demands [116–119]. Therefore, energy consumption is a global issue due to the increased amount of carbon emissions [118, 119]. Therefore, energy efficient solutions, such as the ability to shut down

infrastructure nodes or adaptive transmission strategy according to the traffic, will lead to green wireless communications. Such solutions will help not only operators (due to reduction on the operational costs, for instance) and users (longer battery life), but the environment as a whole.

Therefore, in this section we focus on the energy efficiency of some wireless cooperative schemes. For that sake, we define the total energy consumption per bit of each scheme, which takes into account the required power for the transmission, the power consumption of the RF circuitry, and the bit rate. According to [119, 131, 132] the energy consumption of the RF circuitry is much larger than the baseband processing consumption. Thus, we have ignored the baseband processing consumption in the subsequent analysis.

We considered the same RF circuitry model introduced in [133], as shown in Figure 8. Thus, we account for the following blocks at the transmitter: Digital-to-Analog Converter (DAC), mixer, transmit filters and frequency synthesizer, whose power consumptions are respectively given by P_{DAC}, P_{mix}, P_{fil_tx} and P_{syn}. Thus, the consumed power of the transmit hardware is given by $P_{\mathrm{TX}} = P_{\mathrm{DAC}} + P_{mix} + P_{fil\_tx} + P_{syn}$. Given that and the power consumption estimated values presented in [133], we attain $P_{\mathrm{TX}} = 97.9$ mW. Moreover, at the receiver side, also according to [133], we consider the following blocks: frequency synthesizer, Low-Noise Amplifier (LNA), mixer, Intermediate Frequency

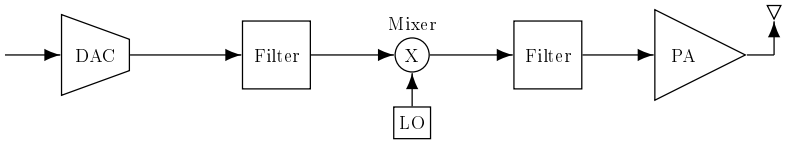

(a) Transmitter: analog circuit blocks

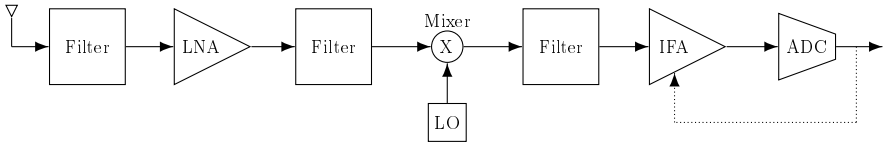

(b) Transmitter: analog circuit blocks

Fig 8. Transmitter and receiver analog circuit blocks. Notice that in the transmitter (a) we account for DAC, mixer, transmit filters and frequency synthesizer. While at the reception side (b) we have the reception filters, LNA, mixer, frequency synthesizer, IFA and ADC.

Amplifier (IFA), receive filters and ADC, whose power consumptions are respectively given by P_{syn}, P_{LNA}, P_{mix}, P_{IFA}, P_{fil_rx} and P_{ADC}. Thus, $P_{\mathrm{RX}} = P_{syn} + P_{\mathrm{LNA}} + P_{mix} + P_{\mathrm{IFA}} + P_{fil\_rx} + P_{\mathrm{ADC}}$. Based on the power consumption values presented in [133], we calculate the receiver circuitry (namely) consumption as $P_{\mathrm{RX}} = 112.2$ mW and we assume a drain efficiency of $\eta = 0.35$, which is within the range of a power amplifier that operates under M-QAM modulation as pointed out in [133]

In what follows, we determine the total consumed energy per bit of the direct scheme as:

$$\mathcal{E}_{dir} = \frac{P_{\mathrm{AMP,S}} + P_{\mathrm{TX}} + P_{\mathrm{RX}}}{\mathcal{R}}, \tag{58}$$

where $P_{\mathrm{AMP,S}} = P_{\mathrm{S}}/\eta$ is the power amplifier consumption for the source transmission, η is the drain efficiency of the power amplifier, P_{TX} and P_{RX} are the power consumed by the internal circuitry for transmitting and receiving, respectively.

In the case of the HD incremental cooperative schemes, the total consumed energy per bit depends on the outage probability on the source-destination and source-relay links:

$$\mathcal{E}_{\mathrm{HD}} = \frac{P_{\mathrm{AMP,S}} + P_{\mathrm{TX}} + 2P_{\mathrm{RX}}}{\mathcal{R}} + \mathcal{P}_{\mathrm{SD}} \cdot (1 - \mathcal{P}_{\mathrm{SR}}) \cdot \Omega, \tag{59}$$

The first term in (59) corresponds to the consumed energy if destination could decode the packet correctly in the first time slot, then no retransmission is required. The second term in (59) corresponds to the consumed energy when the relay cooperates. In the case of the SC scheme, as only the relay transmits in the second time slot, then $\Omega = \frac{P_{\mathrm{AMP,S}} + P_{\mathrm{TX}} + P_{\mathrm{RX}}}{\mathcal{R}}$, where $P_{\mathrm{AMP,S}} = P_{\mathrm{R}}/\eta$. On the other hand, in the IRST scheme both source and relay transmit in the second time slot, so that $\Omega = \frac{P_{\mathrm{AMP,S}} + P_{\mathrm{AMP,S}} + 2P_{\mathrm{TX}} + P_{\mathrm{RX}}}{\mathcal{R}}$. The additional power consumption of the retransmission request messages is negligible, as shown in [122], and therefore is not considered here.

In the case of FD relaying, the total consumed energy per bit depends on the outage probability of the source-relay link, and it is given by:

$$\mathcal{E}_{\mathrm{FD}} = \frac{P_{\mathrm{AMP,S}} + P_{\mathrm{TX}} + 2P_{\mathrm{RX}}}{\mathcal{R}} + (1 - \mathcal{P}_{SR}) \cdot \frac{P_{\mathrm{AMP,S}} + P_{\mathrm{TX}}}{\mathcal{R}}. \tag{60}$$

Notice that the first term in (60) corresponds to the transmission from the source, which is heard by both relay and destination. The second term in (60) refers to the transmission from the relay. It is relevant to note that (60) depends only on the outage probability of the source-relay link once the relay is always overhearing source's transmissions, and that the relay only cooperates if it was able to decode the message from the source. It is also important to note that in the presence of self-interference, the outage in the source-relay link in FD relaying is higher than the outage in the source-relay link in HD relaying.

3.6 Power and rate allocation

Now, we investigate the power and rate allocation between source and relay in order to establish a performance benchmark. The choice of power and rate is such that maximizes the throughput. Thus, we formalize the problem as:

$$\begin{aligned} \max_{\mathcal{R}, P_{\mathrm{S}}^{\star}} \quad & \mathcal{T} \\ \text{subject to} \quad & P_{\mathrm{S}}^{\star} + P_{\mathrm{R}}^{\star} \leq 2P \\ & \mathcal{R}_{min} \leq \mathcal{R} \leq \mathcal{R}_{max} \end{aligned} \tag{61}$$

where $\mathcal{T}$ can be $\mathcal{T}_{\mathrm{FDMH}}$, $\mathcal{T}_{\mathrm{FDBM}}$, $\mathcal{T}_{\mathrm{IRST}}$ or $\mathcal{T}_{\mathrm{dir}}$, and P is the used power for direct transmission. The maximization can be performed with respect to $\mathcal{R}$ and $P_{\mathrm{S}}^{\star}$.

Since our goal is to compare the different HD and FD schemes, we do not focus on the proposal of particular Power Allocation (PA) and Rate Allocation (RA) solutions, but we resort to numerically efficient algorithms. Moreover, performing a closed form analysis of these equations is not possible since the equations are not jointly concave for all variables [134, 135]. Nevertheless, we recall that a local maximum can be found by constraining the equation to a particular interval of interest. Moreover, several efficient numerical solutions exist for such classical constrained nonlinear optimization problem [134–136]. For instance, we run a Sequential Quadratic Programming (SQP) method [136] using MATLAB. Further, for the RA analysis we considered that $\mathcal{R}$ could vary from $\mathcal{R}_{min} = 1$ bits/s/Hz to $\mathcal{R}_{max} = 10$ bits/s/Hz. Such values where arbitrarily set; however, those values reflect a practical operational rate range in current cellular standards such as [137].

Thus, at each SNR value we numerically determine the attempted rate $\mathcal{R}$ which maximizes the throughput. Additionally, for PA we determine the values of $P_{\mathrm{S}}^{\star}$, and therefore $P_{\mathrm{R}}^{\star}$. Notice that we opt for a sum power constraint, and therefore we assume $P_{\mathrm{S}}^{\star} + P_{\mathrm{R}}^{\star} = 2\,P$. Hence, all schemes under analysis have the same power budget, which facilitates the comparison among methods. We recall that such an assumption is commonly used in the literature, see for instance [104, 138]. Then, the two parameters ($P_{\mathrm{S}}^{\star}$, and $\mathcal{R}$) are jointly numerically optimized.

3.7 Numerical results

Next we investigate the outage, throughput and energy efficiency of FDMH, FDBM, IRST and SC. But first let us assume a log-distance path loss model such that $d_{ij}^{-\nu}$, where the decay exponent is $\nu = 4$ and d_{ij} is the distance between nodes i and j. Moreover, we normalize the distance between source and destination to one and we suppose that the relay is positioned in the middle of such straight line between source and destination, thus $d_{\mathrm{RD}} = 1 - d_{\mathrm{SR}}$.For simplicity and easy of comparison among the methods under analysis, we assume equal power allocation at source and relay, thus $P_{\mathrm{S}} = P_{\mathrm{R}}$.

Based on [48], we consider two levels of self-interference: the ideal case, in which $\Omega_{\mathrm{RR}} = 0$ ($-\infty$ dB); and the more practical case of $\Omega_{\mathrm{RR}} = -8$ dB. Notice that henceforth these assumptions hold for all numerical results unless stated otherwise.

Fig. 9.a) presents the outage probability as a function of $\overline{\gamma}_{\mathrm{SD}} = \frac{P_{\mathrm{S}}}{N_0} = P_{\mathrm{S}}$, when $\mathcal{R} = 2$ bits/s/Hz, $d_{\mathrm{SR}} = 0.5$ and $\rho = 0$. We can notice that IRST outperforms the other methods. For FD relaying the performance decreases significantly with the increase of the self-interference. In Fig. 9.b) we consider a similar scenario, but when $\mathcal{R} = 8$ bits/s/Hz and $\rho = 0$, where we can see that IRST increases its advantage over the other schemes with the increase in the attempted rate. Therefore, at least in terms of outage probability, HD is considerably superior than FD relaying. That is reasonable since in FD mode destination sees a superposition of source and relay signals, which increases the error probability at destination. Moreover, it is clear that the self-interference results in a floor in the outage of FDBM, compromising the performance.

In order to show the impact of ρ, Fig. 10 shows the outage probability versus ρ for different relay positions d_{SR}. We assume that $\gamma_{\mathrm{SD}} = 0$ dB (black curves)

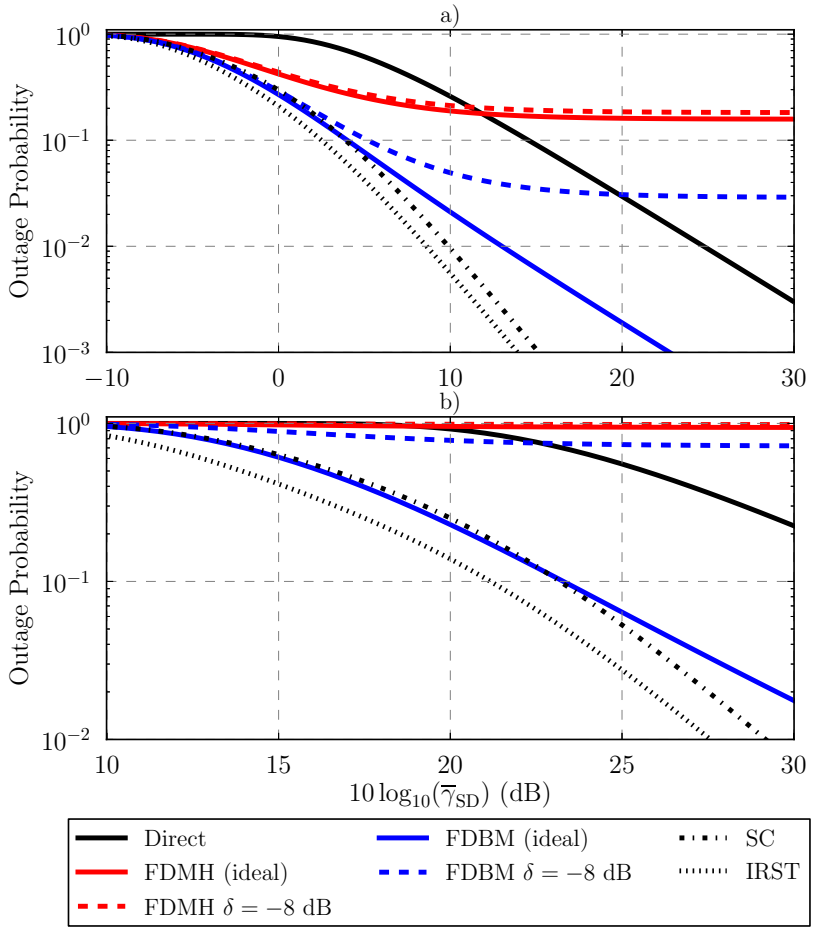

Fig 9. Outage probability as a function of the SNR $\overline{\gamma}_{\mathrm{SD}} = \frac{P_{\mathrm{S}}}{N_0} = P_{\mathrm{S}}$ for $d_{\mathrm{SR}} = 0.5$, $\rho = 0$, and a) $\mathcal{R}$ =2 bits/s/Hz and b) $\mathcal{R}$ =8 bits/s/Hz. We compare ideal FD relaying to practical FD relaying as well as to HD schemes, direct transmission is shown as reference. Modified from [45] © John Wiley & Sons 2015.

or $\gamma_{\mathrm{SD}} = 10$ dB (blue curves), and that $d_{\mathrm{SR}} \in \{1/3, 1/2, 2/3\}$. Notice that in this case $\rho = 0$ turns out to be the best choice. Therefore, next we assume that the correlation coefficient of the FDBM scheme is null ($\rho = 0$), which turns the FDBM scheme into a joint decoding method (at the destination). Additionally, a similar result, showing that $\rho = 0$ might be the optimum choice, was presented in [98, Figure 4], in a different context.

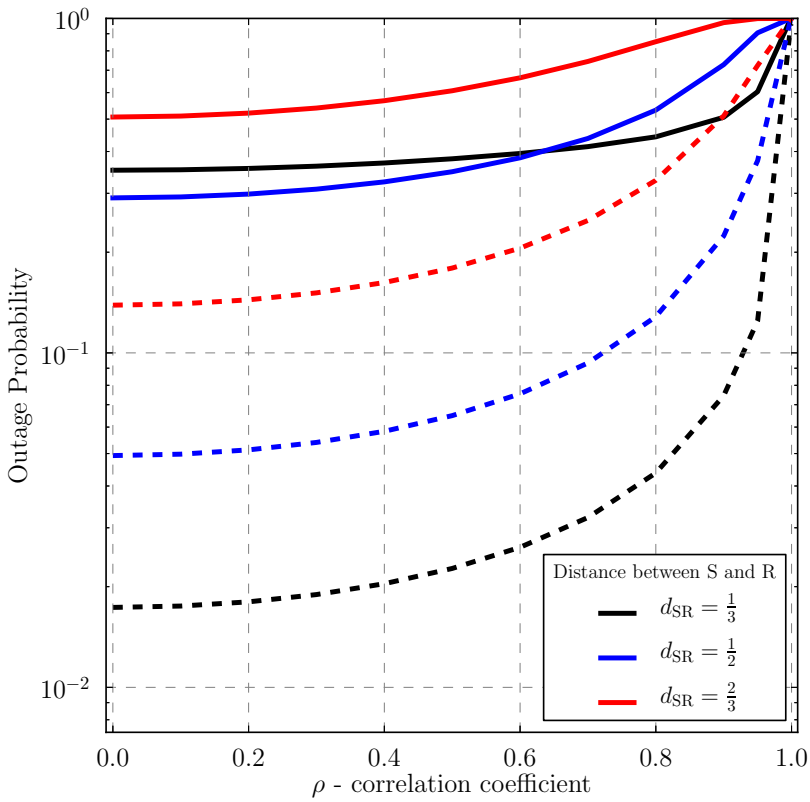

Fig 10. Outage versus ρ for $\gamma_{SD} = 0$ dB (solid line) or $\gamma_{SD} = 10$ dB (dashed line), and that $d_{SR} \in \{1/3, 1/2, 2/3\}$, for an ideal FD relay and for the case of a FD relay with self-interference. Modified from [45] © John Wiley & Sons 2015.

When the throughput is the metric to be considered, as shown in Fig. 11, we can see that FDBM can considerably outperform the other methods[3]. However, for higher values of $\mathcal{R}$ and for practical values of the self-interference the performance of FDBM considerably decreases. For $\mathcal{R} = 8$ bits/s/Hz and $\Omega_{RR} = -8$ dB, IRST, SC and even the direct transmission can outperform FDBM in terms of throughput. Moreover, we can note that in terms of throughput the simple SC scheme performs very close to IRST. In Fig. 12 we investigate the throughput as a function of $\mathcal{R}$, considering fixed SNR values of $\overline{\gamma}_{SD} = 0$ dB and $\overline{\gamma}_{SD} = 15$

[3] The throughput of a single direct (non-cooperative) transmission is defined as $\mathcal{T}_{dir} = \mathcal{R}(1 - \mathcal{P}_{SD})$.

dB. In the case of a low SNR as in Fig 12.a), FD relaying is a better option even with self-interference. However, in the case of a higher SNR as in Fig 12.b) this is not true, as FDBM with self-interference is outperformed by IRST and SC for many attempted rates $\mathcal{R}$. The reason for this reduced performance of FDBM is that the self-interference results in a floor in the outage of FDBM, which gets close to one as $\mathcal{R}$ grows.

We can clearly see from the above results that there are values of SNR and $\mathcal{R}$ for which FD relaying considerably outperforms the HD strategies while, by its turn, in some cases HD relaying becomes much more attractive. Therefore, an interesting approach to increase the performance of cooperative systems would be to adopt a hybrid strategy in which the nodes would be able to shift between FD and HD mode according to its operating region.

3.7.1 Energy efficiency

In order to analyse the trade-off between throughput gains and energy consumption, we normalize the throughput by the total energy consumed. The normalized throughput, given in b/s/Hz/J, is shown in Fig. 13 for $\mathcal{R} = 2$ bits/s/Hz and $\mathcal{R} = 8$ bits/s/Hz. Assuming that both source and relay are using the same power, i.e., $P_{\mathrm{S}} = P_{\mathrm{R}}$ and also the same rate, Fig. 13 show that the ideal FDBM scheme in general outperforms the other strategies, with an exception to the IRST scheme which outperforms FDBM in the low SNR region and with a high rate (Fig. 13-*b*)). However, recall that in practice it is still not possible to achieve the performance of ideal FDBM, due to the presence of the self-interference. By its turn, the practical FDBM scheme (with self-interference) is considerably outperformed by both HD relaying schemes for a high rate in the whole SNR range (Fig. 13-*b*)), while in the case of a low attempted rate (Fig. 13-*a*)) it performs better than the HD schemes. Therefore, for high attempted rates it may be considerably more efficient to use HD incremental relaying than FD relaying.

In Fig. 14-*a*) we analyze the trade-off between throughput and power consumption as a function of $\mathcal{R}$ when $\overline{\gamma}_{\mathrm{SD}} = 0$ dB. From the figure we can conclude that for such a low SNR value the FDBM scheme considerably outperforms HD relaying in case of attempted rates up to 4 bits/s/Hz, even in the presence of an strong self-interference signal. On the other hand, at higher attempted information rates the IRST scheme becomes advantageous when compared to the

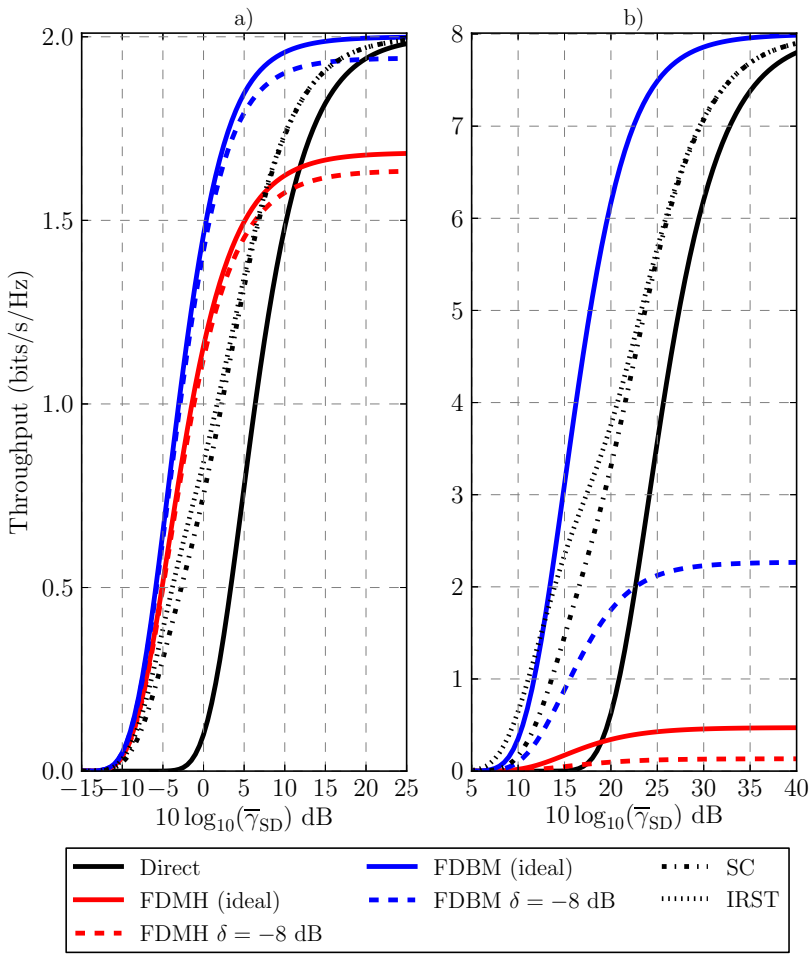

Fig 11. Throughput (bits/s/Hz) as a function of $\overline{\gamma}_{SD}$ for *a)* $\mathcal{R}$ **=2 bits/s/Hz and** *b)* $\mathcal{R}$ **=8 bits/s/Hz. Modified from [45] © John Wiley & Sons 2015.**

FDBM strategy, once the HD schemes has much lower outage probabilities at such high information rates. By its turn, when $\overline{\gamma}_{SD} = 15$ dB (Fig. 14-*b*)), the conclusions are significantly different as shown in Fig.14. At this higher SNR value, the direct transmission presents itself as a better option for attempted rates up to 4 bits/s/Hz, as retransmissions are rarely required. In case of higher attempted information rates the HD schemes considerably outperform FDBM and the direct transmission. Our analysis shows that FD relaying is feasible and

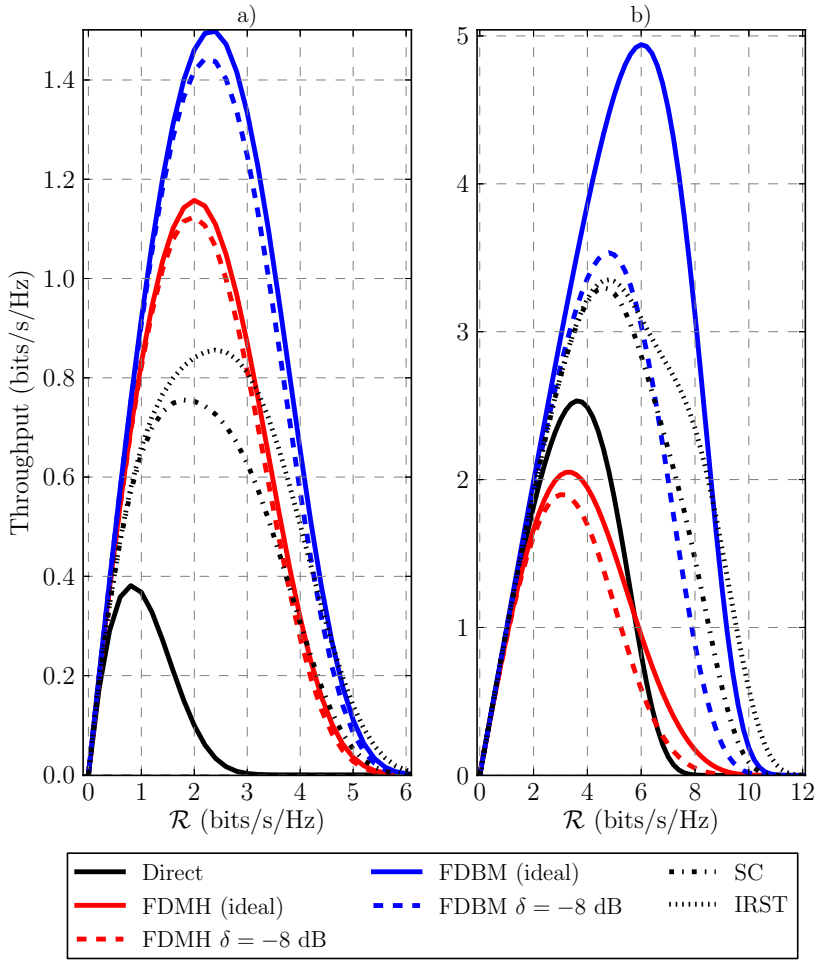

Fig 12. Throughput (bits/s/Hz) as a function of the target transmission rate $\mathcal{R}$, for HD and FD schemes when *a)* $\overline{\gamma}_{\mathrm{SD}} = 0$ **dB and** *b)* $\overline{\gamma}_{\mathrm{SD}} = 15$ **dB. Modified from [45] © John Wiley & Sons 2015.**

it is a good approach at low SNR and/or low information rate regions. By its turn, HD schemes become a more interesting strategy at high-SNR and high information rate regions.

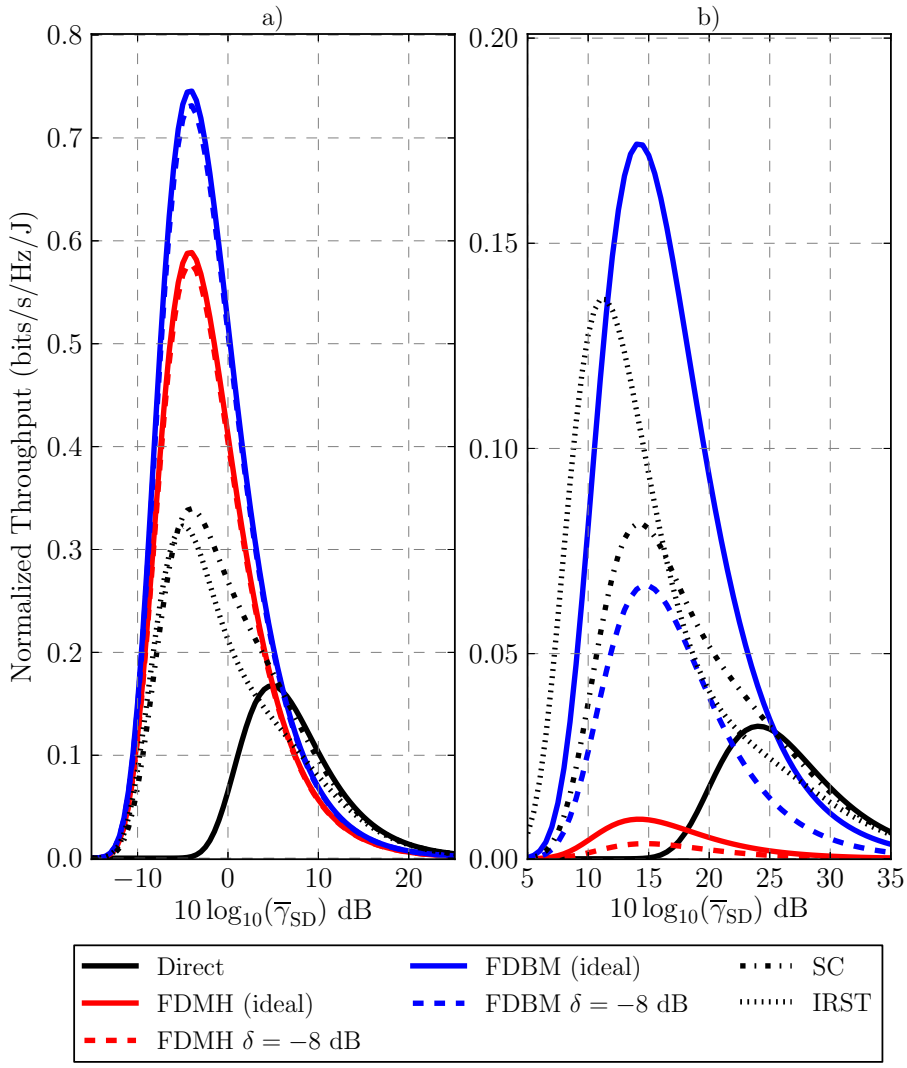

Fig 13. Normalized throughput (bits/s/Hz/J) versus $\overline{\gamma}_{\mathrm{SD}}$ for: *a)* $\mathcal{R}$ **=2 bits/s/Hz and** *b)* $\mathcal{R}$ **=8 bits/s/Hz; and under equal power allocation. Modified from [45] © John Wiley & Sons 2015.**

3.7.2 Joint allocation and energy efficiency

Fig. 15 shows the throughput with PA and RA as a function of the SNR. From the figure we can see that the ideal FDBM relaying outperforms IRST. Nevertheless, when we consider the self-interference, the performance of IRST becomes very competitive, specially from the mid to high SNR region. Note that at high spectral efficiency or $\Omega_{\mathrm{RR}} \neq 0$ dB the outage probability of the FDMH

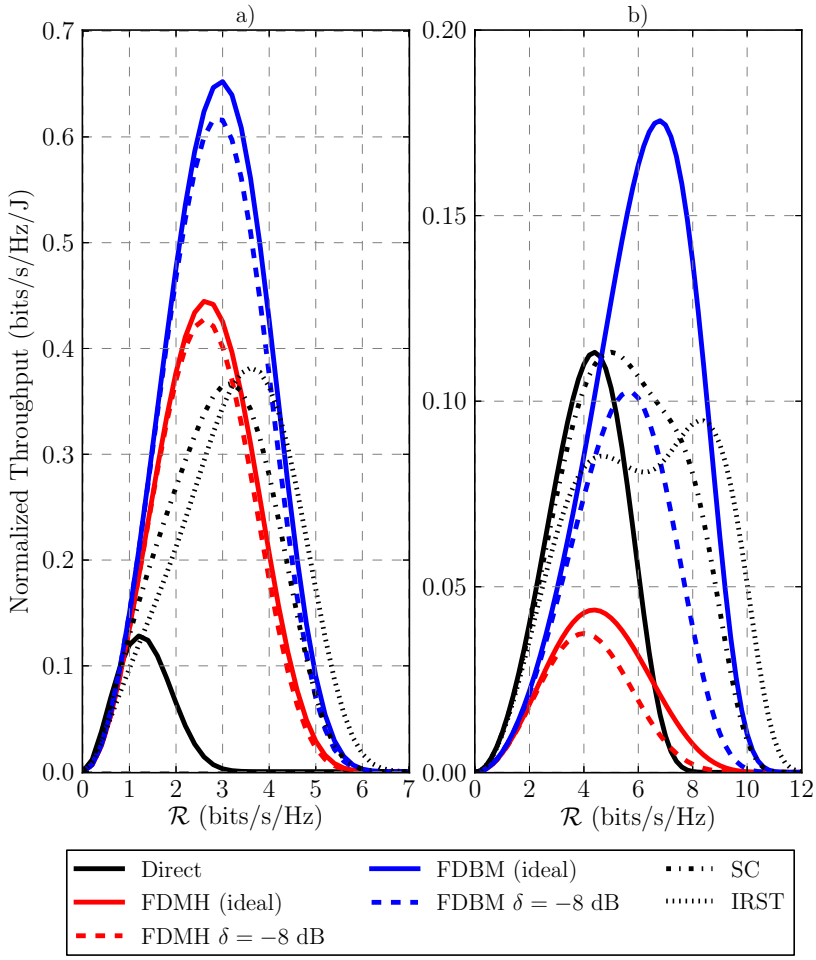

Fig 14. Normalized Throughput (bits/s/Hz) versus $\mathcal{R}$ for: *a)* $\overline{\gamma}_{\mathrm{SD}} = 0$ **dB and** *b)* $\overline{\gamma}_{\mathrm{SD}} = 15$ **dB. Modified from [45] © John Wiley & Sons 2015.**

scheme is close to one. Therefore, the performance of FDMH even with PA and RA is worse than the direct transmission.

In Fig. 16 we present the power allocated to the source as a function of the SNR. We can notice that most of the available power is allocated to the source ($P_{\mathrm{S}}^{\star}$) in the IRST and FDBM schemes, consequently less power is allocated to the relay. However, in the FD-MH scheme $P_{\mathrm{S}}^{\star}$ decreases and more power is allocated to the relay. We recall that the performance of FDMH is also limited by the source-destination link which is seen as interference at the destination. Thus,

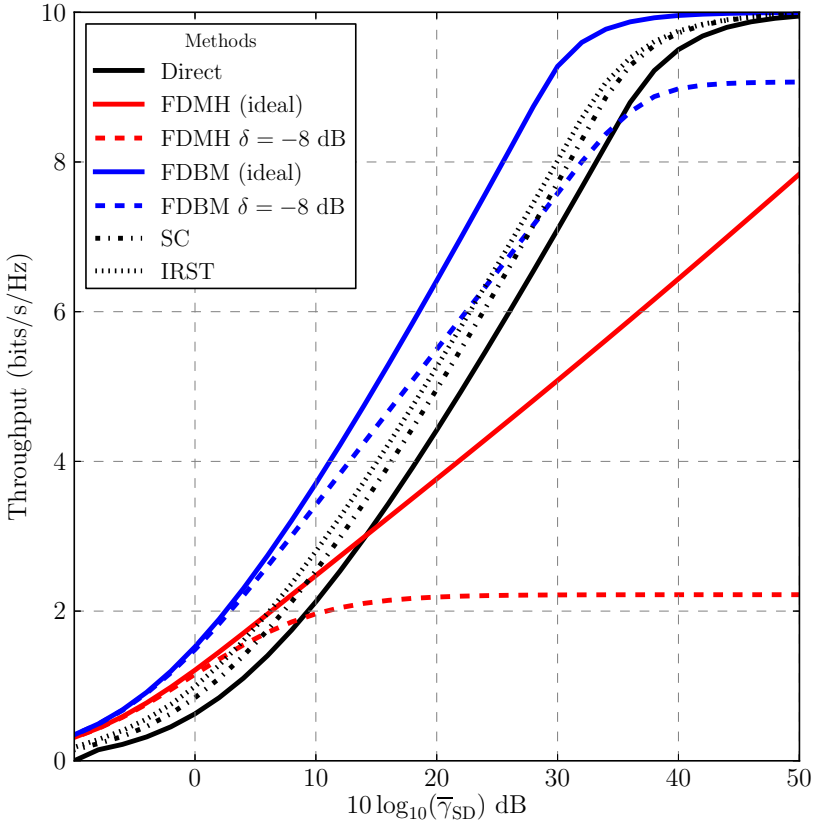

Fig 15. Throughput as function of $\overline{\gamma}_{\mathrm{SD}}$ accounting for joint power and rate allocation. Notice that there is a trade-off between FD ($\delta = -8$ dB) and HD schemes because of the residual self-interference. Modified from [45] © John Wiley & Sons 2015.

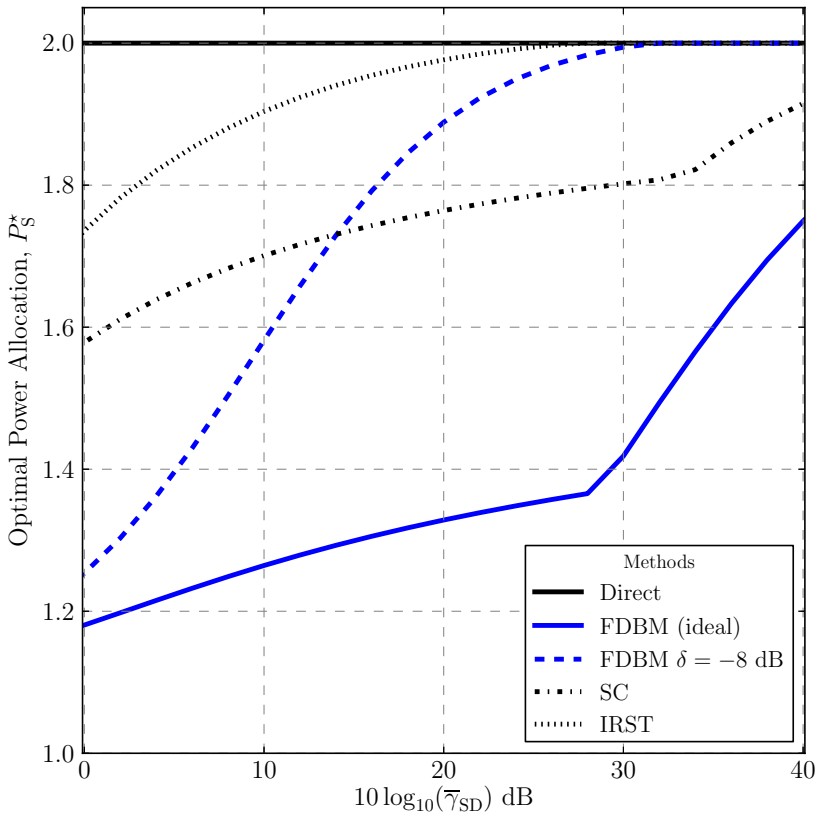

Fig 16. Optimal power allocation at the source as a function of $\overline{\gamma}_{SD}$. We assume a total power budget of $P = 2$ for all schemes and that $P_S + P_R = P$. Modified from [45] © John Wiley & Sons 2015.

reducing the transmit power at the source lowers the interference level at the destination. Moreover, In terms of RA, as shown in Fig. 17, HD and FD schemes perform alike, except for the FDMH scheme which employs a less aggressive RA strategy, due to the reasons discussed before.

Further, in Fig. 18 we evaluate the jointly impact of PA, RA and energy efficiency. Therefore, we can conclude that conversely to the discussion presented at the end of Section 3.5, if PA and RA are employed then FD relaying (even in the presence of strong self-interference) becomes more attractive from low- to high-SNR. Additionally, it is hard to notice from the figure but the direct

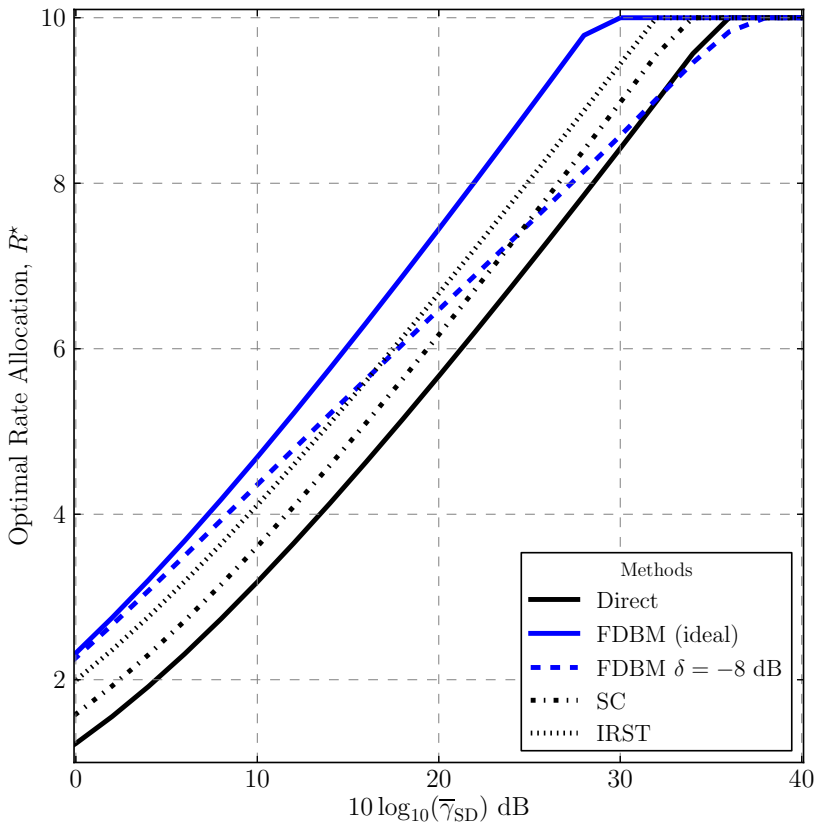

Fig 17. Optimal rate allocation at the source as a function of $\overline{\gamma}_{\mathrm{SD}}$. We assume a total power budget of $P = 2$ for all schemes, and that under cooperation $P_{\mathrm{S}} + P_{\mathrm{R}} = P$. Notice that rate range is limited by a maximum transmission rate of 10 bits/s/Hz. Modified from [45] © John Wiley & Sons 2015.

transmission is the most energy efficient scheme in the very high SNR region. That is reasonable since in the very high SNR region the cooperation from the relay is unnecessary, only increasing the energy consumption, since the source-destination link is very strong.

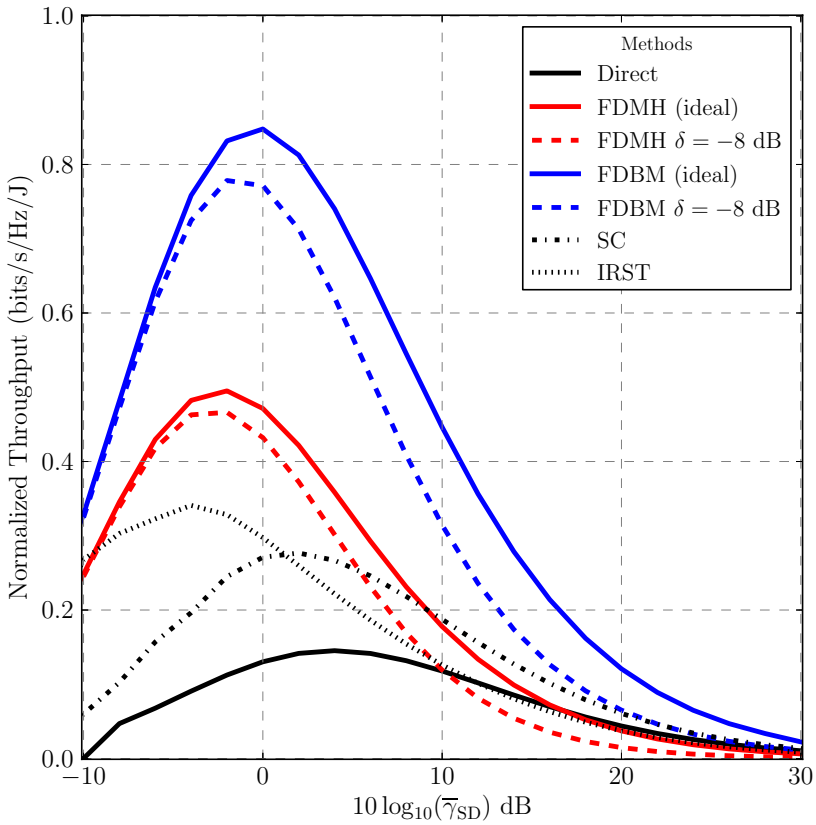

Fig 18. Normalized throughput (bits/s/Hz/J) as a function of as a function of $\overline{\gamma}_{\mathrm{SD}}$ when power and rate allocation are carried out. Modified from [45] © John Wiley & Sons 2015.

3.8 Final remarks and conclusions

We analytically evaluated the performance of some cooperative FD and HD schemes in terms of the outage probability, throughput and energy efficiency. In the FD scheme we took into account the self-interference caused by the relay transmitted signal into the relay received signal.

Surprisingly, our results show that incremental cooperative HD schemes can outperform practical (with self-interference) cooperative FD relaying. The reason for that is twofold: *i)* the presence of the self-interference causes a floor in

the outage probability of FDBM relaying, which reduces the maximum achievable throughput; *ii)* as we consider incremental protocols for HD relaying, HD cooperation is able to achieve the same maximum throughput as ideal FD relaying (without self-interference). For instance, in the case of a high SNR or of a high attempted information rate, incremental cooperative HD relaying can achieve a better trade-off between throughput and energy consumption. Thus, we observe that there is a trade-off between FD and HD relaying depending SNR region and transmission rate that the network operates. For instance, in a scenario with high SNR and high rate requirement HD solutions are more suitable, except for very low values of residual self-interference. Thus, an hybrid solution where the relay operates under FD or HD mode would be a valuable solution. The switch point would be determined by the network parameters such as, for instance, transmission rate, SNR or a given outage threshold.

4 Performance of full-duplex block-Markov relaying with self-interference in Nakagami-m fading

4.1 Motivation and related work

Cooperative systems operate either in HD or FD mode [7]. In the former, the relay transmits and receives the signal in orthogonal channels, whereas in FD mode the transmission and reception are performed at the same time and at the same frequency band. Owing to this fact, HD relays require the use of additional system resources, and FD relays arise as a viable option to alleviate this problem. However, although ideal FD relaying can achieve higher capacity than HD relaying [7], its use introduces self interference that is inherent to the practical FD approach – as discussed in Section 2.2. Nevertheless, the works [40, 43, 48] showed that FD relays can still achieve good performance, even in the presence of high interference levels.

In this chapter, we investigate the performance under Nakagami-m fading of the best known FD relaying protocol, the FDBM protocol [7, 98, 108]. It is noteworthy that FDBM relaying is the best performance achieving relaying scheme based on the DF protocol [7]. Notice that the FDBM is envisaged to operate as a combination of block Markov encoding at source and relay, associated with coding for cooperative multiple access channel and superposition coding [77, 108]. The achievability of the FDBM is proved in [108]. In addition, an extension to quasi-static fading channels was presented in [7, 98]. As mentioned in Section 2.2 we assume here regular encoding and backward decoding, opposed to irregular encoding and superposition decoding given that both strategies perform alike [7].

We assume a practical FD relaying scenario, where the relay suffers from residual self-interference as discussed earlier. Moreover, differently from Chapter 3, herein we extend the our model and we consider arbitrary Nakagami-m fading channels in all the links. So that we can emulate different configurations of (non-)LoS.

Moreover, the main contributions of this chapter can be briefly summarized as:

- We provide closed-form approximate expressions for the outage probability and throughput. Our derivations rely on efficient approximations proposed in the literature for the sum of Gamma RVs [139–141].
- Additionally, we introduce a new accurate approximation for the product of two Nakagami-m RVs. Such methodology alleviates considerably the complexity inherent to the exact formulations. Moreover, the accuracy of the proposed approximations is verified by Monte Carlo simulations.

Next, we introduce the system model and assumptions employed herein. Then, we introduce a new statistical method to evaluate the product of two Nakagami-m RVs and its play in the outage probability formulation of the FDBM protocol. In what follows, we introduce some numerical results and discussions.

4.2 Problem setting and general assumptions

Consider a dual-hop cooperative system composed by source, one relay, and one destination, such that the source communicates with the destination via a direct link and also through the help of the relay, as shown in Fig. 3b. Moreover, the relay operates in the FD mode so that the transmission and reception occur simultaneously. This causes self interference, which is the residual self-interference after the application of some interference cancellation technique, as discussed in Section 2.2 – for further details on residual self-interference refer to [26, 30, 41, 42, 48].

In addition, all channels are quasi-static, independent and non-necessarily identically Nakagami-m distributed, thus $\mathsf{Nakagami}(m_{ij}, \Omega_{ij})$, with PDF given as [142]

$$f_H(h) = \frac{2\, m^m\, h^{2m-1}}{\Omega^m\, \Gamma(m)} \exp\left(-\frac{m\, h^2}{\Omega}\right) \tag{62}$$

where $m \triangleq m_{ij} \geq \frac{1}{2}$ being the Nakagami-m fading parameter pertaining to the link between $i \in \{\mathrm{S}, \mathrm{R}\}$ and $j \in \{\mathrm{R}, \mathrm{D}\}$, h_{ij} denotes the Nakagami-m channel coefficient and $\Omega \triangleq \Omega_{ij} \triangleq \mathrm{E}\left[|h_{ij}|^2\right] \triangleq d_{ij}^{-\nu}$ represents the corresponding average fading power. Notice that $\Omega_{\mathrm{RR}} \triangleq \mathrm{E}\left[|h_{\mathrm{RR}}|^2\right] \triangleq \delta$, where δ represents residual

self-interference cancellation coefficient, which encompass active and passive cancellation techniques [26, 30] – please refer to [35, 37–39] for further details on self-interference cancellation techniques. We assume perfect CSI at the receivers and the noise terms are complex additive white Gaussian RVs with $N_0 \triangleq \sigma_w^2 = 1$, where N_0 is the one-sided noise power spectral density.

Since the channel follows Nakagami-m distribution the squared envelope follows Gamma distribution [142]; therefore, the PDF of SNR – notice that Γ is a RV representing the SNR, which is distributed as $\Gamma \sim \mathsf{Gamma}(m, \overline{\gamma})$) – is given as [142]

$$f_{\Gamma}(\gamma) = \frac{m^m \, \gamma^{m-1}}{\overline{\gamma} \, \Gamma(m)} \exp\left(-\frac{m\,\gamma}{\overline{\gamma}}\right), \tag{63}$$

where $\overline{\gamma} \triangleq \overline{\gamma}_{ij} \triangleq P_i \, \frac{\Omega_{ij}}{m_{ij}}$, and notice that $\overline{\gamma}_{\mathrm{RR}} \triangleq P_{\mathrm{R}} \, \frac{\Omega_{\mathrm{RR}}}{m_{\mathrm{RR}}}$.

4.2.1 Full-duplex block Markov (FDBM) under general fading

Herein, we focus on the analysis of the FDBM cooperative scheme [7], which can be seen as the composite of a BC and a MAC. In the broadcast phase, the message is transmitted from the source to both relay and destination. The MAC stage is composed by the signals coming from source and relay to the destination. Therefore, differently from HD relaying schemes, the presence of self interference in FD relaying implies that the transmission from the relay interferes in its own reception.

Based on [7, 108], the mutual information, denoted as achievable rate in Section 2.2, at the source-relay link can be written as[4]

$$\mathcal{I}_{\mathrm{SR}} = \log_2\left(1 + \left(1-\rho^2\right) \frac{\left|h_{\mathrm{SR}}\right|^2 P_{\mathrm{S}}}{\left|h_{\mathrm{RR}}\right|^2 P_{\mathrm{R}} + 1}\right), \tag{64}$$

while the mutual information from the MAC is given by

$$\mathcal{I}_{\mathrm{MAC}} = \log_2\left(1 + P_{\mathrm{S}} \, \left|h_{\mathrm{SD}}\right|^2 + P_{\mathrm{R}} \, \left|h_{\mathrm{RD}}\right|^2 + 2\sqrt{P_{\mathrm{S}} \, P_{\mathrm{R}}} \, \mathrm{Re}\left(\rho \, h_{\mathrm{SD}} \, h_{\mathrm{RD}}^*\right)\right), \tag{65}$$

[4] Notice that in Chapter 2 the mutual information of source-relay link is defined as (4). We opt to redefine the expressions in order to improve readability.

where ρ is the correlation coefficient between x and $\tilde{x}$ [7, 98, 108]. Thus, the overall mutual information of FDBM is [7, 98, 108]

$$\mathcal{I}_{\mathrm{FDBM}} = \min\left\{\mathcal{I}_{\mathrm{SR}}\,,\,\mathcal{I}_{\mathrm{MAC}}\right\}. \tag{66}$$

4.3 Outage probability and throughput analysis

Next we address the overall outage probability of the FDBM protocol, namely $\mathcal{P}_{\mathrm{FDBM}}$, which is given by the following theorem.

Theorem 4.1. *(Outage probability of the FDBM) Let all RVs be independent and identically distributed (*i.i.d.*), then the outage probability of the FDBM protocol is*

$$\mathcal{P}_{\mathrm{FDBM}} = \mathcal{P}_{\mathrm{SR}} + \mathcal{P}_{\mathrm{MAC}} - \mathcal{P}_{\mathrm{SR}}\,\mathcal{P}_{\mathrm{MAC}}, \tag{67}$$

where $\mathcal{P}_{\mathrm{SR}} = \Pr\left[\mathcal{I}_{\mathrm{SR}} < \mathcal{R}\right]$ *and* $\mathcal{P}_{\mathrm{MAC}} = \Pr\left[\mathcal{I}_{\mathrm{MAC}} < \mathcal{R}\right]$.

Proof. Proof is straightforward since we rely on standard statistics and on the independence of all RV, which gives us [130]

$$\mathcal{P}_{\mathrm{FDBM}} = \Pr\left[\min\left\{\,\mathcal{I}_{SR}, \mathcal{I}_{\mathrm{MAC}}\,\right\} < \mathcal{R}\right] \tag{68}$$

$$= 1 - \left(1 - \mathcal{P}_{\mathrm{SR}}\right)\left(1 - \mathcal{P}_{\mathrm{MAC}}\right), \tag{69}$$

and that concludes the proof. □

4.3.1 Outage probability of the BC phase

Next, in order to determine (67), firstly we assess $\mathcal{P}_{SR}$ which is expressed through the following theorem.

Lemma 4.1. *(Outage probability of the source-relay link) Let all RVs be independent and the transmission rate be* $\mathcal{R}$*, then the outage probability of the FDBM protocol is*

$$\mathcal{P}_{\mathrm{SR}} = 1 - \sum_{k=0}^{m_{\mathrm{SR}}-1} \frac{\vartheta_{\mathrm{RR}}^{m_{\mathrm{RR}}}\,\vartheta_{\mathrm{SR}}^{k}\,e^{-\vartheta_{\mathrm{SR}}}}{\Gamma\left(k+1\right)}\,\mathsf{U}\left(m_{\mathrm{RR}}\,,\,k+m_{\mathrm{RR}}+1\,,\,\vartheta_{\mathrm{RR}}+\vartheta_{\mathrm{SR}}\right), \tag{70}$$

where the fading figure $m_{\mathrm{SR}} \in \mathbb{Z}^{\star}$, *while* $m_{\mathrm{RR}} > 0.5$. *Additionally,* $\vartheta_{\mathrm{RR}} = \frac{m_{\mathrm{RR}}}{P_{\mathrm{R}}\,\Omega_{\mathrm{RR}}}$, $\vartheta_{\mathrm{SR}} = \frac{(2^{\mathcal{R}}-1)\,m_{\mathrm{SR}}}{(1-\rho^2)\,P_{\mathrm{S}}\,\Omega_{\mathrm{SR}}}$, *and* $\mathrm{U}(\cdot,\cdot,\cdot)$ *denotes the confluent hypergeometric function of the second kind [143, Eq. 13.2.5].*

Proof. In order to solve the outage probability of the source-relay link we proceed as follows

$$\mathcal{P}_{SR} = \Pr\left[\mathcal{I}_{SR} < \mathcal{R}\right] \tag{71}$$

$$= \Pr\left[\left(1-\rho^2\right)\frac{\left|h_{SR}\right|^2 P_S \kappa_{SR}}{\left|h_{RR}\right|^2 P_R + 1} < 2^{\mathcal{R}} - 1\right] \tag{72}$$

$$= \Pr\left[\frac{X}{Y+1} < 2^{\mathcal{R}} - 1\right] \tag{73}$$

$$= \Pr\left[Z < 2^{\mathcal{R}} - 1\right] \tag{74}$$

where the auxiliary RVs $X \sim \mathrm{Gamma}(\alpha_x, \beta_x)$ and $Y \sim \mathrm{Gamma}(\alpha_y, \beta_y)$ represent the SNR of the source-relay and self-interference links, respectively, [142]. Notice that for easy of notation $\alpha_x = m_{\mathrm{SR}}$ and $\beta_x = (1-\rho^2)\,P_{\mathrm{S}}\,d_{\mathrm{SR}}^{-\nu}\,\frac{\Omega_{\mathrm{SR}}}{m_{\mathrm{SR}}}$, while $\alpha_y = m_{\mathrm{RR}}$ and $\beta_y = P_{\mathrm{R}}\,\delta\,\frac{\Omega_{\mathrm{RR}}}{m_{\mathrm{RR}}}$. Then, applying the concepts of probability theory [130], the PDF of Z can be expressed as

$$f_Z(z) = \int_0^{\infty} (t+1) f_X(z(t+1)) f_W(t+1) dt, \tag{75}$$

where $W = Y + 1$, whose PDF can be attained from the PDF of Y by making a transformation of RVs. Thus, by substituting appropriately the PDFs of X and W in (75), it follows that

$$f_Z(z) = \frac{z^{\alpha_x - 1}\, e^{-\frac{z}{\beta_x}}}{\Gamma(\alpha_x)\,\beta_x^{\alpha_x}\,\beta_y^{\alpha_y}} \mathrm{U}\left(\alpha_y, \alpha_x + \alpha_y + 1, \frac{z}{\beta_x} + \frac{1}{\beta_y}\right). \tag{76}$$

From (76), the CDF of Z can be attained as

$$F_Z(\epsilon) = 1 - \int_0^{\infty} \frac{(\beta_y)^{-\alpha_y} t^{\alpha_y - 1}}{\Gamma(\alpha_x)\Gamma(\alpha_y)} \exp\left(-\frac{t}{\beta_y}\right) \Gamma\left(\alpha_x\,,\, \frac{(t+1)\epsilon}{\beta_x}\right) dt\,, \tag{77}$$

$$= 1 - I_1 \tag{78}$$

Now, in order to attain I_1 in (78), we resort to [144, Eq. 8.352-7]

$$\Gamma(n,x) = (n-1)!\exp(-x)\sum_{k=0}^{n-1}\frac{x^k}{k!}, \tag{79}$$

which, after solving the required integral and after some algebraic manipulations, yields

$$I_1 = \sum_{k=0}^{\alpha_x-1}\frac{1}{k!}\left(\frac{\epsilon}{\beta_x}\right)^k \beta_y^{-\alpha_y}\,\exp\left(\frac{\epsilon}{\beta_x}\right)\mathrm{U}\left(\alpha_y\,,k+\alpha_y+1\,,\frac{1}{\beta_y}+\frac{\epsilon}{\beta_x}\right). \tag{80}$$

Finally, by putting $\epsilon = 2^{\mathcal{R}}-1$ in (80), and plugging this latter into (77), (70) is obtained, which concludes the proof. □

Remark 4.1. *It is noteworthy that the distribution of the ratio between two Gamma RVs is a known result as discussed in [145, 146]. However, the distribution of the RV Z turns out to be a more intricate problem than what is presented in [145, 146], since it involves the ratio between a Gamma RV and a Generalized Gamma RV $W \sim \mathsf{GGamma}(\alpha_w, \beta_w, 1, 1)$ [147, 148]. Thus, Lemma 4.1 provides a simple and easy to evaluate CDF to the ratio Z, since the CDF involves a summation of well known functions.*

Remark 4.2. *In (70), note that even though m_{SR} is restricted to be a positive integer, it is possible to evaluate a great number of fading scenarios. Notice that the fading figure of the self-interference $m_{\mathrm{RR}} > 0.5$ has no restrictions. Moreover, the formulation in* (70) *includes the results of [43] as a special case.*

4.3.2 Outage probability of the MAC phase

In order to evaluate the outage probability of the MAC phase of the FD protocol, we first need to assess the PDF and CDF of the equivalent SNR in (65). However, this turns out to be a cumbersome task due to the presence of sums of products in (65). Thus, we tackle this issue through the following lemma.

Lemma 4.2. *Assuming that all channel gains are Nakagami-m distributed we*

define the mutual information of the MAC phase of the FDBM protocol as

$$\mathcal{I}_{\mathrm{MAC}} = \log_2\left(1 + P_{\mathrm{S}}\,|h_{\mathrm{SD}}|^2 + P_{\mathrm{R}}\,|\,h_{\mathrm{RD}}|^2 + 2\sqrt{P_{\mathrm{S}}\,P_{\mathrm{R}}}\,\rho\,h_{\mathrm{SD}}\,h_{\mathrm{RD}}\right), \tag{81}$$

$$= \log_2\left(1 + \Phi\right). \tag{82}$$

Proof. Proof comes straightforward from the properties of the Nakagami-m distribution, since all RVs are Nakagami-m distributed and only assume positive real values, we rewrite (65) as in (82). □

Thus, in order to evaluate $\mathcal{P}_{\mathrm{MAC}}$, we need to find the PDF and CDF of Φ, which is indeed a quite complex task due to the sum and product of RVs presented in Φ. To circumvent this issue, herein we propose a highly accurate approximate framework that leads to simple closed-form expressions.

Theorem 4.2. *The product of two Nakagami-m RVs is approximated by a single Gamma RV (i.e., $\Lambda \sim \mathsf{Gamma}(\xi, \varrho)$), whose parameters are expressed as*

$$\xi = \left(\frac{\Gamma\left(m_{\mathrm{SD}}\right)\Gamma\left(m_{\mathrm{SD}}+1\right)\Gamma\left(m_{\mathrm{RD}}\right)\Gamma\left(m_{\mathrm{RD}}+1\right)}{\Gamma\left(m_{\mathrm{SD}}+\frac{1}{2}\right)^2\Gamma\left(m_{\mathrm{RD}}+\frac{1}{2}\right)^2} - 1\right)^{-1} \tag{83}$$

$$\varrho = \sqrt{\frac{\Omega_{\mathrm{SD}}}{m_{\mathrm{SD}}}\frac{\Omega_{\mathrm{RD}}}{m_{\mathrm{RD}}}}\frac{\Gamma\left(m_{\mathrm{SD}}+\frac{1}{2}\right)\Gamma\left(m_{\mathrm{RD}}+\frac{1}{2}\right)}{\Gamma\left(m_{\mathrm{SD}}\right)\Gamma\left(m_{\mathrm{RD}}\right)}\frac{1}{\xi}, \tag{84}$$

where $\Gamma(\cdot)$ indicates the Gamma function [144, Eq. 8.310-1].

Proof. Firstly, relying on the idea presented in [149], we propose to approximate the product of two Nakagami-m RVs (i.e., $\Upsilon = h_{\mathrm{SD}}\,h_{\mathrm{RD}}$) by a single Gamma RV (i.e., $\Lambda \sim \mathsf{Gamma}(\xi, \varrho)$), whose parameters ξ and ϱ can be estimated according to the method of the moments [130]. Therefore, by matching $\mathrm{E}\left[\Upsilon\right]$ with $\mathrm{E}\left[\Lambda\right]$ and $\mathrm{E}\left[\Upsilon^2\right]$ with $\mathrm{E}\left[\Lambda^2\right]$ [130], and after some algebraic manipulations, ξ and ϱ are written as a function of the parameters of the Nakagami-m RVs h_{SD} and h_{RD}. Bearing this in mind, let us define the first and second moments of Λ as $\mathrm{E}\left[\Lambda\right] = \xi\varrho$ and $\mathrm{E}\left[\Lambda^2\right] = \xi(1+\xi)\varrho^2$ [130]. From [149, Eq. 9], the n-th moment of $\Upsilon = h_{\mathrm{SD}}h_{\mathrm{RD}}$ can be determined as

$$\mathrm{E}\left[\Upsilon^n\right] = \frac{\Gamma(m_{\mathrm{SD}}+\frac{n}{2})\Gamma(m_{\mathrm{RD}}+\frac{n}{2})}{\Gamma(m_{\mathrm{SD}})\Gamma(m_{RD})}\left(\frac{\Omega_{\mathrm{SD}}}{m_{\mathrm{SD}}}\right)^{\frac{n}{2}}\left(\frac{\Omega_{\mathrm{RD}}}{m_{\mathrm{RD}}}\right)^{\frac{n}{2}}. \tag{85}$$

□

Remark 4.3. *It is noteworthy that, in [149], an exact formulation for the PDF of the product of Nakagami-m RVs was derived. Herein, differently from [149] but still making use of its formulation, we propose to approximate the product of two Nakagami-m RVs by a single Gamma RV. Then, we can easily write the sum in* (81) *as the sum of Gamma RVs, which leads to simple closed-form expressions.*

By considering distinct values of m_{ij} and Ω_{ij}, Fig.19 shows the proposed approximation for the product of two Nakagami-m RVs. Interestingly, in addition to be new, our proposed approximation will show to be very precise, as we shall see later in this section, agreeing very well with the actual PDF of the product of two Nakagami-m RVs, which was derived in [149, Eq. 6], and with Monte Carlo simulations. Note that the approximation of the product of two Nakagami-m RVs applies for independent and not necessarily identically distributed RVs.

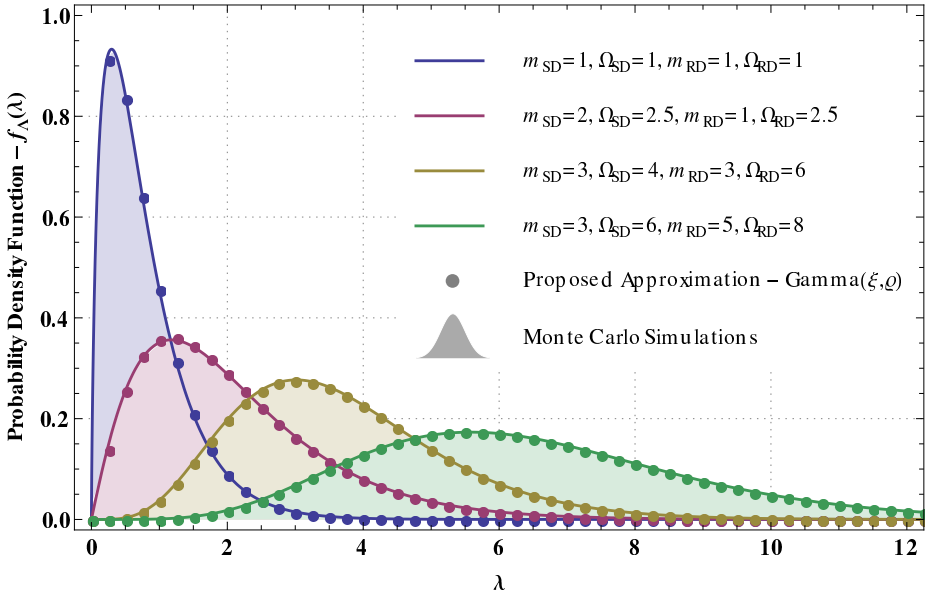

Fig 19. Approximation of the product of Nakagami-m RV to a single Gamma RV for different parameters. Modified from [46] © IEEE 2015.

In what follows, we compare our proposed approximation to the approximation introduced in [150]. As we can see from Fig. 20, our proposed approximation (colored lines) is tight compared to [150] (black, solid lines) and to the closed-form expression from [149, Eq. 6] (colored markers). The histogram is also included for comparison, and is generated using 800.000 samples for each set of m_{ij} and Ω_{ij}. Moreover, notice that both approximations overlap for the Rayleigh case $m_{ij} = 1$. Additionally, the proposed approximation is tight with the increase of the fading figure m_{ij} and scale parameter Ω_{ij}.

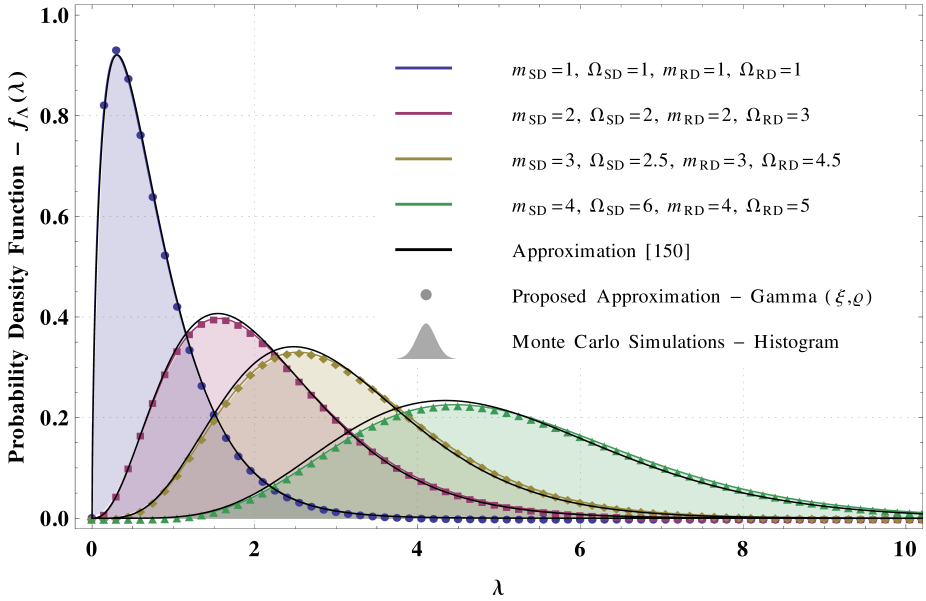

Fig 20. Approximation of the product of Nakagami-m RV to a single Gamma RV for different parameters. Proposed approximation (colored lines) is compared to [150] (black lines) and to the closed-form solution introduced in [149, Eq. 6]. The histogram is also included for comparison.

Remark 4.4. *Notice that [150] can also be used to approximate the product of independent Gamma and Gaussian RVs. Herein, our comparison focused on the product of independent Nakagami-m RVs. Additionally, [150] the authors address the case where all RVs have the same fading figure, thus* $m_{ij} = m > 0.5$*, with distinct shape parameter* Ω_{ij}*. Differently from [150], our proposed*

approximation relax this constraint on the fading figure, thus $m_{ij} > 0.5$.

Kullback-Leibler divergence

We have evaluated the proposed approximation through the Kullback-Leibler divergence, which measures the information lost when a probability distribution P is approximate by another distribution Q[77]. The Kullback-Leibler divergence is defined as [77]:

$$D_{\mathrm{KL}}(P||Q) = \int_{-\infty}^{\infty} \ln\left(\frac{p_X(x)}{q_X(x)}\right) p_X(x) dx. \tag{86}$$

Note that the lower is the value of $D_{\mathrm{KL}}(P||Q)$, the better is the approximation. Now, let us define [149, Eq. (6)]

$$p_X(x) = \frac{4\,x^{m_{\mathrm{SR}}+m_{\mathrm{RD}}-1}}{\Gamma(m_{\mathrm{SR}})\,\Gamma(m_{\mathrm{RD}})} \left(\frac{\Omega_{\mathrm{SR}}}{m_{\mathrm{SR}}}\,\frac{\Omega_{\mathrm{RD}}}{m_{\mathrm{RD}}}\right)^{-\frac{m_{\mathrm{SR}}+m_{\mathrm{RD}}}{2}} \mathrm{K}_{\nu}\left(2\,x\sqrt{\frac{m_{\mathrm{SR}}\,m_{\mathrm{RD}}}{\Omega_{\mathrm{SR}}\,\Omega_{\mathrm{RD}}}}\right) \tag{87}$$

as the PDF of the product of two Nakagami-m RVs, where $\nu = m_{\mathrm{SR}} - m_{\mathrm{RD}}$ and $\mathrm{K}_{\nu}(\cdot)$ is the modified Bessel function of the second kind [144, Eq. 8.432-6][5]. Then the PDF of our proposed approximation, represented in (86) by $q_X(x)$, follows $\Lambda \sim \mathsf{Gamma}(\xi, \varrho)$.

Now, with the exact and approximated PDFs the Kullback-Leibler divergence can be evaluated for different values of P_{S}, m_{SR}, m_{RD}, Ω_{SR} and Ω_{RD}, as shown in Fig. 21. In Fig. 21 we assume $\overline{\gamma} = \overline{\gamma}_{\mathrm{SD}} = \overline{\gamma}_{\mathrm{RD}}$ represents the average SNR and $N_0 = 1$. Moreover, note that the amount of information lost by the approximation is almost negligible and does not vary with the SNR of the source-destination and relay-destination links.

We recall that $D_{\mathrm{KL}}(P||Q) = 0$ if and only if $P = Q$ [77, 151], which means that the smaller the value of $D_{\mathrm{KL}}(P||Q)$ the better is the proposed approximation. In that sense, notice that for all cases under analysis the Kullback-Leibler divergence is at most in the order of 10^{-3}, which indicates that the approximation is accurate. This can be also observed in Fig. 19, note that the proposed approximation and the actual PDF and simulations agree well.

[5] Notice that ν in (87) refers to the order of the modified Bessel function rather than the path loss exponent.

Next, Table 3 shows the Kullback-Leibler divergence between [149, Eq. 6] *i)* the approximation in [150]; and *ii)* the proposed approximation. We assume $\Omega_{\mathrm{SD}} = \Omega_{\mathrm{RD}} = 0$ dB, while $m_{ij} \in \{1, 2, 3, 4, 5, 10\}$, with $i \in \{\mathrm{S}, \mathrm{R}\}$ and $j \in \{\mathrm{D}\}$. Notice that the approximation proposed in [150] presents a better fit for the Rayleigh case when compared our proposed approximation; however, as the fading figure increases (larger values of m_{ij}) our proposed approximation has a better fit since $D_{\mathrm{KL}}(P||Q)$ tends to zero.

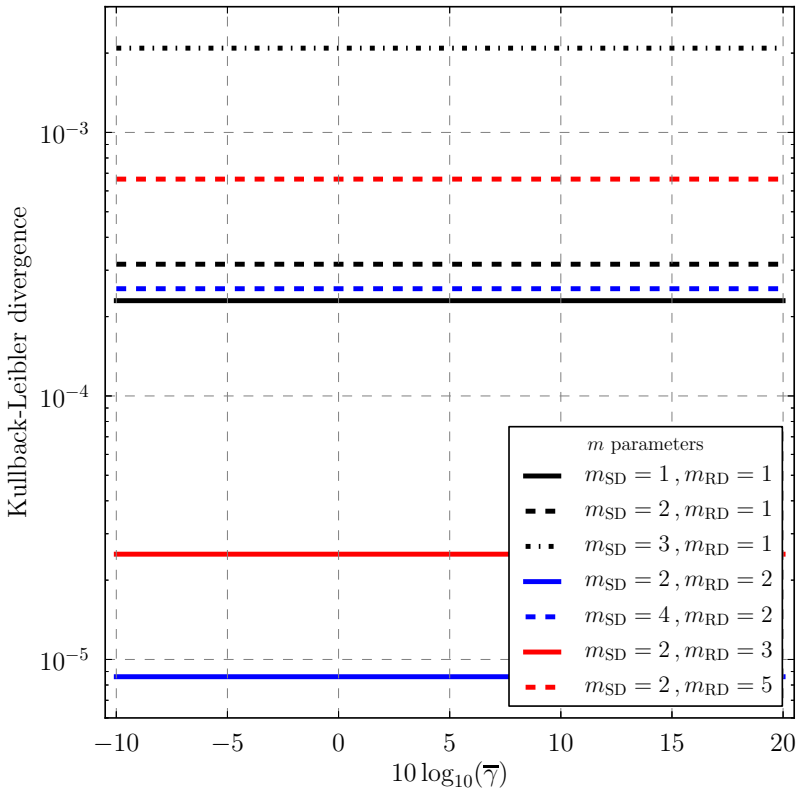

Fig 21. Kullback-Leibler divergence versus the average SNR, where $\overline{\gamma} = \overline{\gamma}_{\mathrm{SD}} = \overline{\gamma}_{\mathrm{RD}}$. Notice that the proposed approximation is accurate for a large number of combinations of m-parameters.

Table 3. Kullback-Leibler divergence: comparison between closed-form expression [149, Eq. 6] with *i)* approximation [150] and *ii)* proposed approximation.

	Kullback-Leibler divergence (KLd)	
m_{ij}	*i)* Approximation [150]	*ii)* Proposed Approximation
1	1.625×10^{-4}	2.298×10^{-4}
2	5.932×10^{-4}	8.600×10^{-6}
3	1.849×10^{-3}	1.071×10^{-6}
4	3.527×10^{-3}	2.378×10^{-7}
5	5.415×10^{-3}	7.374×10^{-8}
10	1.592×10^{-2}	1.987×10^{-9}

4.3.3 Sum of gamma random variables

Once the parameters of Λ are properly determined, Φ becomes the sum of three different Gamma RVs.

Lemma 4.3. *The PDF of Φ is approximated by the PDF of a single Gamma RV such that $\Phi \sim \mathsf{Gamma}(m, \Omega/m)$) [139–141], whose parameters are*

$$\Omega = P_{\mathrm{S}}\,\Omega_{\mathrm{SD}} + P_{\mathrm{R}}\,\Omega_{\mathrm{RD}} + 2\sqrt{P_{\mathrm{S}}\,P_{\mathrm{R}}}\,\rho\,\xi\,\varrho, \tag{88}$$

$$m = \left(\frac{\left(P_{\mathrm{S}}\,\Omega_{\mathrm{SD}}\right)^2 m_{\mathrm{RD}} + \left(P_{\mathrm{R}}\,\Omega_{\mathrm{RD}}\right)^2 m_{\mathrm{SD}} + 4\,P_{\mathrm{S}}\,P_{\mathrm{R}}\,\rho^2\,m_{\mathrm{SD}}\,m_{\mathrm{RD}}\,\xi\,\varrho^2}{m_{\mathrm{SD}}\,m_{\mathrm{RD}}\Omega^2}\right)^{-1}. \tag{89}$$

Proof. Please refer to [139–141] for detailed approximation on the sum of Gamma RVs. □

Finally, an accurate, easy-to-compute approximate expression for $\mathcal{P}_{\mathrm{MAC}}$ is given in the following theorem.

Theorem 4.3. *Assuming a transmission rate of $\mathcal{R}$, the outage probability of the MAC phase of the FDBM protocol is*

$$\mathcal{P}_{MAC} \approx 1 - \frac{\Gamma\left(m, \frac{m(2^{\mathcal{R}}-1)}{\Omega}\right)}{\Gamma\left(m\right)}, \tag{90}$$

where $\Gamma(\cdot,\cdot)$ indicates incomplete Gamma function [144, Eq. 8.350-2].

Proof. From Theorem 4.2 we have that the product of two Nakagami-m RVs can be approximated by a single Gamma RV. Then, we resort to Lemma 4.3 for the sum of Gamma RVs, and therefore we can express Φ as a single Gamma RV according to $\Phi \sim \mathsf{Gamma}(m, \Omega/m)$, whose CDF is given as in (90). □

Assuming a transmission rate of $\mathcal{R}$, the average rate of all successful transmissions, gives us the average information rate, spectral efficiency, seen at the destination is

$$\mathcal{T} = \mathcal{R}\,(1 - \mathcal{P}_{\mathrm{FDBM}}) \tag{91}$$

$$= \mathcal{R}\,(1 - \mathcal{P}_{SR})\,(1 - \mathcal{P}_{\mathrm{MAC}})\,. \tag{92}$$

Remark 4.5. *Differently from [43], where the analysis was based on $\rho = 0$, and from [97], where self interference was not taken into account, our methodology offers a more general framework that captures the effects of ρ, different power allocations and allows us to emulate different configurations of (non-) LoS scenarios.*

4.4 Numerical results and discussions

In this Section, representative numerical examples are presented for the outage probability and throughput of the considered FDBM encoding cooperative scheme. Unless otherwise stated, we assume $N_0 = 1$, $d_{ij} = 1$, $\nu = 4$, $\rho = 0.2$, and $\mathcal{R} = 2$ bits/s/Hz. Monte Carlo simulations are also presented to validate the analytical derivations. We have used at least 10^6 repetitions in order to generate the simulations points.

Based on (70), Fig. 22 shows the outage probability of the source-relay link for different values of m_{SR}, m_{RR}, and Ω_{RR}. For the plots, we consider $m_{\mathrm{SR}} \in \{1, 2\}$, $\Omega_{\mathrm{SR}} = 2$, $m_{\mathrm{RR}} \in \{1, 2\}$, $\Omega_{\mathrm{RR}} = 1$ and $\delta \in \left\{10^{-1}, 10^{-2}, 10^{-4}\right\}$. Note that the system performance improves when:

a) the fading severity of the source-relay link decreases (i.e., when m_{SR} increases);

b) the antenna isolation at the relay (which is inversely proportional to δ) increases.

It is worth noting that the better is the antenna isolation component, the lower is the impact of the parameter m_{RR}. This occurs mainly due to the residual self interference, which is dominated by the scattering component of the channel, once the LoS component was assumed to be considerably reduced by antenna isolation (as considered in [48] and demonstrated in [25]).

Fig. 23 shows the overall outage probability as a function of ρ by setting $P_{\mathrm{S}} = P_{\mathrm{R}} = 20$ dB, $m_{ij} \in \{1, 2, 3\}$, and $\Omega_{ij} = 2$, except for $\Omega_{\mathrm{RR}} = 1$ and $\delta = 10^{-4}$. Again, Monte Carlo simulations are presented to corroborate our analysis. Notice that all channels are subject to Rayleigh fading when $m_{ij} = 1$, which encompass the results presented in [43]. As expected, note that if the messages x and $\tilde{x}$ are fully correlated, the system is in outage. Also, the outage

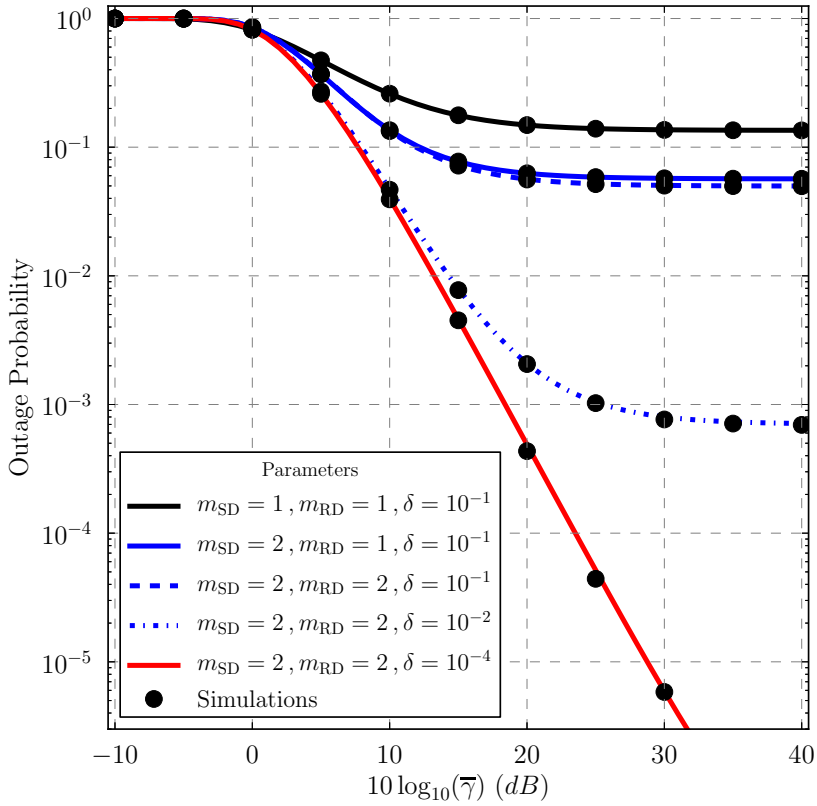

Fig 22. Outage probability of the source-relay link as a function of the average SNR $\overline{\gamma}$ for different fading setups. Modified from [46] © IEEE 2015.

performance varies with ρ and there exists a range in which the outage can be minimized. Interestingly, it can be seen that the parameters m_{RR}, m_{SD}, and m_{RD} have low impact on the system performance. However, a large m_{SR} can considerably reduce the outage probability, since the relay decodes with high probability the source's message and consequently increases reliability, which lowers the outage probability.

Fig. 24 depicts the overall outage probability as a function of $\overline{\gamma}$. In the plots, we set $P_{\mathrm{S}} = P_{\mathrm{R}}$, $m_{ij} = 1$ except for m_{SR}, which assume the values indicated in the plot. Note that the poorer the antenna separation is, the worse is the FDBM performance compared to the ideal case ($\delta = 0$). Note also that the performance considerably improves at high SNR region when the fading severi-

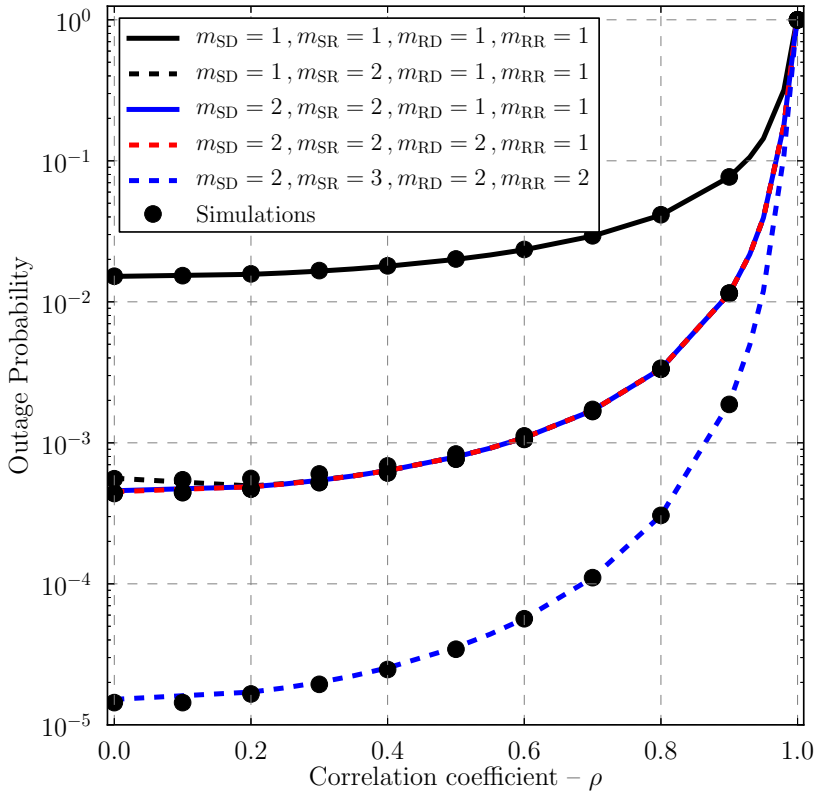

Fig 23. Overall outage probability as a function of correlation coefficient ρ for distinct fading configurations. Modified from [46] © IEEE 2015.

ties (m parameter) of the source-relay, source-destination and relay-destination channels decrease.

Fig. 25 shows the throughput as a function of $\overline{\gamma}$. Again, we set $P_{\mathrm{S}} = P_{\mathrm{R}}$, $m_{\mathrm{SR}} = 2$ and $m_{\mathrm{RR}} = 1$. In order to avoid entanglement among the curves, simulation results have been omitted but indeed they match very well with the analytical curves. Interestingly, it can be seen that, at low SNR, a random channel variation is preferred. This is because of higher values for the fading parameters imply that the links become increasingly deterministic and, consequently, the encoding becomes a hard task at low SNR. In this case, fading is beneficial for the system throughput. On the other hand, from medium to high SNR regions, fading becomes harmful. Thus, increasing the deterministic na-

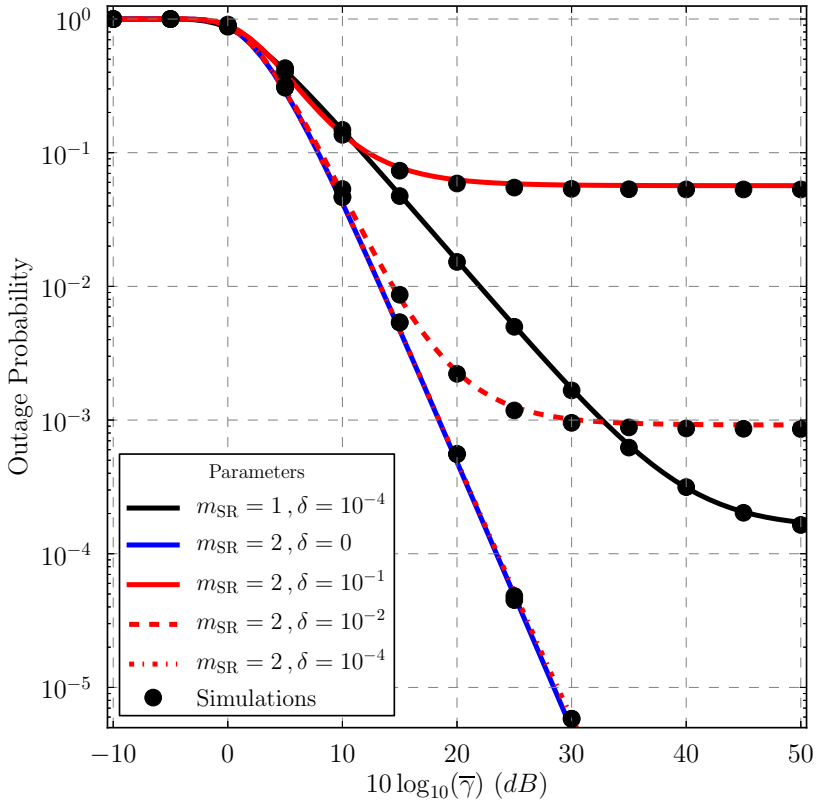

Fig 24. Overall outage probability as a function the average SNR $\overline{\gamma}$ for distinct fading parameters. Modified from [46] © IEEE 2015.

ture of the channels (i.e., increasing the values of the fading parameters) yields a higher system throughput.

4.5 Final remarks and conclusions

In this chapter we investigate the performance of a FDBM relaying scheme with self interference at the relay under independent non-identically distributed Nakagami-m fading. Then, relying on efficient approximations for the sum of Gamma RVs, and based on a new, accurate approximation for the product of two Nakagami-m RVs, we attain tight closed-form approximate expressions for the

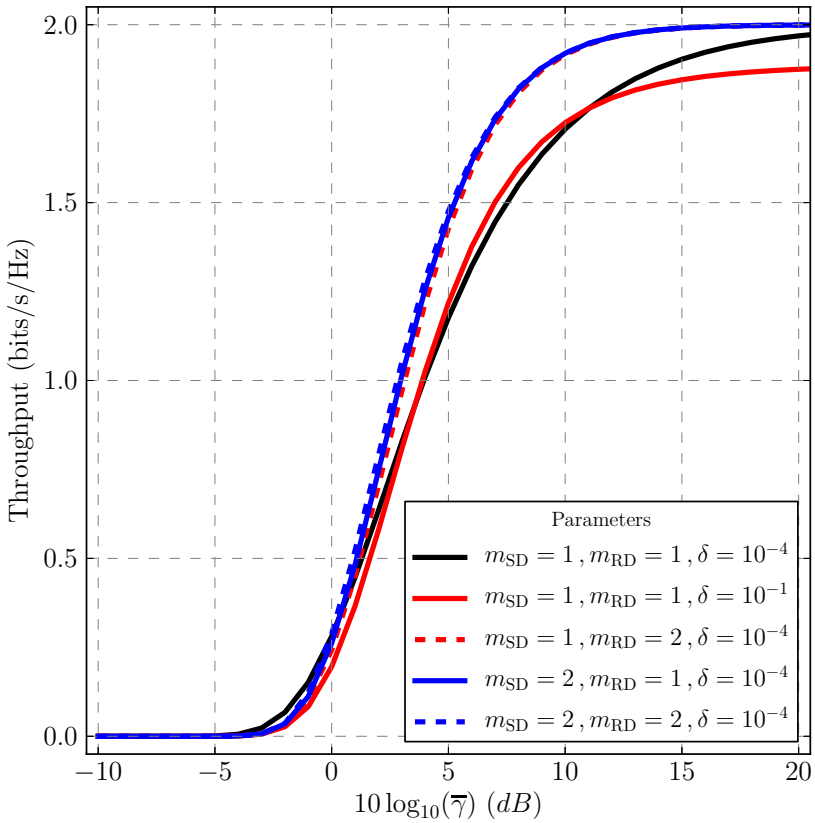

Fig 25. Throughput as a function of the average SNR $\overline{\gamma}$ for distinct fading parameters.Modified from [46] © IEEE 2015.

outage probability of the second phase of the FD cooperative protocol, namely (90). The outage probability of the broadcast phase is attained in closed-form as shown in (70) and is valid for integer m parameters. With those expressions we can then derive tight closed-form approximate expressions for the overall outage probability and throughput, which are analyzed through representative numerical results, that also show the accuracy of the proposed approximations.

Moreover, the finding in this chapter allows us to better understand effects of the residual self-interference on a FD relaying setup, since distinct (non-) LoS configurations can be emulated, which can be directly related to the quality of the antenna isolation and self-interference cancellation employed at the FD relay. Additionally, our results show that the deployment of the relay considerably affects performance, for instance, if the relay is positioned with some LoS to the source or destination large gains can be achieved mid-high SNR region. Therefore, this results can be used on the design and deployment cooperative networks to boost performance in order to attend the demands of high QoS of the upcoming wireless systems [11–14], especially the cases of cell-range extension.

5 On the performance of secure full-duplex relaying networks under composite fading channels

5.1 Motivation and related Work

Chapter 3 and 4 provide us a comprehensive analysis of FD relying schemes, where we covered a wide range of scenarios and applications. Herein and differently from the previous chapters, we add one more constraint to our analysis by focusing on the aspect of security at wireless networks.

Wireless communication systems are naturally vulnerable to the attack of eavesdroppers due to the broadcast nature of the wireless medium. Therefore, security issues play an important role in the system design [49–51, 152–154]. Traditionally, security methods rely on cryptographic techniques employed at the upper layers of the network [155]. However, wireless networks are steadily growing and becoming decentralized, which in practice poses challenges to key distribution and maintenance [49]. Owing to this fact, PHY security has reappeared as a way to increase security with reduced complexity, increasing the difficulty for attackers to decipher private information [49–51, 152, 153]. The key idea behind this strategy is to exploit the spatial-temporal characteristics of the wireless channel to ensure secure data transmission.

In this context lies the analysis introduced herein. Even though the comprehensive analysis of FD introduced on the previous chapters, it is not possible to infer what would be the performance of FD relaying under secrecy constraints. Therefore, herein we extend our FD scenario in order to account for the presence of an malicious eavesdropper and, additionally, we assume an even more general fading setting, as we shall discuss next. Hence, we investigate the performance benchmark of secure FD relaying systems, which serves as a guideline to the design of the next generation of wireless networks.

In what follows, we provide an overview of PHY security and cooperative security, and then we introduce three scenarios and the new metrics used in each case.

5.1.1 Brief overview on PHY security

A pioneering work on PHY security is that of Wyner, in [156], where it is proved that there are codes for the wire-tap channel that guarantee both low error probabilities and a certain degree of confidentiality. The wire-tap channel is composed by two legitimate users, commonly known as Alice and Bob, communicating in the presence of an eavesdropper, which is commonly known as Eve. Alice and Bob communicate through the main channel while Eve observes, through the eavesdropper channel, a degraded version of the message seen by Bob. Later, in [157], the secrecy capacity of a Gaussian wire-tap channel is defined as the difference between the capacity of the main channel and that of the eavesdropper channel. Recently, those results are extended to wireless scenarios [158, 159]. For instance, in [158] PHY security for a quasi-static Rayleigh fading wire-tap channel with single-antenna devices is investigated. In [159], it is assumed that the eavesdropper may have multiple antennas, showing that when selection combining is used, one multi-antenna eavesdropper damages as much as multiple single-antenna eavesdroppers.

The case of MIMO techniques, in which Alice, Bob and Eve may be equipped with multiple antennas, is initially investigated in [160, 161], in the Gaussian MIMO wire-tap channel. Later on, in [162], secrecy outage probability expressions are derived for a codebook-based beamforming over Rayleigh fading supposing that Alice and Eve have multiple antennas, while Bob is a single-antenna device. Such codebook-based beamforming assumes that the transmitter uses a predefined codebook, known to both transmitter and receiver, and that a feedback channel is available. In [163], both Bob and Eve are assumed to have multiple antennas while Alice is a single-antenna device. Considering that the receivers employ Maximum Ratio Combining (MRC), the authors derive closed-form expressions for the secrecy outage probability and show that the use of multiple receive antennas can enhance security. Further, in [52, 56] Alice employs transmit antenna selection (TAS) while Bob is a single-antenna user and Eve applies MRC among its multiple receive antennas. In that work, it is shown that Eve is not able to exploit diversity from Alice's antennas, which enhances security. The scenario of [52] is extended in [164], where the performance gap between using SC or MRC at Bob and Eve is investigated. Results show that both SC and MRC achieve the same secrecy diversity order regardless of the small

performance gap between SC and MRC. The work in [164] is further extended in [165] to analyze the effects of antenna correlation on the secrecy performance. High correlation at Bob impacts negatively on the secrecy performance, while high correlation at Eve offers benefits to the secrecy. The overall effect is positive at low SNR, while it becomes negative at high SNR.

5.1.2 Cooperative security

Along the last years, cooperative communications have also been considered in the scope of PHY security [111, 154, 166–168]. In [111] the relay-eavesdropper channel is introduced and secrecy rates are characterized. In the relay-eavesdropper channel a trusted relay node helps the communication between source (Alice) and destination (Bob) through traditional cooperation or by confusing the eavesdropper (Eve) with independent codewords. Secure communication in multiple relay networks is investigated in [166], where the relays operate under DF protocol. In [167], the case of multiple eavesdroppers is considered, so that the relays may employ AF, DF or cooperative jamming to improve security. As pointed out in [51, 167] cooperative jamming arises as an interesting solution since legitimate transmitters improve the secrecy rate by introducing noise or structured signals in order to confuse the eavesdropper. Further, in [169], relay selection with secrecy constraints is performed, where a first relay is chosen to cooperate with the source, while a second relay is selected for jamming the eavesdropper. Additionally, a summary of the recent advances in cooperative security at PHY is given in [51, 154, Sect. V].

Most of the works focus on HD cooperative schemes with little attention to FD relaying, which are spectrally efficient compared to HD schemes. This, motivates us to focus our attention on FD schemes, since in HD mode, the relay transmits and receives the signal in orthogonal channels [7], whereas in FD mode the transmission and reception are performed at the same time and at the same frequency band [7]. Furthermore, as pointed out in [25–28, 30–47, 68, 69] FD operation is feasible and the the extent the gains attainable by FD nodes is directly related to the quality of the self-interference cancellation employed at the FD node. Moreover, self-interference can be modeled as a fading channel which allows the emulation of various (non-) LoS configurations [26, 46].

Secrecy and full-duplex

Recently, FD transmission is employed as a way to enhance security, since a FD node is able to receive while jamming the eavesdroppers [170–173]. The use of FD nodes for jamming purposed eliminates the need for external helpers, which provides system robustness. For instance, in [170] the authors design the system in order to jointly mitigate the self-interference associated with the FD operation and optimize the jamming transmission. Similar solutions are proposed in [171, 172] where artificial noise is generated and transmitted towards the eavesdropper. One advantage of [172] is that the authors proposed a method such that the own transmit signal can used as artificial noise in a two-way communication setting. Conversely to [170–172], in [173] the authors investigate the impact of a MIMO FD eavesdropper, which selects some of its antennas to send jamming signals to the destination while receiving at the remaining ones. The authors also discuss some potential countermeasures to such a malicious attack.

Cooperative FD relying is investigated in [57, 174]. In [174] the authors investigate a three node cooperative network operating under AF protocol and in the presence of a jammer. By its turn, in [57] the performance of FD cooperative network is investigated in terms secrecy outage probability.

Yet, in [175] the authors investigate secure communication of a FD base station. Thus, the authors characterize the secure transmission rates for UL and DL. The authors show that optimal performance in terms of secrecy rate can be achieved but the base station should either transmit information or jamming in a SISO setting, while for the MIMO case, the base station can optimally allocate resources for both, transmission and jamming.

As we have seen, FD communication becomes a viable solution not only to boost performance, but also to enhance security. And, as we shall see next, it is in this context that asses the performance of secure FD relaying.

5.1.3 Outline and summary of contributions

In this chapter, we assume a cooperative network in the presence of a multi-antenna eavesdropper, where the source communicates with the destination with the help of a FD relay, which suffers self-interference. We also employ a general channel model which encompasses Nakagami-m fading as well as Log-Normal

shadowing, which is known as composite fading channel [176–179].

Malicious users focus their attack on eavesdropping, hence we consider three scenarios dependent on the availability ofCSI at Alice. The scenarios and contributions are briefly summarized next:

- Full CSI: Alice has the CSI of all users (legitimate or malicious), thus perfect secrecy is achievable. Information on the eavesdroppers' channels can be attained when the eavesdropper is part of the network such that its active transmissions can be monitored [158, 167]. Therefore, we focus on the average secrecy rate as the performance metric, for which we present an accurate approximation in closed-form.
- Partial CSI: This scenario corresponds to the case where Eve is a passive and hostile eavesdropper in the network [52, 158, 164, 165]. Alice has only information about the legitimate channels and has the statistics of the eavesdroppers' channel so that perfect secrecy cannot be guaranteed at all times. Therefore, we resort to secrecy outage probability as the performance metric. We provide accurate approximation in closed-form for the secrecy outage probability.
- No CSI: This scenario addresses the cases where feedback of instantaneous CSI is either costly or infeasible [180, 181]. Therefore, Alice only has channel statistics of the users. Besides secrecy outage probability, another relevant metric is reliability outage, which we analytically characterized in closed-form.

Additionally, besides the mathematical framework developed for this analysis, another contribution is the extensive numerical results and discussions provided herein. We show that secure FD relaying is feasible in all scenarios under consideration, even though our results show that the self-interference at the relay considerably affects performance. Therefore, the better the isolation and cancellation employed at the relay, the higher is the security achieved. Additionally, we also investigate the impact of the number of antennas at Eve on the overall performance of each scenario. All in all, we demonstrate that even though experiencing strong self-interference FD relaying is feasible under secrecy constraints even in the presence of sophisticated multiple antenna eavesdropper.

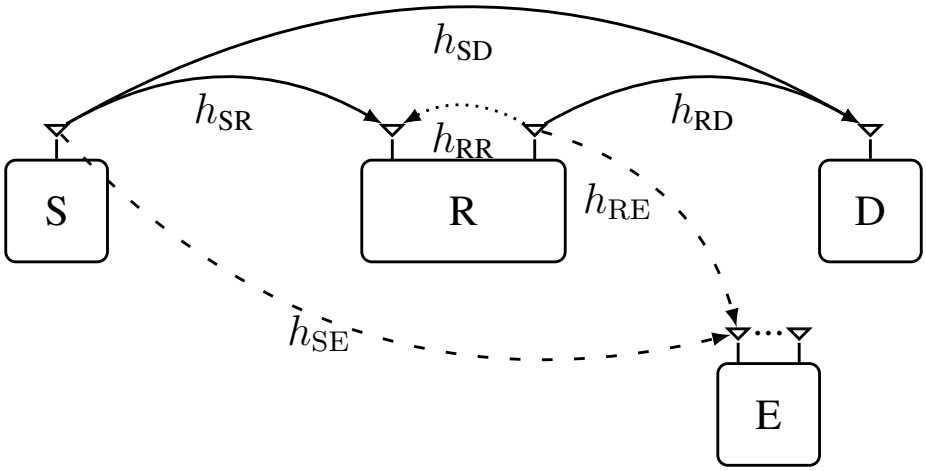

Fig 26. Cooperative network composed by Alice, relay (R) and Bob in the presence of a multi-antenna eavesdropper (E). Notice that Alice and Bob play the role of source (S) and destination (D), respectively, while the relay is a helper chosen by the source.

5.2 System model

Consider a cooperative network consisting of three legitimate single-antenna users: Alice, relay and Bob, communicating in the presence of an eavesdropper (E), which has N_{E} antennas, according to Fig. 26. Following the typical terminology of cooperative communications and introduced in Chapter 2, Alice plays the role of source (S), while Bob represents the destination (D) and the relay (R) is a known node to the source which is chosen as a helper [166, 167]. We assume that Eve is a more resourceful and sophisticated node and thus employs MRC among its multiple antennas, which is a worst case scenario in terms of secrecy for the legitimate link [52, 164, 165].

Moreover, we consider that the relay operates in FD mode and employs the DF protocol. As discussed before, FD cooperative protocols outperform HD one; however, such gains come at a cost of self-interference [26, 33, 37–39, 41, 42]. Please refer to [26, 33, 37–39, 41] for further details on the self-interference mitigation. Nevertheless, due to such high potential, FD communication has received considerable attention in recent years and has become a promising technology to increase spectral efficiency [26, 41, 42, 45–47, 68, 69].

5.2.1 Composite fading channel

Radio links are affected by path loss, large-scale shadowing and multipath fading which are assumed to be mutually independent and multiplicative phenomena [176]. In order to account for these channel impairments we adopt a composite fading distribution, which is widely used in the literature [68, 69, 176–179]. The fading follows Nakagami-m distribution while shadowing is modeled as Log-Normal (LN) random variable (RV) [176, 177]. Thus, the squared-envelop of the channel coefficient follows a Gamma-LN distribution, whose probability density function (PDF) is given as [176]

$$f_R(r) = \int_0^\infty \left(\frac{m}{\omega}\right)^m \frac{r^{m-1}}{\Gamma(m)} \exp\left(-\frac{m}{\omega}r\right) \frac{\xi}{\sqrt{2\pi}\sigma\omega} \exp\left[-\frac{\left(\xi \ln\omega - \mu_{\Omega_p}\right)^2}{2\sigma^2_{\Omega_p}}\right] \mathrm{d}\omega, \quad (93)$$

where m is the shape parameter of the Nakagami-m distribution, $\xi = \ln(10)/10$, Ω_p is the mean squared-envelop, μ_{Ω_p} and σ_{Ω_p} is the mean and standard deviation of Ω_p, respectively.

Moreover, as proposed in [177], the composite squared envelop is well approximated by a single LN RV, whose parameters depend on the actual distribution and are defined as: shape $\mu_{\mathrm{dB}} = \xi\left[\psi(m) - \ln(m)\right] + \mu_{\Omega_p}$ and log-scale $\sigma^2_{\mathrm{dB}} = \xi^2\zeta(2, m) + \sigma^2_{\Omega_p}$.

Let us introduce next the framework to calculate the sum of LN RVs, which will be useful as we shall see in the next sections.

Sum of LN RVs

Motivated by the fact that the density of $Z = \sum_k \gamma_{\mathrm{ij}_k}$, a RV representing the sum of k independent LN RVs, has no exact closed-form expression [182–186] and that its distribution is heavy-tailed and positively skewed [187], we resort to an approximation of the sum of LN RVs by a single LN RV [184]. To do so, we employ higher order statistics to recover the distribution of the sum of LN RVs, namely cumulant-based framework. Moreover, we resort to the cumulant-based framework due to the following reasons: *i)* cumulants are easy-to-compute due to the additivity property; *ii)* the original parameters of the network are given explicitly in the expressions (numerical methods are often

required in order to obtain the parameters of the approximated PDF, see for instance [184, 188, 189]); and *iii)* this approximation offers a good match for the scenarios under consideration, as we shall see next.

In what follows, let us introduce some definition related to the cumulants and their properties.

Definition 5.1. *Let $Z = \sum_k \gamma_{ij_k}$ be a RV representing the sum of k independent LN RVs, and $\iota = \sqrt{-1}$ be the imaginary unity. Then, the characteristic function of Z is the function $\Psi : \mathbb{R} \to \mathbb{C}$, which is defined as [130, Ch. 5]*

$$\Psi_Z(\omega) = \mathrm{E}\left[e^{\iota\,\omega Z}\right]. \tag{94}$$

The corresponding n-th cumulant is obtained from higher order derivatives of (94) as shown next [130, 143, 190, Ch. 26].

Lemma 5.1 (**Cumulants of a RV**). *Let Z be a RV and $\Psi_Z(\omega)$ its CF. The nth cumulant is denoted by κ_n where $n \in \mathbb{N}$. Provided that the nth moment exists and is finite; then $\Psi_Z(\omega)$ is differentiable n times. Therefore,*

$$\kappa_n = \frac{1}{\iota^n}\left[\frac{\partial^n}{\partial\omega^n}\ln\Psi_Z(\omega)\right]_{\omega=0}. \tag{95}$$

Proof. See [143, Ch. 26] and [190]. □

Remark 5.1. ***Relation between cumulants and moments*** *The cumulant generating function can be written as the logarithm of the moment generating function, which allows us to simply write the cumulants as a function of the raw moments [143, Ch. 26][190], such that the first cumulant is $\kappa_1 = \mathrm{E}[W]$ while the second is given as $\kappa_2 = \mathrm{E}\left[W^2\right] - \mathrm{E}[W]^2$ [143, Ch. 26][190], where W is a RV distributed as $W \sim \mathsf{LN}(\mu, \sigma)$, whose moment generating function is [130]*

$$\mathrm{E}[W^n] \triangleq \exp\left(n\,\mu + \frac{n^2\,\sigma^2}{2}\right). \tag{96}$$

Definition 5.2 (**Cumulants additivity property**). *Let X and Y be two independent RVs, whose cumulants are κ_n^X and κ_n^Y, respectively. Then, the cumulants of the sum of $X + Y$ are the sum of the individual cumulants, therefore $\kappa_n^{X+Y} \triangleq \kappa_n^X + \kappa_n^Y$ [191].*

Resorting to the approximation of the sum of LN RVs by a single LN RV [184], we estimate the parameters of the single LN RV from the cumulants as [143, 190, Ch. 26]

$$\mu = \ln\left(\frac{\kappa_1^2}{\sqrt{\kappa_1^2+\kappa_2}}\right), \text{ and } \sigma^2 = \ln\left(1+\frac{\kappa_2}{\kappa_1^2}\right), \tag{97}$$

where μ is the mean and σ^2 is the variance of the equivalent $\mathsf{Normal}(\mu, \sigma^2)$ distribution in the logarithmic scale.

Remark 5.2. *It is noteworthy that the sum of LN RVs is still an open problem, several approximations have been proposed over the years [182–186, 188, 189, 192]. For instance, [178, 183] give an overview of the most known methods, while [68, 69, 179, 184–186, 188] rely on higher order statistics to approximate the sum of LN RVs. We recall that some of those methods resort to numerical methods to determine the parameters of the approximated PDF, while the cumulant-based framework the parameters of the approximated PDF are a function of the original parameters of the network.*

In what follows, we provide an example of the cumulant-based framework. Fig. 27 depicts the approximated CDF of the sum of $N \in \{1, 2, 3, 4\}$ LN RVs, whose parameters are obtained from (97). We assume $m = 4$, $\mu_{\Omega_p} = 0$ dB and $\sigma_{\Omega_p} = 8$ dB. Notice that the sum is tight, especially at the tail of the CDF, for a small number of terms in summation. As N grows large, the cumulant-based approximation becomes loose at the head portion of the CDF, while still matches at the extreme portion of the tail of the CDF.

It is noteworthy that a given approximation may be more suitable than other depending on the intended application. For example, when the sum of LN RVs arises from various signal components, and the performance metric is outage probability, then the tail of the CDF needs to be computed accurately as pointed out in [188].

5.2.2 Secure cooperative communication: channel model

The DF protocol can be decomposed into two phases: broadcast and multiple access. In the first phase, the source broadcasts its message to relay and destination. Differently from HD cooperative schemes, the multiple access phase starts

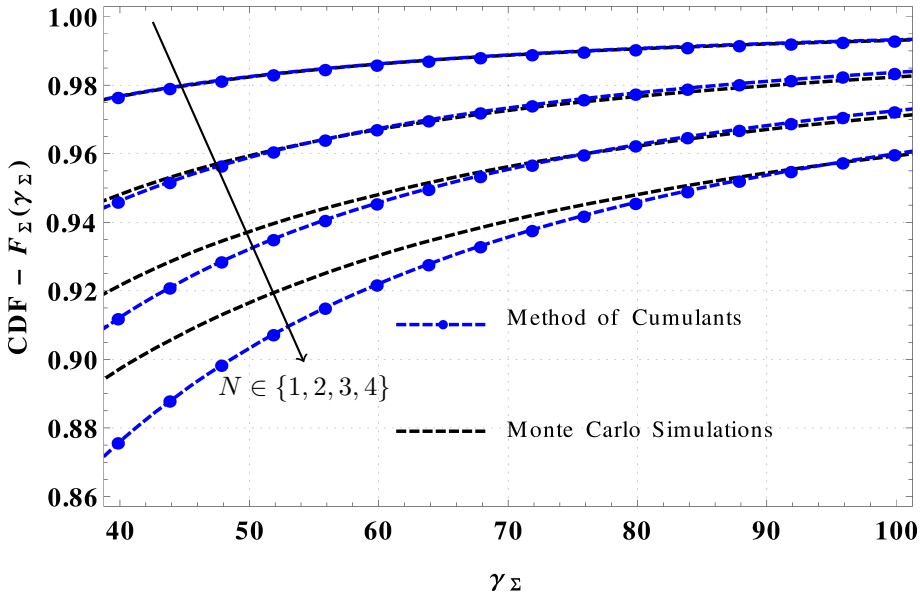

Fig 27. Approximated CDF of the sum $N \in \{1,2,3,4\}$ LN RVs. Notice that Monte Carlo simulations are shown as reference (dashed lines). The blue lines represent the cumulant-based approximation.

simultaneously with the broadcast phase under the FD mode, in which the relay forwards the received message to the destination. Thus, the received signal at the relay is

$$y_{\mathrm{SR}} = \sqrt{P_{\mathrm{S}} d_{\mathrm{SR}}^{-\nu}}\, h_{\mathrm{SR}} \cdot x + \sqrt{P_{\mathrm{R}}\, \delta}\, h_{\mathrm{RR}} \cdot \tilde{x} + w_{\mathrm{R}}, \tag{98}$$

while the received signal at the destination is

$$y_{\mathrm{SD}} = \sqrt{P_{\mathrm{S}} d_{\mathrm{SD}}^{-\nu}}\, h_{\mathrm{SD}} \cdot x + \sqrt{P_{\mathrm{R}}\, d_{\mathrm{RD}}^{-\nu}}\, h_{\mathrm{RD}} \cdot \tilde{x} + w_{\mathrm{D}}, \tag{99}$$

where h_{ij}, $\mathrm{i} \in \{\mathrm{S},\mathrm{R}\}$ and $\mathrm{j} \in \{\mathrm{R},\mathrm{D}\}$, denotes channel coefficient, P_i is the transmit power, d_{ij} represents the distance between the nodes i and j, and ν denotes the path loss exponent. Additionally, w_{j} is zero-mean complex Gaussian noise with variance $\sigma_w^2 = 1$. In addition, x represents the transmitted symbol with unitary energy, while $\tilde{x}$ is the transmitted symbol re-encoded by the relay.

Remark 5.3 (Encoding at the relay:). *A more detailed description of the decoding/encoding scheme will be given later, but it is noteworthy that x and $\tilde{x}$*

are not identical once the relay can use a different codeword from the source and not even when source and relay use the same codebook due to delay. Notice that the message is divided into L blocks, as shown in Fig. 5.

Remark 5.4 (**Processing delay:**). *Due to the inherent characteristics of the encoding/decoding scheme we adopt. Then, $\tilde{x}$ is delayed compared to x [42, 108] such that $\tilde{x}[l] = x[l-\tau]$, where $1 \leq l \leq L$ and τ represents the processing and block delay $\tau \geq 1$ blocks, which we assume hereafter to be $\tau = 1$. As pointed out in [42] this delay is large enough to guarantee that the simultaneously received signals are uncorrelated, and therefore can be jointly decoded.*

A first analysis on such decoding schemes for FD relaying suffering from residual self-interference is done in [45], which is later extended in [47], where the authors generalize the backward decoding scheme for any delay and number of blocks and show that performance is not affected for large L.

Further, consider all channels as quasi-static and follow composite Nakagami-m Log-Normal distribution, whose squared-envelop is given by (93). Moreover, the relay suffers from self-interference, which we model as a composite fading channel denoted by h_{RR}, and δ represents the overall self-interference attenuation factor. Thus, we recall that the composite fading channel model adopted allows us to emulate different conditions of (non-) LoS and its effects on the residual self-interference [41, 45]. Additionally, since all RVs are independent, the instantaneous SNRs of the legitimate links are LN distributed as $\Gamma_{\mathrm{ij}} \sim \mathsf{LN}(\mu_{\mathrm{ij}}, \sigma_{\mathrm{ij}})$ [177]. The SINR at the relay is $\Gamma_{\mathrm{R}} = \dfrac{\Gamma_{\mathrm{SR}}}{\Gamma_{\mathrm{RR}}}$, which is also a LN RV defined as $\Gamma_{\mathrm{R}} \sim \mathsf{LN}(\mu_{\mathrm{R}}, \sigma_{\mathrm{R}})$, where $\mu_{\mathrm{R}} = \mu_{\mathrm{SR}} - \mu_{\mathrm{RR}}$ and $\sigma_{\mathrm{R}} = (\sigma_{\mathrm{SR}}^2 + \sigma_{\mathrm{RR}}^2)^{\frac{1}{2}}$ [130]. Given that the moment generation function of LN RVs is known in closed-form, the first two cumulants of Γ_{ij} can be readily attained through Lemma 5.1 as κ_1^{ij} and κ_2^{ij}. With that and relying on the additivity property [130], we obtain the cumulants of the overall SNR at the destination, $\Gamma_{\mathrm{D}} = \Gamma_{\mathrm{SD}} + \Gamma_{\mathrm{RD}}$, and then with help of (97) the sum of two LN RVs can be simply written as a single LN RV as $\Gamma_{\mathrm{D}} \sim \mathsf{LN}(\mu_{\mathrm{D}}, \sigma_{\mathrm{D}})$.

Eavesdropper channel

The eavesdropper is a more resourceful node compared to the legitimate nodes and its intention is to attack the cooperative network by eavesdropping. Such

assumption allows us to evaluate the worst case for the legitimate channel, since the legitimate user has unfavorable conditions compared to the eavesdropper. Further, the eavesdropper is equipped with N_{E} antennas and applies MRC to the received signals. Bearing this in mind, the $N_{\mathrm{E}} \times 1$ received signal can be represented by

$$\mathbf{y}_{\mathrm{SE}} = \sqrt{P_{\mathrm{S}} d_{\mathrm{SE}}^{-\nu}}\, \mathbf{h}_{\mathrm{SE}} \cdot \mathbf{x} + \sqrt{P_{\mathrm{R}}\, d_{\mathrm{RE}}^{-\nu}}\, \mathbf{h}_{\mathrm{RE}} \cdot \tilde{\mathbf{x}} + \mathbf{w}_{\mathrm{E}}, \tag{100}$$

where $\mathbf{h}_{\mathrm{ij}}$, $\mathrm{i} \in \{\mathrm{S}, \mathrm{R}\}$ and $\mathrm{j} \in \{\mathrm{E}\}$ denotes the channel coefficients vectors ($N_{\mathrm{E}} \times 1$) at the eavesdropper. Additionally, $\mathbf{w}_{\mathrm{E}}$ ($N_{\mathrm{E}} \times 1$) is zero-mean complex Gaussian noise with unity variance.

From Lemma 5.1 we attain the cumulants of γ_{iE_k}, and then from Definition 5.2, once all RVs are independent, we obtain the cumulants of $\Gamma_{\mathrm{iE}} = \sum_k \gamma_{\mathrm{iE}_k}$ as $N_{\mathrm{E}}\, \kappa_n^{\mathrm{iE}}$, where $i \in \{\mathrm{S}, \mathrm{R}\}$ and $1 \leq k \leq N_{\mathrm{E}}$. Then, since Γ_{SE} and Γ_{RE} are independent we resort again to Definition 5.2 and define the cumulants of $\Gamma_{\mathrm{E}} = \Gamma_{\mathrm{SE}} + \Gamma_{\mathrm{RE}}$ as $\kappa_n = N_{\mathrm{E}}(\kappa_n^{\mathrm{SE}} + \kappa_n^{\mathrm{RE}})$, which allows us to write $\Gamma_{\mathrm{E}} \sim \mathrm{LN}(\mu_{\mathrm{E}}\,, \sigma_{\mathrm{E}})$, whose parameters are $\mu_{\mathrm{E}} = \ln\left(\kappa_1^2\right) - \ln(\sqrt{\kappa_1^2 + \kappa_2})$ and $\sigma_{\mathrm{E}} = \sqrt{\ln\left(\kappa_1^2 + \kappa_2\right) - \ln(\kappa_1^2)}$.

As an example, Fig. 28 shows the approximated CDF of the sum of $N \in \{2, 4\}$ LN RVs, since $N_{\mathrm{E}} \in \{1, 2\}$, for $m = 4$, $\mu_{\Omega_p} = -20$ dB and $\sigma_{\Omega_p} = 12$ dB. Notice that such parameters are commonly used in PHY-security scenarios, and specially the cases involving small cell deployments [52, 56, 158, 179, 188]. For comparison, we numerically approximate the sum of LN RVs by a single LN RV using Monte Carlo simulations and the method FindParameters from Mathematica 9, this result is depicted in Fig. 28 as a dashed line. It is noteworthy that numerical parameter estimation is common in the literature, see for instance [184, 188, 189].

As commented above in Fig 27, the cumulant-based approximation offer a good match for a small number of terms in the summation, which can be also observed in Fig. 28. Moreover, the approximation becomes more tight at the tail of the CDF.

In what follows, we address the encoding and decoding of the FD cooperative network.

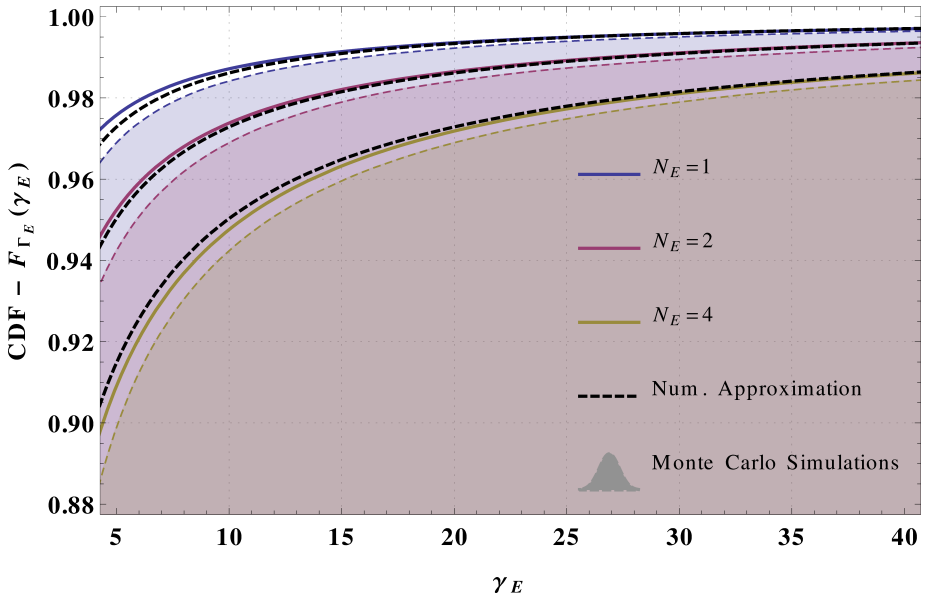

Fig 28. Approximated CDF of the sum of $N \in \{2, 4, 8\}$ LN RVs, thus $N_E \in \{1, 2, 4\}$. Monte Carlo simulations are shown as reference as well as a numerical approximation by a single LN RV.

5.2.3 Encoding and decoding for full-duplex relaying

The DF scheme initially proposed in [108] is extended to fading scenarios in [7, 45] and to secrecy context in [111, 166]. The DF protocol proposed in [108] relies on a combination of block Markov encoding at the source and relay, associated with coding for cooperative multiple access channel and superposition coding [7, 108]. As pointed out in [7] the same achievable rates for the DF protocol proposed in [108] (named irregular encoding and successive decoding [7]) can be achieved through different strategies: regular encoding and sliding-window decoding [109]; and regular encoding and backward decoding [110]. Moreover, as indicated in [7], both strategies are more suitable for quasi-static fading channels, once they are less likely to fail in the intermediate decoding steps.

Therefore, hereafter we assume regular encoding and backward decoding [7, 110, 111][6]. Notice that such strategy is also assumed in [111, 166] for the relay-eavesdropper channel, and [111] additionally provides detailed encod-

[6] Please refer to [7] for further details on regular encoding and backward decoding for the DF protocol, and to [111, Th. 2] for an analysis on the relay-eavesdropper channel.

ing/decoding process and proof of achievability. As aforementioned, Fig. 5 depicts the block transmission scheme with backward decoding where the message is divided into L blocks, notice that even though the relay is delayed by one block with respect to the source, performance is not affected for large L [108]. We recall that the backward decoding scheme is generalized in [47] for any number of delayed and total number of blocks. In that work it is shown that performance is not affected as far the ratio between delay and number of blocks is small.

Lemma 5.2. *The achievable rate of the DF protocol using regular encoding and backward decoding is expressed as*

$$\mathcal{R}_{FD} = \min\left\{\mathcal{R}_{SR}\,,\,\mathcal{R}_{SRD}\right\}, \tag{101}$$

where the achievable rate of the source-relay link is

$$\mathcal{R}_{SR} = \log_2\left(1 + \frac{\gamma_{SR}}{\gamma_{RR}+1}\right), \tag{102}$$

and the achievable rate due to the multiple access phase is

$$\mathcal{R}_{SRD} = \log_2\left(1 + \gamma_{SD} + \gamma_{RD}\right). \tag{103}$$

Proof. Please refer to [7, Sect. IV-B] and [110]. Notice that we account for the self-interference at the relay in (102). □

The destination is able to jointly decode the messages from source and relay in an iterative process dependent of backward decoding [7, 47, 166]. Decoding process serves to combine the transmissions from source and relay at the current time slot using advanced detection techniques and the acquired knowledge from previously received frames [47].

Remark 5.5 (Eavesdropper's achievable rate). *Assuming that the eavesdropper uses the above encoding/decoding process, the achievable rate is* $\mathcal{R}_E = \log_2\left(1 + \gamma_{SE} + \gamma_{RE}\right)$ *[111, Th. 2] and [166].*

5.2.4 Scenarios and assumptions

We investigate the secrecy performance of a cooperative network in three distinct scenarios depending on the availability of CSI at the source:

1. Full CSI: the eavesdropper is part of the network and its active transmissions are monitored [158, 167], therefore the source has CSI of all users and adapt the rate in order to achieve perfect secrecy.
2. Partial CSI: the eavesdropper is a passive and hostile eavesdropper in the network [52, 158, 164, 165], therefore the source has only knows the legitimate channels and perfect secrecy is not guaranteed at all times [158].
3. No CSI: feedback of instantaneous CSI is either costly or infeasible [180, 181] such that no CSI is available, thus, as we shall see next, the source resorts to fixed Wyner codes to secure its communication [180, 181].

5.3 Scenario 1: full CSI - average secrecy rate

Suppose that the source is able to acquire the CSI from the eavesdropper, which is one of the users of the network. For instance, this may be the case when the source wants to communicate privately to a certain user (*i.e.*, a specific subscriber) without being eavesdropped by other legitimate receivers. This scenario represents the active eavesdropping, so that the legitimate users are aware of the eavesdropper presence [164, 165]. Therefore, the source can adapt its transmission rate accordingly in order to achieve perfect secrecy. In such a scenario, the average secrecy capacity is an insightful metric once it quantifies the average secrecy rate [158].

Recall from the secrecy capacity of the non-cooperative wiretap channel is given as the difference between the capacity of the legitimate and eavesdropper's channels, namely $\mathcal{C}_s = \mathcal{C}_{\mathrm{M}} - \mathcal{C}_{\mathrm{E}}$ [157, 158, 161]. Similarly, we can also write the achievable rates of the cooperative wiretap channel as the difference difference between the achievable rates of the the legitimate and eavesdropper's channels as introduced in [111] where the relay-eavesdropper channel as well as the achievable rates of DF and noise forward protocols are introduced. Later, these initial result are extended to a multiple relay settings in [166, 167]. Relying on similar

approach of [111] we write the achievable cooperative secrecy rate as

$$\mathcal{R}_s = \left[\mathcal{R}_{\mathrm{FD}} - \mathcal{R}_{\mathrm{E}}\right]^+, \tag{104}$$

$$= \left[\min\left\{\log_2\left(\frac{1+\frac{\gamma_{\mathrm{SR}}}{\gamma_{\mathrm{RR}}+1}}{1+\gamma_{\mathrm{SE}}+\gamma_{\mathrm{RE}}}\right), \log_2\left(\frac{1+\gamma_{\mathrm{SD}}+\gamma_{\mathrm{RD}}}{1+\gamma_{\mathrm{SE}}+\gamma_{\mathrm{RE}}}\right)\right\}\right]^+ \tag{105}$$

$$= \left[\min\left\{\log_2\left(\frac{1+\gamma_{\mathrm{R}}}{1+\gamma_{\mathrm{E}}}\right), \log_2\left(\frac{1+\gamma_{\mathrm{D}}}{1+\gamma_{\mathrm{E}}}\right)\right\}\right]^+ \tag{106}$$

where $[x]^+ \triangleq \max\{x, 0\}$.

Based on the average rate derivation for traditional relaying in [193] and given the cooperative secrecy rates from [111], and given that all RVs are independent we can rewrite (104) as

$$\mathcal{R}_s = \left[\log_2\left(1+\min\left\{\gamma_{\mathrm{R}}, \gamma_{\mathrm{D}}\right\}\right) - \log_2\left(1+\gamma_{\mathrm{E}}\right)\right]^+, \tag{107}$$

$$= \left[\log_2\left(1+\gamma_{\mathrm{FD}}\right) - \log_2\left(1+\gamma_{\mathrm{E}}\right)\right]^+. \tag{108}$$

Let us introduce here a new RV defined as $\Gamma_{\mathrm{FD}} = \min\{\Gamma_{\mathrm{R}}, \Gamma_{\mathrm{D}}\}$, whose PDF and CDF are given as

$$f_{\Gamma_{\mathrm{FD}}}(\gamma_{\mathrm{FD}}) = \exp\left(-\frac{(\mu_{\mathrm{R}} - \ln(\gamma_{\mathrm{FD}}))^2}{2\sigma_{\mathrm{R}}^2}\right)\frac{\operatorname{erfc}\left(\frac{-\mu_{\mathrm{D}}+\ln(\gamma_{\mathrm{FD}})}{\sqrt{2}\,\sigma_{\mathrm{D}}}\right)}{2\sqrt{2\pi}\,\sigma_{\mathrm{R}}\,\gamma_{\mathrm{FD}}} + \exp\left(-\frac{(\mu_{\mathrm{D}} - \ln(\gamma_{\mathrm{FD}}))^2}{2\sigma_{\mathrm{D}}^2}\right)\frac{\operatorname{erfc}\left(\frac{-\mu_{\mathrm{R}}+\ln(\gamma_{\mathrm{FD}})}{\sqrt{2}\,\sigma_{\mathrm{R}}}\right)}{2\sqrt{2\pi}\,\sigma_{\mathrm{D}}\,\gamma_{\mathrm{FD}}}, \tag{109}$$

$$F_{\Gamma_{\mathrm{FD}}}(z) = 1 - \frac{1}{4}\operatorname{erfc}\left(\frac{-\mu_{\mathrm{R}}+\ln(z)}{\sqrt{2}\,\sigma_R}\right)\operatorname{erfc}\left(\frac{-\mu_{\mathrm{D}}+\ln(z)}{\sqrt{2}\,\sigma_D}\right), \tag{110}$$

where the LN parameters μ_{i} and σ_{i} $i \in \{R, D\}$ are attained through the proposed framework in Section 5.2.1. Notice that $\operatorname{erfc}(\cdot)$ is the complementary error function [143, Eq. 7.1.2]. Thus, we know that Γ_{R} and Γ_{D} are LN distributed, thus the PDF $\Gamma_{\mathrm{FD}} = \min\{\Gamma_{\mathrm{R}}, \Gamma_{\mathrm{D}}\}$ can be readily attained through standard statistical methods [130], which results in (109). Then, by integrating (109) from 0 to z, we attain the CDF of Γ_{FD} as in (110).

The average secrecy rate is given by taking the expected value of (108) over

all possible channel realizations as shown in the following lemma.

Lemma 5.3. *Assuming the non-negativity of the secrecy rate and the independence of RVs, a general from for the average secrecy rate is given as*

$$\overline{\mathcal{R}}_s = \int_0^\infty \int_0^\infty \mathcal{R}_s \, f_{\Gamma_{FD}}(\gamma_{FD}) \, f_{\Gamma_E}(\gamma_E) \, \mathrm{d}\gamma_{FD} \, \mathrm{d}\gamma_E, \tag{111}$$

$$= \frac{1}{\ln 2} \int_0^\infty \frac{F_{\Gamma_E}(\gamma_E)}{1+\gamma_E} \left[1 - F_{\Gamma_{FD}}(\gamma_E)\right] \mathrm{d}\gamma_E. \tag{112}$$

Proof. Let us introduce two new RVs variables that denote the SNR of main and eavesdroppers channels, respectively, Γ_{D} and Γ_{E}, with PDFs $f_{\Gamma_{\mathrm{D}}}(\gamma_{\mathrm{D}})$ and $f_{\Gamma_{\mathrm{E}}}(\gamma_{\mathrm{E}})$, while its CDFs are represented by $F_{\Gamma_{\mathrm{D}}}(\gamma_{\mathrm{D}})$ and $F_{\Gamma_{\mathrm{E}}}(\gamma_{\mathrm{E}})$. Then, averaging the instantaneous secrecy rate in (104) over γ_{D} and γ_{E}, the average secrecy rate is given as

$$\overline{\mathcal{R}}_s = \int_0^\infty \int_0^\infty \mathcal{R}_s \, f_{\Gamma_{\mathrm{D}}}(\gamma_{\mathrm{D}}) \, f_{\Gamma_{\mathrm{E}}}(\gamma_{\mathrm{E}}) \, \mathrm{d}\gamma_{\mathrm{D}} \, \mathrm{d}\gamma_{\mathrm{E}}, \tag{113}$$

$$= \int_0^\infty \Xi f_{\Gamma_{\mathrm{D}}}(\gamma_{\mathrm{D}}) \, \mathrm{d}\gamma_{\mathrm{D}}. \tag{114}$$

Then, by applying integration by parts into Ξ we attain

$$\Xi = \int_0^{\gamma_{\mathrm{D}}} \left[\log_2(1+\gamma_{\mathrm{D}}) - \log_2(1+\gamma_{\mathrm{E}})\right] f_{\Gamma_{\mathrm{E}}}(\gamma_{\mathrm{E}}) \, \mathrm{d}\gamma_{\mathrm{E}} \tag{115}$$

$$= \log_2(1+\gamma_{\mathrm{D}}) \, F_{\Gamma_{\mathrm{E}}}(\gamma_{\mathrm{D}}) - \int_0^{\gamma_{\mathrm{D}}} \log_2(1+\gamma_{\mathrm{E}}) \, f_{\Gamma_{\mathrm{E}}}(\gamma_{\mathrm{D}}) \, \mathrm{d}\gamma_{\mathrm{E}} \tag{116}$$

$$= \log_2(1+\gamma_{\mathrm{D}}) \, F_{\Gamma_{\mathrm{E}}}(\gamma_{\mathrm{D}}) - \left(\log_2(1+\gamma_{\mathrm{D}}) \, F_{\Gamma_{\mathrm{E}}}(\gamma_{\mathrm{D}}) - \frac{1}{\ln 2} \int_0^{\gamma_{\mathrm{D}}} \frac{F_{\Gamma_{\mathrm{E}}}(\gamma_{\mathrm{E}})}{1+\gamma_{\mathrm{E}}} \, \mathrm{d}\gamma_{\mathrm{E}} \right) \tag{117}$$

$$= \frac{1}{\ln 2} \int_0^{\gamma_{\mathrm{D}}} \frac{F_{\Gamma_{\mathrm{E}}}(\gamma_{\mathrm{E}})}{1+\gamma_{\mathrm{E}}} \, \mathrm{d}\gamma_{\mathrm{E}}. \tag{118}$$

Then, plugging (118) into (114) and changing the order of integration, we arrive

at

$$\overline{\mathcal{R}}_s = \int_0^{\infty} \left(\frac{1}{\ln 2} \int_0^{\gamma_{\mathrm{D}}} \frac{F_{\Gamma_{\mathrm{E}}}(\gamma_{\mathrm{E}})}{1+\gamma_{\mathrm{E}}} \mathrm{d}\gamma_{\mathrm{E}} \right) f_{\Gamma_{\mathrm{D}}}(\gamma_{\mathrm{D}}) \mathrm{d}\gamma_{\mathrm{D}} \tag{119}$$

$$= \frac{1}{\ln 2} \int_0^{\infty} \frac{F_{\Gamma_{\mathrm{E}}}(\gamma_{\mathrm{E}})}{1+\gamma_{\mathrm{E}}} \left(\int_{\gamma_{\mathrm{E}}}^{\infty} f_{\Gamma_{\mathrm{D}}}(\gamma_{\mathrm{D}}) \mathrm{d}\gamma_{\mathrm{D}} \right) \mathrm{d}\gamma_{\mathrm{E}} \tag{120}$$

$$= \frac{1}{\ln 2} \int_0^{\infty} \frac{F_{\Gamma_{\mathrm{E}}}(\gamma_{\mathrm{E}})}{1+\gamma_{\mathrm{E}}} \left[1 - F_{\Gamma_{\mathrm{D}}}(\gamma_{\mathrm{E}}) \right] \mathrm{d}\gamma_{\mathrm{E}}. \tag{121}$$

□

From (110) we known the CDFs of Γ_{FD} and Γ_{E}, then with help of Lemma 5.3 we define the the average secrecy rate (bits/s/Hz) is

$$\overline{\mathcal{R}}_s = \frac{1}{\ln 2} \int_0^{\infty} \frac{\operatorname{erfc}(\eta_{\mathrm{E}}) \operatorname{erfc}(\eta_{\mathrm{D}}) \operatorname{erfc}(\eta_{\mathrm{R}})}{8(1+z)} \mathsf{d}z \,, \tag{122}$$

where $\eta_{\mathrm{E}} = \dfrac{\mu_{\mathrm{E}} - \ln(z)}{\sqrt{2}\,\sigma_{\mathrm{E}}}$, $\eta_{\mathrm{D}} = \dfrac{-\mu_{\mathrm{D}} + \ln(z)}{\sqrt{2}\,\sigma_{\mathrm{E}}}$ and $\eta_{\mathrm{R}} = \dfrac{-\mu_{\mathrm{R}} + \ln(z)}{\sqrt{2}\,\sigma_{\mathrm{R}}}$.

Nevertheless, (122) does not have a closed-form solution, and therefore we proposed in the following theorem an approximation to the integral in (122) based on Gauss-Laguerre quadrature [143, Ch. 25.4]. As we shall see in the next section, the proposed approximation proves to be quite accurate.

Remark 5.6. *It is noteworthy that Gauss quadrature methods offer high accuracy, since such methods seek to obtain the best numerical estimate of an integral by selecting optimal abscissas and summation weights in order to evaluate the given function $f(x)$ [194]. Moreover, Gauss quadrature have distinct integration intervals, which allow us to choose the method that best fits the function $f(x)$. For instance, in this work the integration interval is $[0\,, \infty)$, therefore we resort to Gauss-Laguerre quadrature [143, Ch. 25.4], and the abscissas are obtained through Laguerre polynomials [143, Ch. 25.4]. While on the integration interval of $(-\infty\,, \infty)$, Gauss-Hermite quadrature [143, Ch. 25.4] is more suitable. Both methods are discussed in more details as we shall see next.*

In what follows, we assume that perfect CSI at transmitters is available, so

that the average secrecy rate in bits/s/Hz is given by

$$\overline{\mathcal{R}}_s \simeq \frac{1}{\ln 2} \sum_{k=1}^{K} \frac{\omega_k^{\mathrm{L}}\, e^{\chi_k^{\mathrm{L}}}}{8} \operatorname{erfc}\left(\eta_{\mathrm{E}}'\right) \operatorname{erfc}\left(\eta_{\mathrm{R}}'\right) \operatorname{erfc}\left(\eta_{\mathrm{D}}'\right), \tag{123}$$

where η_{i}' with $\mathrm{i} \in \{\mathrm{R}, \mathrm{D}, \mathrm{E}\}$ is written as in η_{i} but replacing z by $e^{\chi_k^{\mathrm{L}}} - 1$, and K is the order of the Laguerre polynomial. Then, we resort to Lemma 5.3 and to Gauss-Laguerre quadrature [143, Ch. 25.4] in order to obtain (123), where χ_k^{L} are the roots of the Laguerre polynomial while

$$\omega_k^{\mathrm{L}} = \frac{\chi_k^{\mathrm{L}}}{\left((K+1)\, \mathrm{L}_{K+1}(\chi_k^{\mathrm{L}})\right)^2}, \tag{124}$$

represent the weights of the Gauss-Laguerre quadrature [143, Ch. 25.4]. Notice that the truncation error can be evaluated analytically, assuming that the $2K$-th derivative exists, as [143, Eq. 25.4.45]

$$\varepsilon = \frac{(K!)^2}{(2K)!}\, f^{(2K)}(\chi_k), \tag{125}$$

where χ_k lies somewhere in the range $0 \leq \chi_k < \infty$, and may be used as a conservative design criterion.

5.4 Scenario 2: partial CSI - secrecy outage probability

Now suppose that the source has no knowledge of the eavesdropper's CSI except for channel statistics, this scenario corresponds to the case where the eavesdropper is a passive and malicious user of the network [52, 158, 164, 165]. Thus, in order to protect its transmission from a possible inimical attack, the source communicates with the destination with a constant secrecy rate $R_s > 0$, which yields a certain secrecy outage probability[7]. Note that the source assumes that the eavesdropper' secrecy rate is $\mathcal{R}_{\mathrm{E}} = \mathcal{R}_{\mathrm{FD}} - R_s$, thus security is compromised as soon as $\mathcal{C}_{\mathrm{E}} > \mathcal{R}_{\mathrm{E}}$. Otherwise, perfect secrecy is assured. Then, secrecy outage probability is the appropriated metric to evaluate the performance of a quasi-

[7] In order to avoid confusion it is noteworthy that the secrecy capacity is denoted by the calligraphic letter $\mathcal{C}$ and the secrecy achievable rate by letter $\mathcal{R}$, while the attempted transmission rate is represented by the letter R.

static fading wiretap channel when the transmitter has no CSI and the receivers have CSI of their own channels only [46, 165].

Bearing this in mind, let $\Gamma_{\mathrm{FD}} = \min\{\Gamma_{\mathrm{R}}, \Gamma_{\mathrm{D}}\}$, then based on [158] the probability of non-zero secrecy rate is given as

$$\begin{aligned}
\Pr[\mathcal{R}_s > 0] &= \Pr\left[\log_2\left(\frac{1+\gamma_{\mathrm{FD}}}{1+\gamma_{\mathrm{E}}}\right) > 0\right] && (126)\\
&= \Pr[\gamma_{\mathrm{FD}} > \gamma_{\mathrm{E}}] \\
&= 1 - \Pr[\gamma_{\mathrm{FD}} < \gamma_{\mathrm{E}}] && (127)\\
&= 1 - \int_0^{\infty} F_{\mathrm{FD}}(z) f_{\mathrm{E}}(z) \mathsf{d}z && (128)\\
&= \int_{-\infty}^{\infty} \frac{e^{-t^2}}{4\sqrt{\pi}} \operatorname{erfc}\left(\frac{\mu_{\mathrm{E}} - \mu_{\mathrm{D}} + \sqrt{2}\,\sigma_{\mathrm{E}}\, t}{\sqrt{2}\,\sigma_{\mathrm{D}}}\right) \operatorname{erfc}\left(\frac{\mu_{\mathrm{E}} - \mu_{\mathrm{R}} + \sqrt{2}\,\sigma_{\mathrm{E}}\, t}{\sqrt{2}\,\sigma_{\mathrm{R}}}\right) \mathsf{d}t. && (129)
\end{aligned}$$

where $\eta_{\mathrm{E}} = \frac{\mu_{\mathrm{E}} - \ln(z)}{\sqrt{2}\,\sigma_{\mathrm{E}}}$, $\eta_{\mathrm{D}} = \frac{-\mu_{\mathrm{D}} + \ln(z)}{\sqrt{2}\,\sigma_{\mathrm{D}}}$ and $\eta_{\mathrm{R}} = \frac{-\mu_{\mathrm{R}} + \ln(z)}{\sqrt{2}\,\sigma_{\mathrm{R}}}$. Unfortunately (128) has no closed-form solution, therefore we resort to semi-analytical solution based on Gauss-Hermite quadrature [143, Ch. 25.4]. Thus, the weights of the Hermite polynomial are given as $\omega_k^{\mathrm{H}} = \sqrt{\pi}\, 2^{K-1}\, K! \,/\, \left(K^2\, \mathrm{H}_{K-1}(\chi_k^{\mathrm{H}})\right)$, where χ_k^{H} are the roots of Hermite polynomial of order K [143, Ch. 25.4]. Bearing this in mind and applying the following substitution $t = -\frac{\mu_{\mathrm{E}} - \ln(z)}{\sqrt{2}\,\sigma_{\mathrm{E}}}$ into (128) we readily attain (129) which can be easily put in the Gauss-Hermite quadrature format. Thus, the probability of strictly positive secrecy rate in composite fading channels is given as

$$\Pr[\mathcal{R}_s > 0] \simeq \sum_{k=0}^{K} \frac{\omega_k^{\mathrm{H}}}{4\sqrt{\pi}} \operatorname{erfc}(\eta_{\mathrm{DE}}) \operatorname{erfc}(\eta_{\mathrm{RE}}), \tag{130}$$

where $\eta_{\mathrm{DE}} = \dfrac{\mu_{\mathrm{E}} - \mu_{\mathrm{D}} + \sqrt{2}\,\sigma_{\mathrm{E}}\, \chi_k^{\mathrm{H}}}{\sqrt{2}\,\sigma_{\mathrm{D}}}$ and $\eta_{\mathrm{RE}} = \dfrac{\mu_{\mathrm{E}} - \mu_{\mathrm{R}} + \sqrt{2}\,\sigma_{\mathrm{E}}\, \chi_k^{\mathrm{H}}}{\sqrt{2}\,\sigma_{\mathrm{R}}}$. With ω_k^{H} and χ_k^{H} being the weights and roots of the Hermite polynomial, respectively, of the Gauss-Hermite quadrature [143, Ch. 25.4].

Next, we determine the secrecy outage probability as $\mathcal{O}_{\mathrm{P}} = \Pr[\mathcal{R}_s < R_s]$. Thus, an outage event occurs whenever the instantaneous secrecy rate $\mathcal{R}_s$ falls

bellow the target secrecy rate R_s fixed by the source. Thus, assuming the non-negativity of the secrecy rate and that only CSI of the legitimate channel is available at the transmitter, we can define the secrecy outage probability, $\mathcal{O}_{\mathrm{P}}$, as the probability that the instantaneous achievable rate $\mathcal{R}_s$ falls below the given secrecy transmission rate R_s in bits/s/Hz. Then, based on [111, 158], we can define the secrecy outage probability under composite fading channels as

$$\begin{aligned}\mathcal{O}_P &= \Pr\left[\mathcal{R}_s < R_s\right] \\ &= \Pr\left[\log_2\left(1+\gamma_{\mathrm{FD}}\right) - \log_2\left(1+\gamma_{\mathrm{E}}\right) < R_s\right] \\ &= \int_0^{\infty} F_{\Gamma_{\mathrm{FD}}}(2^{R_s}(1+z)-1) f_{\mathrm{E}}(z) \mathrm{d}z \end{aligned} \tag{131}$$

Note that the CDF of Γ_{FD} is given in (110). However, (131) does not have a closed-form solution. Therefore, we resort to Gauss-Hermite quadrature [143, Ch. 25.4], and then the secrecy outage probability can be written as

$$\mathcal{O}_{\mathrm{P}} \simeq 1 - \sum_{k=1}^{K} \frac{\omega_k^{\mathrm{H}} \operatorname{erfc}\left(\frac{-\mu_{\mathrm{D}}+\ln(\upsilon_{\mathrm{E}})}{\sqrt{2}\,\sigma_{\mathrm{D}}}\right) \operatorname{erfc}\left(\frac{-\mu_{\mathrm{R}}+\ln(\upsilon_{\mathrm{E}})}{\sqrt{2}\,\sigma_{\mathrm{R}}}\right)}{4\sqrt{\pi}}, \tag{132}$$

where $\upsilon_{\mathrm{E}} = 2^{R_s}\left(\exp\left(\mu_{\mathrm{E}} + \sqrt{2}\sigma_{\mathrm{E}}\,\chi_k^{\mathrm{H}}\right)+1\right) - 1$.

5.5 Scenario 3: no CSI - secrecy outage probability and reliability probability

In this scenario no CSI is available except for the channel statistics, then in the absence of instantaneous CSI, the transmitter cannot adapt its code rate. Such situation may occur when feedback of instantaneous CSI is either too costly or infeasible [180, 181]. In such condition a *à priori* fixed Wyner code is used for all channel conditions, which guarantees perfect secrecy and small error probabilities for a subset of channel states as discussed in [181, Lemma 1]. To do so, the source assumes a constant secrecy rate R_s, while attempting to transmit at a fixed rate R_{FD} such that $R_{\mathrm{FD}} \geq R_s$. Thus, the eavesdropper equivocation rate can be then written as $R_{\mathrm{E}} = R_{\mathrm{FD}} - R_s$ [180].

In this context, two conditions arise in order to guarantee secrecy and relia-

bility [180]:

1. the achievable rate of the legitimate link has to be larger than R_{FD}; and
2. eavesdropper's equivocation rate is less than $R_{\mathrm{FD}} - R_s$.

These conditions guarantee that there is a Wyner code that ensure a reliable and secure communication link [181][8]. Given the two conditions, in this scenario we consider secrecy outage and reliability outage as the performance metrics [180, 181]. Thus, the overall secrecy outage probability is the union of the following events:

– reliability outage - the achievable rate of the legitimate link falls bellow R_{FD}, which in our setting becomes $\mathcal{R}_{\mathrm{DF}} < R_{\mathrm{FD}}$; and
– secrecy outage - eavesdropper's equivocation rate is greater than secrecy gap $(R_{\mathrm{FD}} - R_s)$, equivalently $\mathcal{R}_{\mathrm{E}} > R_{\mathrm{FD}} - R_s$.

Thus, the overall outage probability is given by the following lemma.

Lemma 5.4. *The overall outage probability when no CSI is available at the transmitter and fixed Wyner coding is employed is composed of the union of two independent events: secrecy and reliability outage. Thus, the overall outage probability is given as*

$$\mathcal{O}_N = \Pr\left[\mathcal{R}_{FD} < R_{FD} \bigcup \mathcal{R}_E > R_{FD} - R_s\right] \tag{133}$$

$$= \Pr\left[\mathcal{R}_{FD} < R_{FD}\right] + \Pr\left[\mathcal{R}_E > R_{FD} - R_s\right] - \Pr\left[\mathcal{R}_{FD} < R_{FD}\right] \Pr\left[\mathcal{R}_E > R_{FD} - R_s\right] \tag{134}$$

Proof. Please see [181, Lemma 1] and [180, Sect. IV-A] □

From Lemma 5.4 and under the assumption of no availability of CSI at the source, the overall outage probability becomes

$$\mathcal{O}_{\mathrm{N}} = F_{\Gamma_{\mathrm{FD}}}(\epsilon) + 1 - F_{\Gamma_{\mathrm{E}}}(\varepsilon) - F_{\Gamma_{\mathrm{FD}}}(\epsilon)(1 - F_{\Gamma_{\mathrm{E}}}(\varepsilon)) \tag{135}$$

$$= 1 - F_{\Gamma_{\mathrm{E}}}(\varepsilon) + F_{\Gamma_{\mathrm{FD}}}(\epsilon) F_{\Gamma_{\mathrm{E}}}(\varepsilon)\,, \tag{136}$$

$$= 1 - \frac{1}{8}\operatorname{erfc}(\vartheta_{\mathrm{R}})\operatorname{erfc}(\vartheta_{\mathrm{D}})\operatorname{erfc}(\vartheta_{\mathrm{E}})\,, \tag{137}$$

[8] Please refer to [180, 181] for further details on fixed Wyner codes and code construction.

where $\vartheta_{\mathrm{R}} = (-\mu_{\mathrm{R}} + \ln(\epsilon))/(\sqrt{2}\sigma_{\mathrm{R}})$, $\vartheta_{\mathrm{D}} = (-\mu_{\mathrm{D}} + \ln(\epsilon))/(\sqrt{2}\sigma_{\mathrm{D}})$ and $\vartheta_{\mathrm{E}} = (-\mu_{\mathrm{E}} + \ln(\varepsilon))/(\sqrt{2}\sigma_{\mathrm{E}})$, with $\epsilon = 2^{R_{\mathrm{FD}}} - 1$ and $\varepsilon = 2^{R_{\mathrm{FD}} - R_s} - 1$. Then applying the CDFs of Γ_{FD} and Γ_{E} into (136) and after few algebraic manipulations we attain (137).

5.6 Numerical results and simulations

We assume that the source, the relay and destination are in a straight line, and the relay is positioned at the center. We assume that all nodes are in an indoor environment of small cells deployment as in [195–197], therefore we set the distance between source and destination at 10m, and we consider the relay in between source and destination and equidistant from both. Additionally, we assume a path loss exponent of $\nu = 3$ as well as unitary bandwidth. We assume that all channels experience some LoS, and therefore undergo fading with $m = 16$ (which corresponds to a Rice channel with factor of 14.8 dB), while the shadowing standard deviation is $\sigma_{\Omega_p} = 6$ dB [195–197]. In this setting, we consider that the legitimate cooperative network perceives stronger LoS component than the eavesdropper. Therefore, we assume that the eavesdropper perceives a more harsh environment, since it may not be in same the indoor environment as the legitimated nodes. Thus, we consider $\nu = 4$, $m = 4$ and $\sigma_{\Omega_p} = 12$ dB. We assume that the polynomial order of $K = 24$ since it presents great accuracy. We recall that the error can be analytically estimated which is another advantage of such quadrature methods [143]. All Monte Carlo simulations are performed with 10^6 realizations. Moreover, we consider equal power allocation so that the total power is given as $P_{\mathrm{S}} = P_{\mathrm{R}} = P$. As pointed out in [48], the residual self-interference component is mostly dominated by the shadowing, since most of the LoS is attenuated through antenna isolation. Thus, we model the residual self-interference with $m = 1$ and $\sigma_{\Omega_p} = 10$ dB, and for distinct values of δ.

5.6.1 Average secrecy rate

Fig. 29 shows the average secrecy rate as a function of transmit power P in dBm for different values of self-interference cancellation for $N_{\mathrm{E}} = 2$. Eavesdropper's average SNR is set to $\mu_{\mathrm{E}} = -3.70$ and $\sigma_E = 2.68$, which means that $\mu_{\Omega_p} = -20$ dB and $\sigma_{\Omega_p} = 12$ dB so that the eavesdropper is closer to source and

relay than to the destination. Notice that the more sophisticated is the self-interference cancellation at the relay (lower values of δ), higher is the achievable average secrecy rate. For instance, at high SNR, the average secrecy rate rises about 25% with the reduction of the self-interference from -80 dB to -90 dB. Even though sophisticated interference mitigation schemes have been recently proposed, such cancellation levels, in the order of -90 dB, are still a challenging task to achieve [26, 34].

Next, we investigate the effect on performance of a more sophisticated adversary, thus we assume that the eavesdropper may have $N_{\mathrm{E}} \in \{1, 4\}$ antennas. Then, Fig. 30 shows the average secrecy rate as a function of the transmit power

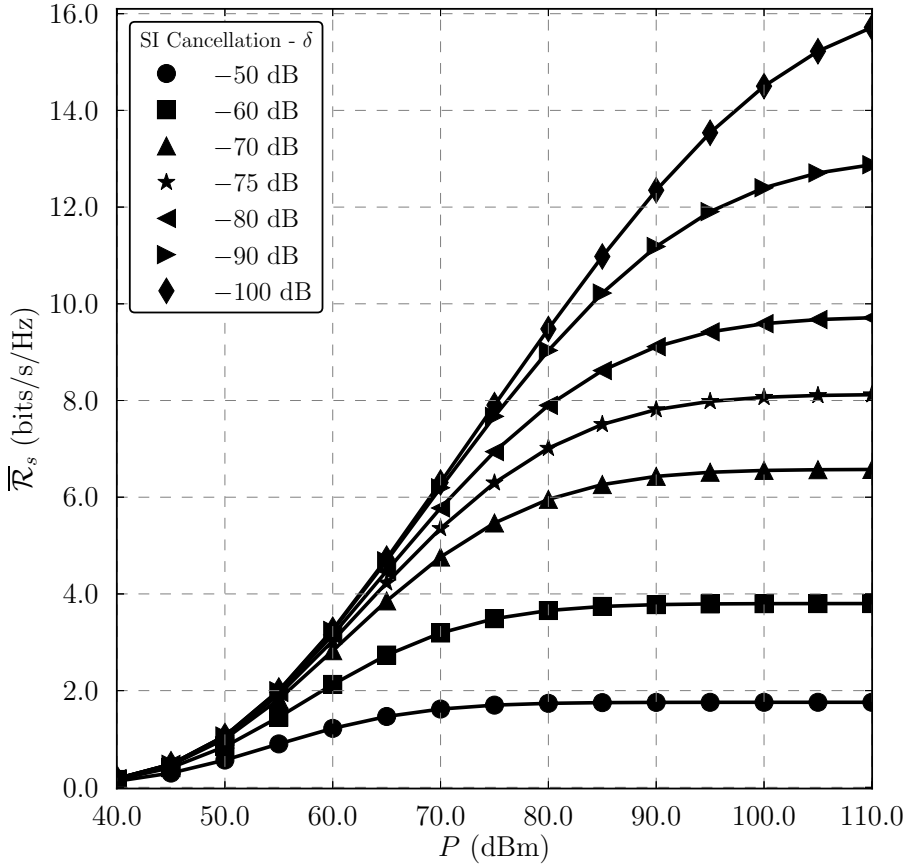

Fig 29. Average secrecy rate $\overline{\mathcal{R}}_s$ as a function of the transmit power P in dBm for different values of δ and $N_{\mathsf{E}} = 1$.

for different values of self-interference cancellation as well as for different number of antennas. The average secrecy rate degrades as the number of antennas grows. Nevertheless, it is still possible to communicate with perfect secrecy. Notice that in terms of secrecy capacity the impact of relatively poor self-interference cancellation ($\delta > -75$ dB) is much worse than that of having a sophisticated eavesdropper (with several receive antennas applying MRC).

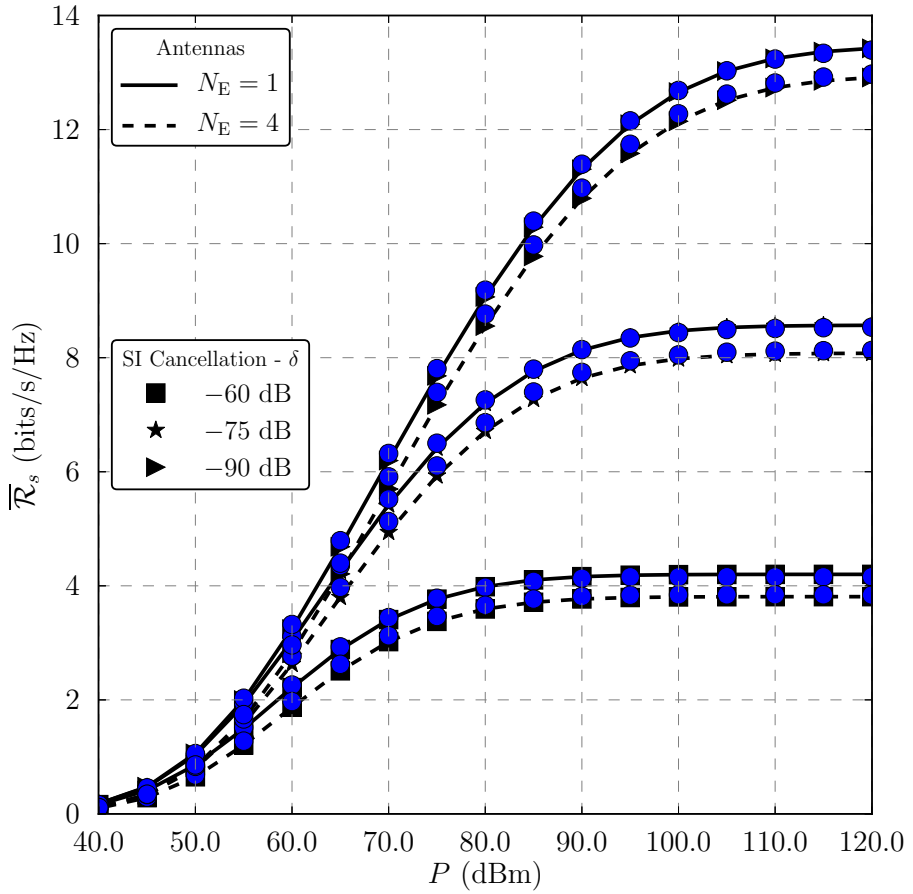

Fig 30. Average secrecy rate $\overline{\mathcal{R}}_s$ as a function of the transmit power P in dBm for different values of δ and number of antennas N_E.

5.6.2 Secrecy outage probability

In the following, we present some numerical results regarding the partial availability of CSI at the transmitters with respect to the eavesdropper. We recall that the transmitters are aware of passive eavesdropping, but have no CSI of the eavesdroppers channels, and therefore, the source attempts to convey with a fixed secure rate R_s. First, in Fig.31 we investigate the probability of non-zero secrecy rate, $\Pr[\mathcal{R}_s > 0]$, as a function of the transmit power for distinct values of δ and number of antennas at the eavesdropper.

From Fig. 31 we observe that the SNR of the eavesdropper increases with the increase of the number of antennas, which is directly reflected into a reduced probability of non-zero secrecy rate. For instance, for $P = 50$ dBm, $N_{\mathrm{E}} = 1$ and $\delta = -90$ dB a probability around 90% of with non-zero secrecy rate is achieved; however, if the eavesdropper has $N_{\mathrm{E}} = 4$ antennas this probability reduces to 72%. Again, the performance increases considerably as the self-interference cancellation improves. For instance, at high SNR regime and $N_{\mathrm{E}} = 4$, up to 15% gain is attainable is if the self-interference cancellation factor improves from $\delta = -75$ dB up to $\delta = -90$ dB at high SNR regime.

Further, Fig. 32 shows the outage probability as a function of the transmit power for distinct values δ, $N_{\mathrm{E}} \in \{1, 2, 4\}$ antennas and $R = 1$ bits/s/Hz. Once again, secrecy outage probability considerably increases with better self-interference attenuation and cancellation at the relay (lower δ). Notice also that as the number of antennas at the eavesdropper increases, the secrecy outage probability decreases since the eavesdropper presents more sophisticated hardware capabilities.

5.6.3 Secrecy outage and reliability probability

Next, we introduce some numerical results regarding the the third scenario, where the source has only channel statistics available. Therefore, the source fixes the transmission rate R_{FD} and the its attempted secure rate R_s. Fig. 33 shows the secrecy outage and reliability probability as a function of the transmit power P in dBm with different values of δ as well as target secrecy rate R_s given a fixed transmission rate $R_{\mathrm{FD}} = 4$ bits/s/Hz. Recall that when the source has only the statistics of the channels, she attempts to convey with a fixed transmis-

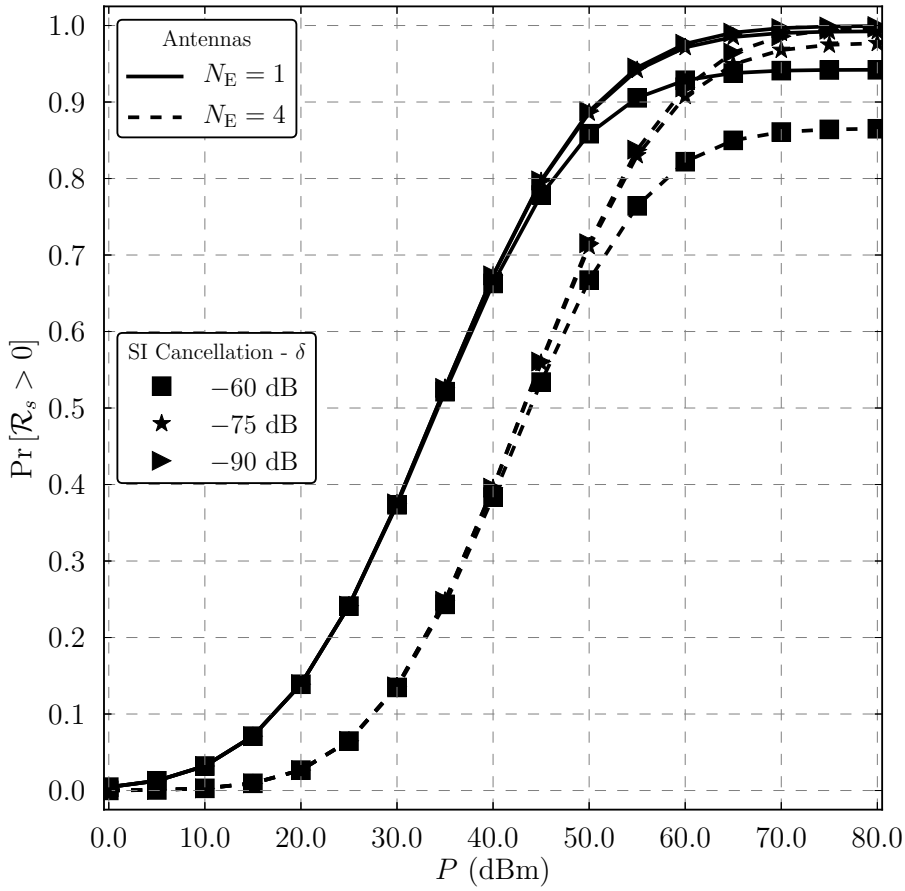

Fig 31. Probability of existence of secrecy rate $\Pr[\mathcal{R}_s > 0]$ as a function of the transmit power P in dBm with different values of δ as well as number of antennas at the eavesdropper (N_{E}) .

sion rate R_{FD} on the main channel, and also fixes a secure rate R_s, which by its turn also fixes the estimated equivocation rate of the eavesdropper. Therefore, whenever the actual equivocation rate at the eavesdropper is greater than the source's prediction, a secrecy outage occurs, while when the main channel does not support R_{FD}, a reliability outage occurs. Notice that as the secrecy gap, namely $R_{\mathrm{FD}} - R_s$, reduces, more secure the system becomes; however, the achieved gain is not in the same order of the reduction on the security gap. For instance, if the source doubles the rate to 2 bits/s/Hz a slight decrease in performance is noticeable since with the increase of R_s there is an increase on

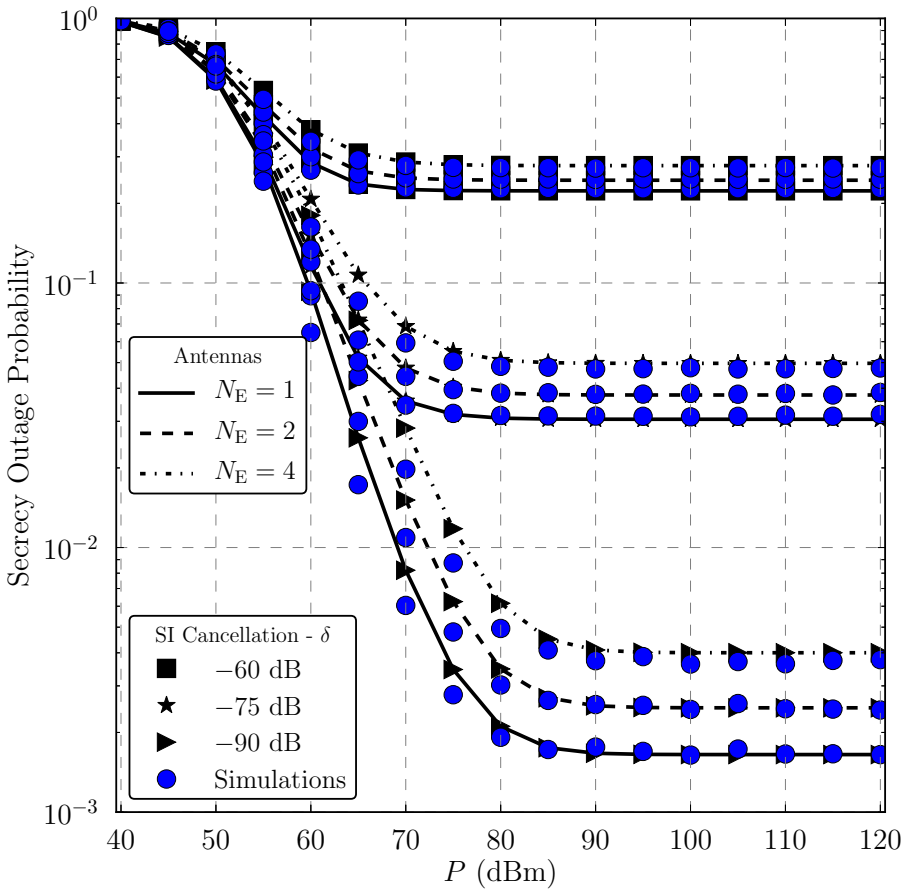

Fig 32. Outage probability, $\Pr[\mathcal{R}_s < R_s]$, as a function of the transmit power P in dBm with different values of δ as well as number of antennas at the eavesdropper, and $R = 1$ bits/s/Hz.

the probability of secrecy outage ($\Pr[\mathcal{R}_{\mathrm{E}} > R_{\mathrm{FD}} - R_s]$) due to the reduction of the secrecy gap. Moreover, notice that secure transmissions are attainable even though no CSI is available at the transmitters.

By its turn, setting the target transmission rate to $R_{\mathrm{FD}} = 8$ bits/s/Hz and assuming that the source transmits with power $P \in \{80, 120\}$ dBm, we evaluate the secrecy outage and reliability probability as a function of the target secrecy rate R_s (bits/s/Hz) in Fig. 34. Note that overall secrecy outage probability gradually increases as the target secrecy rate R_s grows; which means that the source's prediction of the eavesdropper's equivocation rate reduces once R_{FD} is

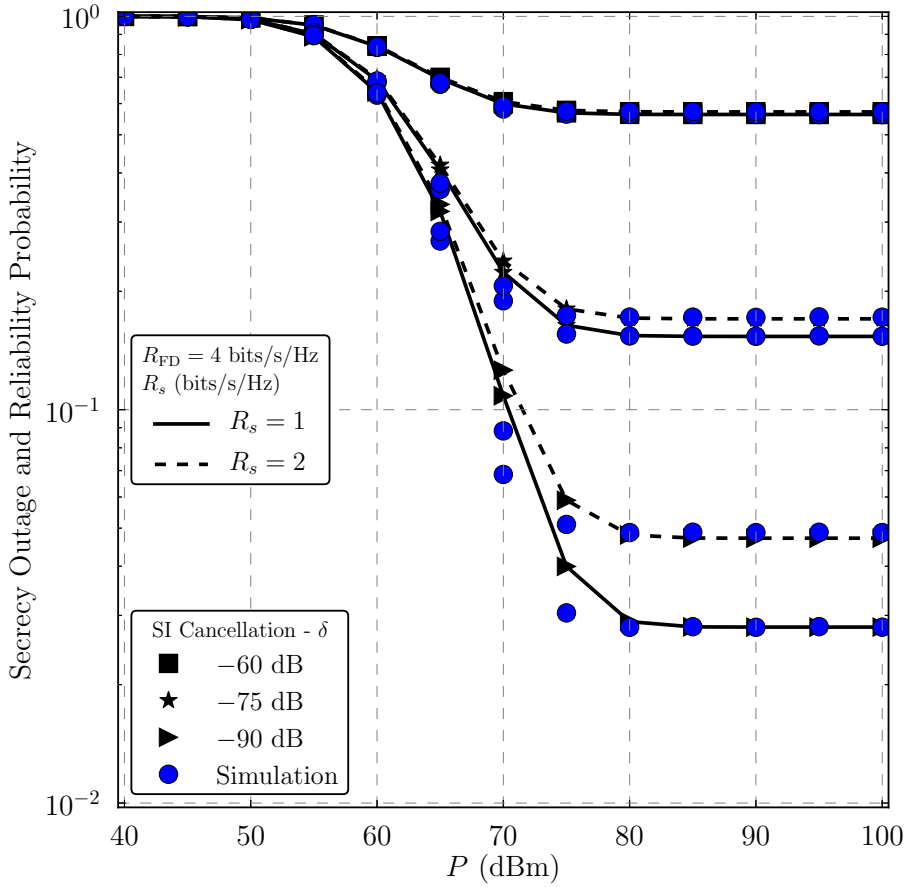

Fig 33. Secrecy outage and reliability probability as a function of the transmit power P in dBm with different values of δ as well as target secrecy rate R_s for $R_{\mathrm{FD}} = 4$ bits/s/Hz, and $N_{\mathrm{E}} = 1$.

fixed, which can also be observed in Fig. 33 as R_s increases. Thus, as the secrecy gap goes to zero the secrecy outage probability hastily tends to unity. Under such circumstances and differently from the second scenario, the source should be more cautious on her predictions of the transmit rates.

Remark 5.7. *It is noteworthy that the analytic results match the Monte Carlo simulations for all three scenarios, especially at high SNR regime. Notice also that there is a slightly shift between the simulations and analytic results, for instance for secrecy outage probability and secrecy outage and reliability probability,*

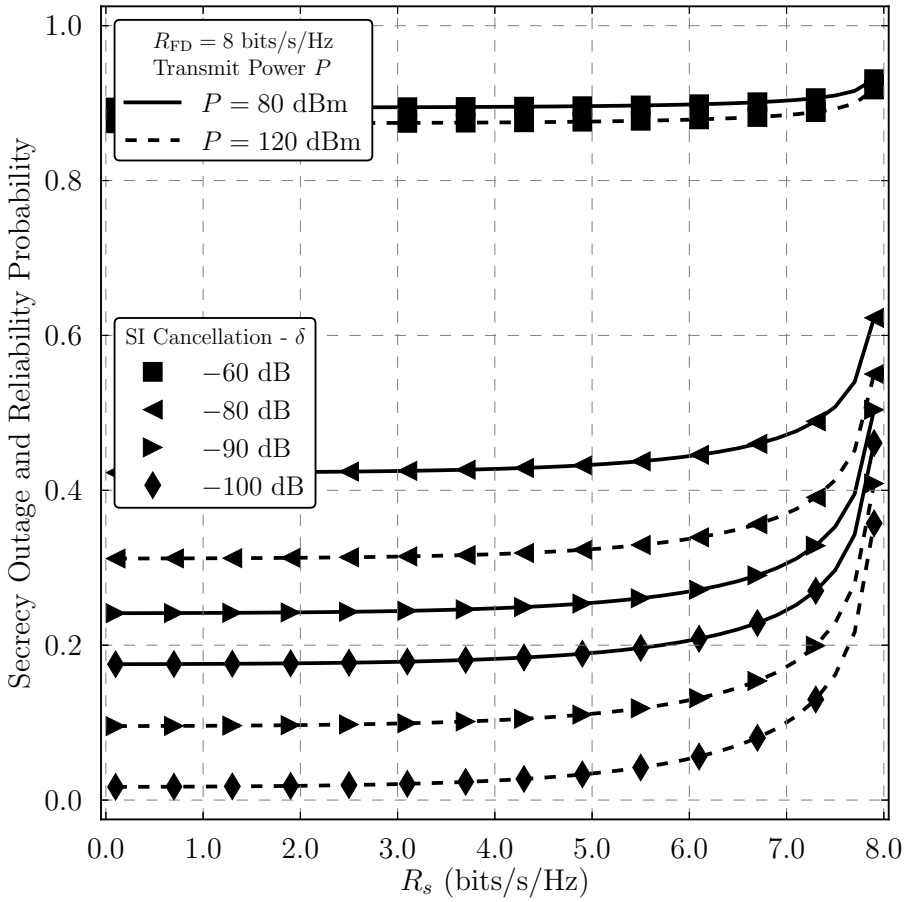

Fig 34. Secrecy outage and reliability probability as a function of the target secrecy rate R_s (bits/s/Hz) with different values of δ as well transmit power $P \in \{80, 120\}$ dBm with fixed attempted transmission rate $R_{\mathsf{FD}} = 8$ bits/s/Hz, and $N_{\mathrm{E}} = 1$.

which occurs because the cumulant-based approximation is more tight at the tail of the CDF. Nonetheless, our results serve as a bound on the performance a secure FD cooperative network under composite fading channel, since we are able to capture the dynamics of the network and the main mechanisms that govern its performance.

5.7 Final remarks and conclusions

This chapter investigates the secrecy performance of a cooperative FD relaying network in the presence of a passive multiple antenna eavesdropper under composite fading channels. Three scenarios are considered based on the CSI availability at the transmitter: *i)* full CSI is available from both intended and unintended receivers; *ii)* only the legitimate channels are known to the source; and *iii)* no CSI is available, except for channel statistics. Thus, in order to assess the performance of each scenario, we address three distinct metrics according to each case such that in *i)* we propose an approximation in closed-form for the average secrecy rate; while in *ii)* an approximation in closed-form is proposed for secrecy outage probability; and in *iii)* we attain closed-form expressions for the secrecy outage and reliability probability.

Furthermore, our results show that the self-interference at the relay, which is modeled as a fading channel, considerably affects performance regardless of the scenario considered. Therefore, the better the isolation and cancellation employed at the relay, the higher the security achieved. Additionally, we also investigate the impact of the number of antennas at the eavesdropper on the overall performance of each scenario. All in all, even though experiencing strong self-interference FD relaying is feasible also under secrecy constraints, even in the presence of sophisticated multiple antenna eavesdropper.

6 Conclusions and future work

In this thesis we studied FD cooperative networks from different perspectives and we provided a comprehensive performance analysis of such networks. We showed that FD relaying is feasible, even when experiencing strong self-interference, and we discussed its application under different scenarios. More importantly, the results attained through this work serve as a benchmark for design as well as deployment of current and future wireless communications technologies. For instance, FD relaying is already foreseen in LTE [11]. Moreover, cooperative systems are foreseen as a key technology also in the upcoming wireless systems [12–14].

In the following sections, we outline the contributions of this thesis chapter by chapter and then point out research directions and future work.

6.1 Contributions

The contributions are summarized as follows:

- **Chapter 2:** We provided a comprehensive overview of the current state-of-the-art on FD communications, more specifically FD relaying, and we revisited some of the main properties of cooperative schemes.
- **Chapter 3:** We assessed the outage probability, throughput and energy efficiency of cooperative FD relaying over Rayleigh fading channels and compared the performance of cooperative FD relaying, as well as a multi-hop FD scheme, to two incremental cooperative HD relaying methods. Besides the mathematical framework provided, we also showed that cooperative HD schemes can achieve a smaller outage probability and a higher throughput than cooperative FD relaying with self-interference. Finally, we drew a discussion on the trade-offs between HD and FD schemes as well as between throughput and energy efficiency.
- **Chapter 4:** We investigated the performance of FDBM relaying protocol under general fading settings. Additionally, we introduced a new accurate approximation for the product of two Nakagami-m RVs as well as for the sum of Gamma RVs. With these results we are able to characterize the outage

probability of the proposed FD relaying protocol in a easy to compute closed-form expression. Our findings allowed us to better understand effects of the residual self-interference on a FD relaying setup, since distinct (non-) LoS configurations can be emulated which can be directly related to the quality of the antenna isolation and self-interference cancellation employed at the FD relay.

– **Chapter 5:** We considered the concept of PHY security and we discussed the main advances on cooperative PHY security associated with FD relaying schemes and composite fading channels. We provided a comprehensive mathematical framework for the performance analysis of secure FD cooperative networks. For each scenario under evaluation, we assessed the appropriate metric, providing ease to compute and in closed-form expressions. We demonstrated that, even though experiencing strong self-interference, FD relaying is feasible also under secrecy constraints.

6.2 Future work and final remarks

We can identify many future directions for the work carried out in this thesis. For instance, we increased the complexity of the fading settings chapter by chapter. In Chapter 3 we focused on Rayleigh fading, while Chapter 4 investigated Nakagami-m fading scenarios. Hence one can extend those results by looking at a more general fading distribution and realistic path loss model. Moreover, recently there has been a upsurge of interest on the unoccupied zones of the spectrum, more specifically on frequencies above 10 GHz, commonly known as Millimeter Wave (mmWave), such that new path loss and fading models are being proposed [14, 198, 199]. Thus, relevant questions arise: How mmWave fading and path loss settings impact performance? How does it impact on network design and deployment? Is FD schemes an viable solution for mmWave scenarios? Could we employ the same tool to mitigate self-interference behaves in such high frequencies? How do we model residual self-interference? Answering these questions is another possible future direction of our work.

Chapter 3 offers performance benchmark and outlines the advantages of power allocation in FD relaying schemes, but do not propose a specific solution. Therefore, power allocation policies are possible extension to this work, since such policies are the focus of current and upcoming wireless communica-

tions technologies. Such technologies aim at lower consumption (green) schemes, such that the longer the user can be connected and the better the user exploit and experiences all the advantages of a fully connected network as envisaged by [12–14].

The results presented in Chapters 3 and 4 can be applied and extended heterogeneous and cognitive radio networks. We already investigated some scenarios [44, 71, 75] were we assess the feasibility of underlay FD relaying and discuss the main advantages and gains attained with FD nodes. In this context, many paths are still open, for instance FD nodes can perform spectrum sensing while conveying information, power allocation policies given all constrains of the primary network are another possibility for future work. Even more paths open, when MIMO nodes are employed. Not only self-interference becomes more intricate problem and harder to cancel, but there are several ways to exploit FD MIMO nodes. For instance, through FD MIMO simultaneous UL and DL of multi-user networks can be assessed, which implicates on re-design of coordination and scheduling mechanisms, opening new challenges for the upcoming wireless networks [12–14]. Further, in [44] heterogeneous networks are investigated, in which FD underlay network can act as a relay for the legacy one. Hence enhancing performance of networks and tackling the issue of backhauling. In a more general framework lies [68, 69], which provide an investigation on how highly dense deployments of small cells perform when full-duplex nodes communicate under composite fading channels. The impact due to extra interference from co-channel users and how that compares to the intrinsic residual self-interference is identified, and performance is compared to benchmark HD scenarios. There are several possible ways to extend these works by considering, for instance, coordination mechanisms in order to reduce the perceived co-channel interference, another possibility is to take into account the temporal and spatial correlations on the outage probability and spectral efficiency.

As pointed out in Chapter 5, wireless communications systems are vulnerable to eavesdropping, and much can be done in this context. For instance, in [52] we propose a network model in which the eavesdropper is not able to exploit additional spatial diversity. One plausible extension is to bring this model to the cooperative context. This, allows us to enhance the performance of the legitimate network by increasing security and confidentiality of legitimate transmissions. Other option is to extend the results presented in Chapter 5 to a MIMO setting,

where a variety of scenarios and metrics can be evaluated, such as diversity-multiplexing trade-off, precoding as well as beamforming for secure relaying, amongst others. Another possible extension, is to investigate the secrecy capacity of interference-limited networks, providing performance analysis on a system level and resorting to Poison Point Process and stochastic geometry. In [54] we started to put some light into such issue.

All in all, as discussed above there are several possible extensions to this work, but not limited to, different fading settings, power allocation policies, heterogeneous and cognitive radio solutions as well as enhanced security solutions.

References

1. Evans D (2011) The Internet of Things: How the Next Evolution of the Internet Is Changing Everything. Cisco White Paper .
2. Solutions N (2011) 2020: Beyond 4G – Radio Evolution for the Gigabit Experience. Nokia White Paper .
3. Ericsson (2013) 5G Radio Access: Research and Vision. Ericsson White Paper .
4. Mietzner J, Schober R, Lampe L, Gerstacker WH & Hoeher PA (2009) Multiple-antenna techniques for wireless communications - a comprehensive literature survey. IEEE Communications Surveys Tutorials 11(2): 87–105.
5. Nosratinia A, Hunter TE & Hedayat A (2004) Cooperative communication in wireless networks. IEEE Communications Magazine 42(10): 74–80.
6. Laneman J, Tse D & Wornell G (2004) Cooperative Diversity in Wireless Networks: Efficient Protocols and Outage Behavior. IEEE Transactions on Information Theory 50(12): 3062–3080.
7. Kramer G, Gastpar M & Gupta P (2005) Cooperative strategies and capacity theorems for relay networks. IEEE Transactions Information Theory 51(9): 3037–3063.
8. Kramer G, Marić I & Yates RD (2006) Cooperative Communications. Foundations and Trends in Networking 1(3-4): 271–425.
9. Gomez-Cuba F, Asorey-Cacheda R & Gonzalez-Castano FJ (2012) A survey on cooperative diversity for wireless networks. IEEE Communications Surveys Tutorials 14(3): 822–835.
10. 3GPP (2010) Overview of 3GPP Release 10. 3GPP Release 10.
11. Li Q, Hu R, Qian Y & Wu G (2012) Cooperative communications for wireless networks: Techniques and applications in LTE-advanced systems. IEEE Wireless Communications 19(2): –.
12. Osseiran A, Boccardi F, Braun V, Kusume K, Marsch P, Maternia M, Queseth O, Schellmann M, Schotten H, Taoka H, Tullberg H, Uusitalo M, Timus B & Fallgren M (2014) Scenarios for 5G mobile and wireless communications: The vision of the METIS project. IEEE Communications Magazine 52(5): 26–35.

13. Wang CX, Haider F, Gao X, You XH, Yang Y, Yuan D, Aggoune H, Haas H, Fletcher S & Hepsaydir E (2014) Cellular architecture and key technologies for 5G wireless communication networks. IEEE Communications Magazine 52(2): 122–130.
14. Boccardi F, Heath RW, Lozano A, Marzetta TL & Popovski P (2014) Five disruptive technology directions for 5G. IEEE Communications Magazine 52(2): 74–80.
15. Meulen ECVD (1971) Three-terminal communication channels. Advances in Applied Probability 3(1): 120–154.
16. Feng D, Jiang C, Lim G, Cimini J L J, Feng G & Li GY (2013) A survey of energy-efficient wireless communications. IEEE Communications Surveys Tutorials 15(1): 167–178.
17. Wang CX, Hong X, Ge X, Cheng X, Zhang G & Thompson J (2010) Cooperative MIMO channel models: A survey. IEEE Communications Magazine 48(2): 80–87.
18. Talha B & Patzold M (2011) Channel models for mobile-to-mobile cooperative communication systems: A state of the art review. IEEE Vehicular Technology Magazine 6(2): 33–43.
19. Letaief K & Zhang W (2009) Cooperative communications for cognitive radio networks. Proceedings of the IEEE 97(5): 878–893.
20. Chen X, Chen HH & Meng W (2014) Cooperative communications for cognitive radio networks: From theory to applications. IEEE Communications Surveys Tutorials 16(3): 1180–1192.
21. Yang D, Fang X & Xue G (2012) Game theory in cooperative communications. IEEE Wireless Communications 19(2): 44–49.
22. Tannious R & Nosratinia A (2008) Spectrally-efficient relay selection with limited feedback. IEEE Journal on Selected Areas in Communications 26(8): 1419–1428.
23. Fan Y, Wang C, Thompson J & Poor HV (2007) Recovering multiplexing loss through successive relaying using repetition coding. IEEE Transactions on Wireless Communications 6(12): 4484–4493.
24. Alves H & Souza RD (2011) Selective decode-and-forward using fixed relays and packet accumulation. IEEE Communications Letters 15(7): 707–709.
25. Duarte M & Sabharwal A (2010) Full-duplex wireless communications using off-the-shelf radios: Feasibility and first results. In: Asilomar Conference

on Signals, Systems and Computers (ASILOMAR).
26. Duarte M, Dick C & Sabharwal A (2012) Experiment-driven characterization of full-duplex wireless systems. IEEE Transactions on Wireless Communications 11(12): 4296 –4307.
27. Choi JI, Hong S, Jain M, Katti S, Levis P & Mehlman J (2012) Beyond full duplex wireless. In: 2012 Conference Record of the Forty Sixth Asilomar Conference on Signals, Systems and Computers (ASILOMAR), pp. 40–44.
28. Bharadia D, McMilin E & Katti S (2013) Full duplex radios. SIGCOMM Comput. Communications Rev. 43(4): 375–386.
29. Sabharwal A, Schniter P, Guo D, Bliss D, Rangarajan S & Wichman R (2014) In-Band Full-Duplex Wireless: Challenges and Opportunities. IEEE Journal on Selected Areas in Communications 32(9): 1637–1652.
30. Hong S, Brand J, Choi J, Jain M, Mehlman J, Katti S & Levis P (2014) Applications of self-interference cancellation in 5G and beyond. IEEE Communications Magazine 52(2): 114–121.
31. Bliss DW, Parker PA & Margetts AR (2007) Simultaneous transmission and reception for improved wireless network performance. In: IEEE/SP 14th Workshop on Statistical Signal Processing – SSP '07, pp. 478–482.
32. Kang YY, Kwak B & Cho JH (2014) An optimal full-duplex AF relay for joint analog and digital domain self-interference cancellation. IEEE Transactions on Communications 62(8): 2758–2772.
33. Everett E, Sahai A & Sabharwal A (2014) Passive self-interference suppression for full-duplex infrastructure nodes. IEEE Transactions on Wireless Communications 13(2): 680–694.
34. Debaillie B, van den Broek DJ, Lavin C, van Liempd B, Klumperink EAM, Palacios C, Craninckx J, Nauta B & Parssinen A (2014) Analog/RF solutions enabling compact full-duplex radios. IEEE Journal on Selected Areas in Communications 32(9): 1662–1673.
35. Li S & Murch RD (2014) An investigation into baseband techniques for single-channel full-duplex wireless communication systems. IEEE Transactions on Wireless Communications 13(9): 4794–4806.
36. He Z, Shao S, Shen Y, Qing C & Tang Y (2014) Performance analysis of RF self-interference cancellation in full-duplex wireless communications. IEEE Wireless Communications Letters 3(4): 405–408.
37. Korpi D, Riihonen T, Syrjala V, Anttila L, Valkama M & Wichman R

(2014) Full-duplex transceiver system calculations: Analysis of ADC and linearity challenges. IEEE Transactions on Wireless Communications 13(7): 3821–3836.

38. Korpi D, Anttila L, Syrjala V & Valkama M (2014) Widely linear digital self-interference cancellation in direct-conversion full-duplex transceiver. IEEE Journal on Selected Areas in Communications 32(9): 1674–1687.
39. Sahai A, Patel G, Dick C & Sabharwal A (2013) On the impact of phase noise on active cancelation in wireless full-duplex. IEEE Transactions on Vehicular Technology 62(9): 4494–4510.
40. Riihonen T, Werner S & Wichman R (2009) Optimized gain control for single-frequency relaying with loop interference. IEEE Transactions Wireless Communications 8(6): 2801–2806.
41. Riihonen T, Werner S & Wichman R (2011) Mitigation of loopback self-interference in full-duplex MIMO relays. IEEE Transactions on Signal Processing 59(12): 5983–5993.
42. Riihonen T, Werner S & Wichman R (2011) Hybrid full-duplex/half-duplex relaying with transmit power adaptation. IEEE Transactions on Wireless Communications 10(9): 3074–3085.
43. Alves H, Fraidenraich G, Souza RD, Bennis M & Latva-aho M (2012) Performance analysis of full duplex and selective and incremental half duplex relaying schemes. In: IEEE Wireless Communications and Networking Conference (WCNC), pp. 771–775.
44. Alves H, Souza RD, Bennis M & Latva-aho M (2012) Enhanced performance of heterogeneous networks through full-duplex relaying. EURASIP Journal on Wireless Communications and Networking 2012(365).
45. Alves H, Souza RD & Fraidenraich G (2013) Outage, throughput and energy efficiency analysis of some half and full duplex cooperative relaying schemes. Transactions on Emerging Telecommunications Technologies .
46. Alves H, da Costa DB, Souza RD & Latva-aho M (2013) Performance of block-markov full duplex relaying with self interference in Nakagami-m fading. IEEE Wireless Communications Letters 2(3): 311–314.
47. Khafagy M, Ismail A, Alouini MS & Aissa S (2013) On the outage performance of full-duplex selective decode-and-forward relaying. IEEE Communications Letters 17(6): 1180–1183.
48. Kwon T, Lim S, Choi S & Hong D (2010) Optimal duplex mode for DF

relay in terms of the outage probability. IEEE Transactions Vehicular Technologies 59(7): 3628–3634.

49. Shiu YS, Chang SY, Wu HC, Huang SCH & Chen HH (2011) Physical layer security in wireless networks: A tutorial. IEEE Wireless Communications 18(2): 66–74.
50. Mathur S, Reznik A, Ye C, Mukherjee R, Rahman A, Shah Y, Trappe W & Mandayam N (2010) Exploiting the physical layer for enhanced security – security and privacy in emerging wireless networks. IEEE Wireless Communications 17(5): 63–70.
51. Bassily R, Ekrem E, He X, Tekin E, Xie J, Bloch M, Ulukus S & Yener A (2013) Cooperative security at the physical layer: A summary of recent advances. IEEE Signal Processing Magazine 30(5): 16–28.
52. Alves H, Souza RD, Debbah M & Bennis M (2012) Performance of transmit antenna selection physical layer security schemes. IEEE Signal Processing Letters 19(6): 372–375.
53. Alves H, Brante G, Souza RD, da Costa DB & Latva-aho M (2015) On the performance of secure full-duplex relaying under composite fading channels. IEEE Signal Processing Letters 22(7): 867–870.
54. Alves H, Lima CHM, Nardelli PJH, Souza RD & Latva-aho M (2015) On the secrecy capacity of interference-limited networks under composite fading channels. IEEE Signal Processing Letters 22(9): 1306–1310.
55. Alves H, Fraidenraich G & Demo Souza R (2011) Throughput performance analysis of some half and full duplex cooperative schemes. In: XXIX Simpósio Brasileiro de Telecomunicações (SBrT 2011), pp. 1–5. Curitiba.
56. Alves H, Demo Souza R & Debbah M (2011) Enhanced physical layer security through transmit antenna selection. In: IEEE GLOBECOM Workshops (GC Wkshps), pp. 879–883.
57. Alves H, Brante G, Souza RD, da Costa DB & Latva-aho M (2014) On the performance of full-duplex relaying under PHY security constraints. In: IEEE International Conference on Acoustics, Speech, and Signal Processing (ICASSP), pp. 1–5. Italy.
58. Alves H, Brante G, Souza RD & Rebelatto JL (2012) Energy efficiency and throughput performance of power and rate allocation on incremental decode-and-forward relaying. Wireless Networks 18(5): 495–505.
59. Alves H, Souza RD, Fraidenraich G & Pellenz ME (2012) Throughput

performance of parallel and repetition coding in incremental decode-and-forward relaying. Wireless Networks 18(8): 881–892.

60. Mafra SB, Souza RD, Rebelatto JL, Fernandez EMG & Alves H (2013) Cooperative overlay secondary transmissions exploiting primary retransmissions. EURASIP Journal on Wireless Communications and Networking 2012(196).
61. Alves H, Demo Souza R, Brante G & Pellenz ME (2011) Performance of type-I and type-II hybrid ARQ in decode and forward relaying. In: IEEE Vehicular Technology Conference (VTC Spring), pp. 1–5.
62. Alves H, Brante G & Demo Souza R (2011) Throughput performance of incremental decode-and-forward using infra-structured relays and rate allocation. In: IEEE International Symposium on Wireless Communication Systems (ISWCS), pp. 106–110.
63. Alves H, Bennis M, Saad W, Debbah M & Latva-aho M (2012) On the fly self-organized base station placement. In: IEEE International Symposium on Wireless Communication Systems (ISWCS), pp. 826–829.
64. Sanguanpuak T, Rajatheva N, Taparugssanagorn A & Alves H (2012) Performance of energy detector over Nakagami-m fading for relay-based cognitive radio networks. In: IEEE International Symposium on Wireless Communication Systems (ISWCS), pp. 546–550.
65. Alves H, Benevides da Costa D, Demo Souza R & Latva-aho M (2013) On the performance of two-way half-duplex and one-way full-duplex relaying. In: IEEE Workshop on Signal Processing Advances in Wireless Communications – Invited Paper (SPAWC), pp. 56–60.
66. Mafra SB, Alves H, da Costa DB, Demo Souza R & Latva-aho M (2013) On the performance of cognitive full-duplex relaying systems under spectrum sharing constraints. In: XXX Simpósio Brasileiro de Telecomunicações (SBrT 2013), pp. 1–5. Fortaleza.
67. Lopez R, Sanchez EF, Souza RD & Alves H (2014) Genetic algorithm aided transmit power control in cognitive radio networks. In: 9th International Conference on Cognitive Radio Oriented Wireless Networks (Crowncom), pp. 1–5. Oulu.
68. Alves H, de Lima CHM, Nardelli PHJ, Souza RD & Latva-aho M (2014) On the average spectral efficiency of interference-limited full-duplex networks. In: 9th International Conference on Cognitive Radio Oriented Wireless

Networks (Crowncom), pp. 1–5. Oulu.

69. de Lima CHM, Nardelli PHJ, Alves H & Latva-aho M (2014) Full-duplex communications in interference networks under composite fading channel. In: European Conference on Networks and Communications (EuCNC'2014), pp. 1–5. Bologna.
70. Nardelli PHJ, de Lima CHM, Alves H, Cardieri P & Latva-aho M (2014) Throughput of wireless networks with poisson distributed nodes using location information. In: Proceedings of 2014 International Telecommunications Symposium (ITS), pp. 1–5. Sao Paulo.
71. Mafra S, Alves H, Da Costa DB, Souza RD, Fernandez E & Latva-aho M (2014) On the performance and optimal power allocation of cognitive full-duplex relaying under spectrum sharing constraints. Wireless Networks -(-): Submitted.
72. Brante G, Alves H, Souza RD & Latva-aho M (2015) Secrecy analysis of transmit antenna selection cooperative schemes with no channel state information at the transmitter. IEEE Transacions on Communications -(-): Accepted – To appear.
73. Nardelli PHJ, de Lima CHM, Alves H, Cardieri P & Latva-aho M (2015) Throughput of wireless networks with poisson distributed nodes using location information. In: Ad-hoc Networks, volume -, p. Accepted. To Appear.
74. Moya DPO, Benítez EEO, Alves H, Santos Filho JCS & Latva-aho M (2014) Exploiting the direct link in full-duplex amplify-and-forward relaying networks. IEEE Signal Processing Letters -(-): Submitted.
75. Benitez EEO, Moya DPO, Alves H, Santos Filho JCS & Latva-aho M (2015) Outage performance of cognitive full-duplex decode-and-forward relaying networks. IEEE Communication Letters -(-): Submitted.
76. Alves H, da Costa DB, Souza RD & Latva-aho M (2015) Performance of full duplex relaying under co-channel interference and Nakagami-m fading. In: VTC-2015, pp. 1–5. Glasgow, Scotland.
77. Cover TM & Thomas JM (2006) Elements of Information Theory. Wiley-Interscience, New Jersey, 2 edition.
78. Larsson EG & Vojcic BR (2005) Cooperative transmit diversity based on superposition modulation. IEEE Communications Letters 9(9): 778–780.
79. Wang C, Fan Y, Thompson JS, Skoglund M & Poor HV (2010) Superposition-Repetition-Coded Successive Decode-And-Forward Relaying

with Limited Destination-Relay Feedback. In: 2010 IEEE Wireless Communication and Networking Conference, pp. 1–6. Sydney, Australia.

80. Yanikomeroglu H, Falconer DD & Periyalwar S (2004) Range extension without capacity penalty in cellular networks with digital fixed relays. In: 2004 IEEE Global Telecommunications Conference, pp. 3053–3057. IEEE, Dallas, Texas.
81. Sadek AK, Han Z & Liu KJR (2010) Distributed relay-assignment protocols for coverage expansion in cooperative wireless networks. IEEE Transactions on Mobile Computing 9(4): 505–515.
82. Valenti MC (2005) Practical relay networks: A generalization of hybrid-ARQ. IEEE Journal on Selected Areas in Communications 23(1): 7–18.
83. Zheng K, Hu L, Wang W & Huang L (2009) Performance analysis of HARQ transmission in cooperative DF relaying systems. Wireless Personal Communications 55(3): 441–455.
84. Hong S & Caire G (2013) Full-duplex relaying with half-duplex relays. CoRR abs/1311.6247.
85. Khandani AK (2013) Two-way (true full-duplex) wireless. In: 2013 13th Canadian Workshop on Information Theory (CWIT), pp. 33–38.
86. Kim TM & Paulraj A (2012) Outage probability of amplify-and-forward cooperation with full duplex relay. In: 2012 IEEE Wireless Communications and Networking Conference (WCNC), pp. 75–79.
87. Baranwal TK, Michalopoulos DS & Schober R (2013) Outage analysis of multihop full duplex relaying. IEEE Communications Letters 17(1): 63–66.
88. Krikidis I & Suraweera HA (2013) Full-duplex cooperative diversity with Alamouti space-time code. IEEE Wireless Communications Letters 2(5): 519–522.
89. Jimenez Rodriguez L, Tran NH & Le-Ngoc T (2014) Performance of full-duplex af relaying in the presence of residual self-interference. IEEE Journal on Selected Areas in Communications 32(9): 1752–1764.
90. Parsaeefard S & Le-Ngoc T (2014) Full-duplex relay with jamming protocol for improving physical-layer security. IEEE Journal on Selected Areas in Communications 32(9): 1–5.
91. Suraweera HA, Michalopoulos DS & Karagiannidis GK (2009) Performance of distributed diversity systems with a single amplify-and-forward relay. IEEE Transactions on Vehicular Technology 58(5): 2603–2608.

92. Nguyen D, Tran LN, Pirinen P & Latva-aho M (2013) Precoding for full duplex multiuser MIMO systems: Spectral and energy efficiency maximization. IEEE Transactions on Signal Processing 61(16): 4038–4050.
93. Lee CH, Lee JH, Shin OS & Kim SC (2010) Sum rate analysis of multi-antenna multiuser relay channel. IET Communications 4(17): 2032–2040.
94. Cirik AC, Rong Y & Hua Y (2014) Achievable rates of full-duplex MIMO radios in fast fading channels with imperfect channel estimation. IEEE Transactions on Signal Processing 62(15): 3874–3886.
95. Huberman S & Le-Ngoc T (2014) Self-interference threshold-based MIMO full-duplex precoding. IEEE Transactions on Vehicular Technology PP(99): 1–1.
96. Huberman S & Le-Ngoc T (2014) Self-interference pricing-based MIMO full-duplex precoding. IEEE Wireless Communications Letters PP(99): 1–1.
97. Zhu Y, Xin Y & Kam PY (2008) Outage probability of Rician fading relay channels. IEEE Transactions Vehicular Technologies 57(4): 2648–2652.
98. Zhu Y, Xin Y & Kam PY (2008) Optimal transmission strategies for rayleigh fading relay channels. IEEE Transactions on Wireless Communications 7(2): 618 –628.
99. Riihonen T, Werner S, Wichman R & Eduardo ZB (2009) On the feasibility of full-duplex relaying in the presence of loop interference. In: 10th IEEE Workshop on Signal Processing Advances in Wireless Communications (SPAWC).
100. Riihonen T, Werner S & Wichman R (2009) Comparison of full-duplex and half-duplex modes with a fixed amplify-and-forward relay. In: Wireless Communications and Networking Conference, 2009. WCNC 2009. IEEE.
101. Krikidis I, Suraweera HA, Yang S & Berberidis K (2012) Full-duplex relaying over block fading channel: A diversity perspective. IEEE Transactions on Wireless Communications 11(12): 4524–4535.
102. Krikidis I, Suraweera HA, Smith PJ & Yuen C (2012) Full-duplex relay selection for amplify-and-forward cooperative networks. IEEE Transactions on Wireless Communications 11(12): 4381–4393.
103. Shang CYA, Smith PJ, Woodward GK & Suraweera HA (2014) Linear transceivers for full duplex mimo relays. In: 2014 Australian Communications Theory Workshop (AusCTW), pp. 11–16.

104. Suraweera HA, Krikidis I, Zheng G, Yuen C & Smith PJ (2014) Low-complexity end-to-end performance optimization in MIMO full-duplex relay systems. IEEE Transactions on Wireless Communications 13(2): 913–927.
105. Ng DWK, Lo ES & Schober R (2012) Dynamic resource allocation in MIMO-OFDMA systems with full-duplex and hybrid relaying. IEEE Transactions on Communications 60(5): 1291–1304.
106. Ngo HQ, Suraweera HA, Matthaiou M & Larsson EG (2014) Multipair full-duplex relaying with massive arrays and linear processing. IEEE Journal on Selected Areas in Communications 32(9): 1721–1737.
107. Gohary RH & Yanikomeroglu H (2014) Grassmannian signalling achieves tight bounds on the ergodic high-SNR capacity of the noncoherent MIMO full-duplex relay channel. IEEE Transactions on Information Theory 60(5): 2480–2494.
108. Cover T & Gamal AE (1979) Capacity Theorems for the Relay Channel. IEEE Transactions on Information Theory 25(5): 572–584.
109. Carleial A (1982) Multiple-access channels with different generalized feedback signals. IEEE Transactions on Information Theory 28(6): 841–850.
110. Zeng CM, Kuhlmann F & Buzo A (1989) Achievability proof of some multiuser channel coding theorems using backward decoding. IEEE Transactions on Information Theory 35(6): 1160–1165.
111. Lai L & El Gamal H (2008) The relay-eavesdropper channel: Cooperation for secrecy. IEEE Transactions on Information Theory 54(9): 4005–4019.
112. Zimmermann E, Herhold P & Fettweis G (2005) On the performance of cooperative relaying protocols in wireless networks. European Transactions on Telecommunications 16(1): 5–16.
113. Zhai C, Xu H, Liu J, Zheng L & Zhou Y (2012) Performance of opportunistic relaying with truncated ARQ over Nakagami-m fading channels. Transactions on Emerging Telecommunications Technologies 23(1): 50–66.
114. Riihonen T, Werner S, Wichman R & Hamalainen J (2009) Outage probabilities in infrastructure-based single-frequency relay links. In: Wireless Communications and Networking Conference, 2009. WCNC 2009. IEEE.
115. Sendonaris A, Erkip E & Aazhang B (2003) User cooperation diversity - Part I: System description. IEEE Transactions on Communications 51(11): 1927–1938.
116. Z Hasan VKB H Boostanimehr (2011) Green cellular networks: A survey,

some research issues and challenges. IEEE Communications Surveys & Tutorials 13(4): 524–540.

117. Hoydis J, Kobayashi M & Debbah M (2011) Green small-cell networks. IEEE Vehicular Technology Magazine 6(1): 37–43.
118. Andreas Eisenblätter RP & Stefa?ski S (2013) Greennets. GreenNets White Paper .
119. Cavalcante RLG, Stanczak S, Schubert M, Eisenblaetter A & Tuerke U (2014) Toward energy-efficient 5g wireless communications technologies: Tools for decoupling the scaling of networks from the growth of operating power. IEEE Signal Processing Magazine 31(6): 24–34.
120. Wang S & Nie J (2010) Energy efficiency optimization of cooperative communication in wireless sensor networks. EURASIP Journal on Wireless Communications and Networking pp. 1–8.
121. Sadek AK, Yu W & Liu KJR (2009) On the energy efficiency of cooperative communications in wireless sensor networks. ACM Transactions on Sensor Networks 6(1): 1–21.
122. Brante G, Kakitani MT & Souza RD (2011) Energy Efficiency Analysis of Some Cooperative and Non-Cooperative Transmission Schemes in Wireless Sensor Networks. IEEE Transactions on Communications 59(10): 2671 –2677.
123. Gomez-Vilardebo J, Perez-Neira A & Najar M (2010) Energy efficient communications over the AWGN relay channel. IEEE Transactions on Wireless Communications 9(1): 32 –37.
124. Zhao B & Valenti MC (2003) Distributed turbo coded diversity for relay channel. Electronics Letters 39(10): 786 – 787.
125. Nam YH, Azarian K, El Gamal H & Schniter P (2005) Cooperation through ARQ. In: IEEE Workshop on Signal Processing Advances in Wireless Communications, pp. 1023–1027.
126. Zhao B & Valenti MC (2005) Practical relay networks: A generalization of hybrid-ARQ. IEEE Journal on Selected Areas in Communications 23(1): 7 –18.
127. Hu J & Duman TM (2007) Low density parity check codes over wireless relay channels. IEEE Transactions on Wireless Communications 6(9): 3384 –3394.
128. Narasimhan R (2008) Throughput-delay performance of half-duplex hybrid-

ARQ relay channels. In: IEEE International Conference on Communications, pp. 986 –990.

129. Khormuji MN & Larsson EG (2009) Cooperative transmission based on decode-and-forward relaying with partial repetition coding. IEEE Transactions on Wireless Communications 8(4): 1716 –1725.
130. Papoulis A & Pillai SU (2001) Probability, Random Variables and Stochastic Processes. McGraw-Hill.
131. Cui S, Goldsmith AJ & Bahai A (2003) Energy-constrained modulation optimization for coded systems. In: IEEE Global Telecommunications Conference, volume 1, pp. 372 – 376.
132. Chen G, Hanson S, Blaauw D & Sylvester D (2010) Circuit design advances for wireless sensing applications. Proceedings of the IEEE 98(11): 1808 – 1827.
133. Cui S, Goldsmith AJ & Bahai A (2005) Energy-constrained modulation optimization. IEEE Transactions on Wireless Communications 4(5): 2349–2360.
134. Boyd S & Vandenberghe L (2004) Convex Optimization. Cambridge University Press, 1 edition.
135. Luo ZQ & Yu W (2006) An introduction to convex optimization for communications and signal processing. IEEE Journal on Selected Areas in Communications, 24(8): 1426 –1438.
136. Cavalcanti FRP & Andersson S (2009) Optimizing Wireless Communication Systems. Springer, 1 edition.
137. 3GPP (2010) Home node b radio frequency RF requirements (FDD). Technical Specification Group Radio Access Networks, 3GPP TR 36.814 version 9.0.0 release 9, Technical Report.
138. Host-Madsen A & Zhang J (2005) Capacity bounds and power allocation for wireless relay channels. IEEE Transactions on Information Theory 51(6): 2020–2040.
139. J C S Santos Filho and M D Yacoub (2004) Nakagami-m approximation to the sum of M non-identical independent Nakagami-m variates. IET Electron. Lett. 40(15): 951–952.
140. D B da Costa, H Ding, M D Yacoub, and J Ge (2012) Two-way relaying in interference-limited AF cooperative networks over Nakagami-m fading. IEEE Transactions Vehicular Technologies 61(8): 3766–3771.

141. D B da Costa, H Ding, and J Ge (2011) Interference-limited relaying transmissions in dual-hop cooperative networks over Nakagami-m fading. IEEE Communications Lett. 15(5): 503–505.
142. Simon MK & Alouini MS (2005) Digital Communication over Fading Channels. Wiley Series in Telecommunications and Signal Processing.
143. Abramowitz M & Stegun IA (1965) Handbook of Mathematical Functions: with Formulas, Graphs, and Math. Tables. Dover.
144. Gradshteyn IS & Ryzhik IM (2007) Table of Integrals, Series, and Products. Academic Press.
145. Springer MD & Thompson WE (1970) The distribution of products of beta, gamma and gaussian random variables. SIAM Journal on Applied Mathematics 18(4): pp. 721–737.
146. Withers CS & Nadarajah S (2013) On the product of gamma random variables. Quality & Quantity 47(1): 545–552.
147. Stacy EW (1962) A generalization of the gamma distribution. The Annals of Mathematical Statistics 33(3): 1187–1192.
148. Crooks GE (2010) The Amoroso Distribution. ArXiv e-prints .
149. Karagiannidis GK, Sagias NC & Mathiopoulos PT (2007) N* Nakagami: A novel stochastic model for cascaded fading channels. IEEE Transactions Communications 55(8): 1453–1458.
150. Chen Y, Karagiannidis G, Lu H & Cao N (2012) Novel approximations to the statistics of products of independent random variables and their applications in wireless communications. IEEE Transactions on Vehicular Technology 61(2): 443–454.
151. Billingsley P (1995) Probability and measure. Wiley-Interscience, New York, 3 edition.
152. Poor HV (2012) Information and inference in the wireless physical layer. IEEE Wireless Communications 19(1): 40–47.
153. Shu Z, Qian Y & Ci S (2013) On physical layer security for cognitive radio networks. IEEE Network 27(3): 28–33.
154. Mukherjee A, Fakoorian SA, Huang J & Swindlehurst A (2014) Principles of physical layer security in multiuser wireless networks: A survey. IEEE Communications Surveys Tutorials 16(3): 1550–1573.
155. E D Silva, A L D Santos, L C P Albini, and M Lima (2008) Identity-based key management in mobile ad hoc networks: Techniques and applications.

IEEE Wireless Communications 15: 46–52.

156. Wyner AD (1975) The wire-tap channel. Bell Sys. Tech. J. 54(8): 1355 –1387.
157. Leung-Yan-Cheong S & Hellman M (1978) The gaussian wire-tap channel. IEEE Transactions on Information Theory 24(4): 451–456.
158. Bloch M, Barros J, Rodrigues MRD & McLaughlin SW (2008) Wireless information-theoretic security. IEEE Transactions on Information Theory 54(6): 2515–2534.
159. Prabhu V & Rodrigues MRD (2011) On wireless channels with M -antenna eavesdroppers: Characterization of the outage probability and ε -outage secrecy capacity. IEEE Transactions on Information Forensics and Security 6(3): 853–860.
160. Khisti A & Wornell GW (2010) Secure transmission with multiple antennas - Part I: The MISOME wiretap channel. IEEE Transactions on Information Theory 56(7): 3088 –3104.
161. Khisti A & Wornell GW (2010) Secure transmission with multiple antennas - Part II: The MIMOME wiretap channel. IEEE Transactions on Information Theory 56(11): 5515 –5532.
162. Bashar S, Ding Z & Li GY (2011) On secrecy of codebook-based transmission beamforming under receiver limited feedback. IEEE Transactions on Wireless Communications 10(4): 1212–1223.
163. He F, Man H & Wang W (2011) Maximal ratio diversity combining enhanced security. IEEE Comm. Letters 15(5).
164. Yang N, Yeoh PL, Elkashlan M, Schober R & Collings IB (2013) Transmit antenna selection for security enhancement in MIMO wiretap channels. IEEE Transactions on Communications 61(1): 144–154.
165. Yang N, Suraweera HA, Collings IB & Yuen C (2013) Physical layer security of TAS/MRC with antenna correlation. IEEE Transactions Information Forensics Sec. 8(1): 254–259.
166. Bassily R & Ulukus S (2012) Secure communication in multiple relay networks through decode-and-forward strategies. Journal of Communications and Neteworks 14(4): 352–363.
167. Dong L, Han Z, Petropulu AP & Poor HV (2010) Improving wireless physical layer security via cooperating relays. IEEE Transactions Signal Process. 58(3): 1875–1888.

168. Gabry F, Li N, Schrammar N, Girnyk M, Rasmussen LK & Skoglund M (2014) On the optimization of the secondary transmitter's strategy in cognitive radio channels with secrecy. IEEE Journal on Selected Areas in Communications 32(3): 451–463.
169. Krikidis I, Thompson J & McLaughlin S (2009) Relay selection for secure cooperative networks with jamming. IEEE Transactions Wireless Communications 8(10): 5003–5011.
170. Zheng G, Krikidis I, Li J, Petropulu A & Ottersten B (2013) Improving physical layer secrecy using full-duplex jamming receivers. IEEE Transactions on Signal Processing 61(20): 4962–4974.
171. Zhou Y, Xiang ZZ, Zhu Y & Xue Z (2014) Application of full-duplex wireless technique into secure MIMO communication: Achievable secrecy rate based optimization. IEEE Signal Processing Letters 21(7): 804–808.
172. Cepheli O, Tedik S & Kurt G (2014) A high data rate wireless communication system with improved secrecy: Full duplex beamforming. IEEE Communications Letters 18(6): 1075–1078.
173. Mukherjee A & Swindlehurst A (2011) A full-duplex active eavesdropper in MIMO wiretap channels: Construction and countermeasures. In: Asilomar Conference on Signals, Systems and Computers (ASILOMAR), pp. 265–269.
174. Zheng G, Jorswieck E & Ottersten B (2013) Cooperative communications against jamming with half-duplex and full-duplex relaying. In: IEEE Vehicular Technology Conference (VTC Spring), pp. 1–5.
175. Zhu F, Gao F, Yao M & Zou H (2014) Joint information- and jamming-beamforming for physical layer security with full duplex base station. IEEE Transactions on Signal Processing 62(24): 6391–6401.
176. Ilow J & Hatzinakos D (1998) Analytic alpha-stable noise modeling in a poisson field of interferers or scatterers. IEEE Transactions on Signal Processing 46(6): 1601–1611.
177. Ho MJ & Stüber GL (1995) Capacity and power control for CDMA microcells. ACM Journal on Wireless Net. 1(3): 355–363.
178. Cardieri P & Rappaport TS (2001) Statistical analysis of co-channel interference in wireless communications systems. Wireless Communications and Mobile Comp. 1(1): 111–121.
179. de Lima CHM, Bennis M & Latva-aho M (2012) Coordination mechanisms

for self-organizing femtocells in two-tier coexistence scenarios. IEEE Transactions on Wireless Communications 11(6).

180. Tang X, Liu R & Spasojevic P (2007) On the achievable secrecy throughput of block fading channels with no channel state information at transmitter. In: CISS'07., pp. 917–922.
181. Tang X, Liu R, Spasojevic P & Poor HV (2009) On the throughput of secure hybrid-ARQ protocols for gaussian block-fading channels. IEEE Transactions on Information Theory 55(4): 1575–1591.
182. Fenton L (1960) The sum of log-normal probability distributions in scatter transmission systems. IRE Transactions on Communications Systems 8(1): 57–67.
183. Beaulieu NC, Abu-Dayya AA & McLane PJ (1995) Estimating the distribution of a sum of independent lognormal random variables. IEEE Transactions on Communications 43(12): 2869–.
184. Wu J, Mehta NB & Zhang J (2005) A flexible lognormal sum approximation method. In: Globecom, pp. 3413–3417. St. Louis, MO.
185. Zhang QT & Song SH (2008) A systematic procedure for accurately approximating lognormal-sum distributions. IEEE Transactions on Vehicular Tech. 57(1): 663–666.
186. Mahmoud ASH (2010) New quadrature-based approximations for the characteristic function and the distribution function of sums of lognormal random variables. IEEE Transactions on Vehicular Technologies 59(7): 3364–3372.
187. Ghasemi A & Sousa ES (2008) Interference aggregation in spectrum-sensing cognitive wireless networks. IEEE Journal of Selected Topics in Signal Processing 2(1): 41–56.
188. de Lima CHM, Bennis M, Ghaboosi K & Latva-aho M (2010) On interference analysis of self-organized femtocells in indoor deployment. In: 2010 IEEE GLOBECOM Workshops (GC Wkshps), pp. 659–663.
189. Filho JCSS, Cardieri P & Yacoub MD (2005) Simple accurate lognormal approximation to lognormal sums. Electronics Letters 41: 1016–1017(1).
190. Lukacs E (1970) Characteristic functions. Hodder Arnold, London, 2 edition.
191. Petrov VV (1975) Sums of independent random variables. Springer-Verlag, New York.

192. Filho JCSS, Cardieri P & Yacoub MD (2006) Highly accurate range-adaptive lognormal approximation to lognormal sum distributions. Electronics Letters 42: 361–363(2).
193. Nikjah R & Beaulieu NC (2009) Exact closed-form expressions for the outage probability and ergodic capacity of decode-and-forward opportunistic relaying. In: IEEE GLOBECOM'09, pp. 1–8.
194. William H Press WTV Saul A Teukolsky & Flannery BP (2007) Numerical Recipes: The Art of Scientific Computing. Cambridge University Press, Cambridge, UK, 3 edition.
195. de Lima CHM, Bennis M & Latva-aho M (2013) Statistical analysis of self-organizing heterogeneous networks with biased cell association and interference avoidance. IEEE Transactions Vehicular Technologies 62(5): 1950–1961. Special Section on Self-Organizing Radio Networks.
196. 3GPP (2009) Evolved Universal Terrestrial Radio Access (E-UTRA); Further advancements for E-UTRA physical layer aspects. Technical Specification Group Radio Access Networks, 3GPP TR 25.820 version 9.0.0 release 9, Technical Report.
197. 3GPP (2010) Channel models for femtocell. CMCC, CATT, Huawei, Qualcomm, Motorola, 3GPP TSG-RAN WG1.
198. Rappaport TS, Sun S, Mayzus R, Zhao H, Azar Y, Wang K, Wong GN, Schulz JK, Samimi M & Gutierrez F (2013) Millimeter wave mobile communications for 5G cellular: It will work! IEEE Access 1: 335–349.
199. Rangan S, Rappaport TS & Erkip E (2014) Millimeter-wave cellular wireless networks: Potentials and challenges. Proceedings of the IEEE 102(3): 366–385.

506. Vasikainen, Soili (2014) Performance management of the university education process

507. Jurmu, Marko (2014) Towards engaging multipurpose public displays : design space and case studies

508. Namal, Suneth (2014) Enhanced communication security and mobility management in small-cell networks

509. Huang, Xiaohua (2014) Methods for facial expression recognition with applications in challenging situations

510. Ala-aho, Pertti (2014) Groundwater-surface water interactions in esker aquifers : from field measurements to fully integrated numerical modelling

511. Torabi Haghighi, Ali (2014) Analysis of lake and river flow regime alteration to assess impacts of hydraulic structures

512. Bordallo López, Miguel (2014) Designing for energy-efficient vision-based interactivity on mobile devices

513. Suopajärvi, Hannu (2014) Bioreducer use in blast furnace ironmaking in Finland : techno-economic assessment and CO_2 emission reduction potential

514. Sobocinski, Maciej (2014) Embedding of bulk piezoelectric structures in Low Temperature Co-fired Ceramic

515. Kulju, Timo (2014) Utilization of phenomena-based modeling in unit operation design

516. Karinkanta, Pasi (2014) Dry fine grinding of Norway spruce (*Picea abies*) wood in impact-based fine grinding mills

517. Tervo, Valtteri (2015) Joint multiuser power allocation and iterative multi-antenna receiver design

518. Jayasinghe, Laddu Keeth Saliya (2015) Analysis on MIMO relaying scenarios in wireless communication systems

519. Partala, Juha (2015) Algebraic methods for cryptographic key exhange

520. Karvonen, Heikki (2015) Energy efficiency improvements for wireless sensor networks by using cross-layer analysis

521. Putaala, Jussi (2015) Reliability and prognostic monitoring methods of electronics interconnections in advanced SMD applications

Book orders:
Granum: Virtual book store
http://granum.uta.fi/granum/

UNIVERSITY OF OULU P.O. Box 8000 FI-90014 UNIVERSITY OF OULU FINLAND

ACTA UNIVERSITATIS OULUENSIS

UNIVERSITY of OULU
OULUN YLIOPISTO

ISBN 978-952-62-0765-0 (Paperback)
ISBN 978-952-62-0766-7 (PDF)
ISSN 0355-3213 (Print)
ISSN 1796-2226 (Online)